

## **Final Report**

**FDOT Contract No: BDV31-977-12**

**UF Project No: 113180**

### **Load and Resistance Factor Design Resistance Factors for Augercast In Place Piles**

Principal Investigators: Michael C. McVay (PI)  
Scott J. Wasman (Co-PI)

Graduate Students: Lin Huang  
Stephen Crawford

Department of Civil and Coastal Engineering  
Engineering School of Sustainable Infrastructure and Environment

University of Florida

P.O. Box 116580

Gainesville, Florida 32611-6580

Developed for the



Rodrigo Herrera, P.E., Project Manager

Juan Castellanos, P.E., Co-Project Manager

*February 2016*

## DISCLAIMER

The opinions, findings, and conclusions expressed in this publication are those of the authors and not necessarily those of the Florida Department of Transportation or the U.S. Department of Transportation.

Prepared in cooperation with the State of Florida  
Department of Transportation and the U.S. Department of  
Transportation.

# SI (MODERN METRIC) CONVERSION FACTORS (from FHWA)

## APPROXIMATE CONVERSIONS TO SI UNITS

SYMBOL	WHEN YOU KNOW	MULTIPLY BY	TO FIND	SYMBOL
<b>LENGTH</b>				
<b>in</b>	inches	25.4	millimeters	mm
<b>ft</b>	feet	0.305	meters	m
<b>yd</b>	yards	0.914	meters	m
<b>mi</b>	miles	1.61	kilometers	km

SYMBOL	WHEN YOU KNOW	MULTIPLY BY	TO FIND	SYMBOL
<b>AREA</b>				
<b>in<sup>2</sup></b>	square inches	645.2	square millimeters	mm <sup>2</sup>
<b>ft<sup>2</sup></b>	square feet	0.093	square meters	m <sup>2</sup>
<b>yd<sup>2</sup></b>	square yard	0.836	square meters	m <sup>2</sup>
<b>ac</b>	acres	0.405	hectares	ha
<b>mi<sup>2</sup></b>	square miles	2.59	square kilometers	km <sup>2</sup>

SYMBOL	WHEN YOU KNOW	MULTIPLY BY	TO FIND	SYMBOL
<b>VOLUME</b>				
<b>fl oz</b>	fluid ounces	29.57	milliliters	mL
<b>gal</b>	gallons	3.785	liters	L
<b>ft<sup>3</sup></b>	cubic feet	0.028	cubic meters	m <sup>3</sup>
<b>yd<sup>3</sup></b>	cubic yards	0.765	cubic meters	m <sup>3</sup>

NOTE: volumes greater than 1000 L shall be shown in m<sup>3</sup>

SYMBOL	WHEN YOU KNOW	MULTIPLY BY	TO FIND	SYMBOL
<b>MASS</b>				
<b>oz</b>	ounces	28.35	grams	g
<b>lb</b>	pounds	0.454	kilograms	kg
<b>T</b>	short tons (2000 lb)	0.907	megagrams (or "metric ton")	Mg (or "t")

SYMBOL	WHEN YOU KNOW	MULTIPLY BY	TO FIND	SYMBOL
<b>TEMPERATURE (exact degrees)</b>				
<b>°F</b>	Fahrenheit	5 (F-32)/9 or (F-32)/1.8	Celsius	°C

SYMBOL	WHEN YOU KNOW	MULTIPLY BY	TO FIND	SYMBOL
<b>ILLUMINATION</b>				
<b>fc</b>	foot-candles	10.76	lux	lx
<b>fl</b>	foot-Lamberts	3.426	candela/m <sup>2</sup>	cd/m <sup>2</sup>

SYMBOL	WHEN YOU KNOW	MULTIPLY BY	TO FIND	SYMBOL
<b>FORCE and PRESSURE or STRESS</b>				
<b>Lbf *</b>	poundforce	4.45	newtons	N
<b>kip</b>	kip force	1000	pounds	lbf
<b>lbf/in<sup>2</sup></b>	poundforce per square inch	6.89	kilopascals	kPa

**APPROXIMATE CONVERSIONS TO SI UNITS**

SYMBOL	WHEN YOU KNOW	MULTIPLY BY	TO FIND	SYMBOL
<b>LENGTH</b>				
<b>mm</b>	millimeters	0.039	inches	in
<b>m</b>	meters	3.28	feet	ft
<b>m</b>	meters	1.09	yards	yd
<b>km</b>	kilometers	0.621	miles	mi

SYMBOL	WHEN YOU KNOW	MULTIPLY BY	TO FIND	SYMBOL
<b>AREA</b>				
<b>mm<sup>2</sup></b>	square millimeters	0.0016	square inches	in <sup>2</sup>
<b>m<sup>2</sup></b>	square meters	10.764	square feet	ft <sup>2</sup>
<b>m<sup>2</sup></b>	square meters	1.195	square yards	yd <sup>2</sup>
<b>ha</b>	hectares	2.47	acres	ac
<b>km<sup>2</sup></b>	square kilometers	0.386	square miles	mi <sup>2</sup>

SYMBOL	WHEN YOU KNOW	MULTIPLY BY	TO FIND	SYMBOL
<b>VOLUME</b>				
<b>mL</b>	milliliters	0.034	fluid ounces	fl oz
<b>L</b>	liters	0.264	gallons	gal
<b>m<sup>3</sup></b>	cubic meters	35.314	cubic feet	ft <sup>3</sup>
<b>m<sup>3</sup></b>	cubic meters	1.307	cubic yards	yd <sup>3</sup>

SYMBOL	WHEN YOU KNOW	MULTIPLY BY	TO FIND	SYMBOL
<b>MASS</b>				
<b>g</b>	grams	0.035	ounces	oz
<b>kg</b>	kilograms	2.202	pounds	lb
<b>Mg (or "t")</b>	megagrams (or "metric ton")	1.103	short tons (2000 lb)	T

SYMBOL	WHEN YOU KNOW	MULTIPLY BY	TO FIND	SYMBOL
<b>TEMPERATURE (exact degrees)</b>				
<b>°C</b>	Celsius	1.8C+32	Fahrenheit	°F

SYMBOL	WHEN YOU KNOW	MULTIPLY BY	TO FIND	SYMBOL
<b>ILLUMINATION</b>				
<b>lx</b>	lux	0.0929	foot-candles	fc
<b>cd/m<sup>2</sup></b>	candela/m <sup>2</sup>	0.2919	foot-Lamberts	fl

SYMBOL	WHEN YOU KNOW	MULTIPLY BY	TO FIND	SYMBOL
<b>FORCE and PRESSURE or STRESS</b>				
<b>N</b>	newtons	0.225	poundforce	lbf
<b>kPa</b>	kilopascals	0.145	poundforce per square inch	lbf/in <sup>2</sup>

\*SI is the symbol for International System of Units. Appropriate rounding should be made to comply with Section 4 of ASTM E380.  
(Revised March 2003)

# TECHNICAL REPORT DOCUMENTATION PAGE

1. Report No.		2. Government Accession No.		3. Recipient's Catalog No.	
4. Title and Subtitle Load and Resistance Factor Design (LRFD) Resistance Factors for Augercast In Place Piles				5. Report Date December 2015	
				6. Performing Organization Code	
7. Author(s) Michael McVay, Scott Wasman, Lin Huang, and Stephen Crawford				8. Performing Organization Report No.	
9. Performing Organization Name and Address University of Florida – Dept. of Civil and Coastal Engineering Engineering School of Sustainable Infrastructure and Environment 365 Weil Hall – P.O. Box 116580 Gainesville, FL 32611-6580				10. Work Unit No. (TRAIS)	
				11. Contract or Grant No. BDV31-977-12	
12. Sponsoring Agency Name and Address  Florida Department of Transportation 605 Suwannee Street, MS 30 Tallahassee, FL 32399				13. Type of Report and Period Covered  Final Report 2/07/14 – 3/15/16	
				14. Sponsoring Agency Code	
15. Supplementary Notes					
<p>16. Abstract: Data from 78 load tests from 21 sites in the State of Florida were collected to develop Load and Resistance Factor Design (LRFD) resistance factors for Auger Cast In Place (ACIP) pile design. Forty-four of the piles were embedded in layers of soil and rock, 4 were only clay, 7 were only sand, 15 were sand and clay layers, and 8 had no borings. Inspection of the load test data revealed the majority (90%) of pile top displacements ranged from 0.1" to 0.3" and only a few reached 1". Because of the relatively small displacements recorded during testing, the majority of the ACIP's top load was carried by skin friction, where the maximum recorded tip resistance was 30% of top load, and occurred in the instance where the pile underwent 1.2" of top displacement. Current practice in the State is to design ACIP to carry the load in side friction only. The procedure has been adopted to address the load transfer characteristics of the relatively thin elements (when compared to drilled shafts for example), avoid issues with punching shear when tipping near the bottom of a calcareous bearing layer (e.g., Limestone), and to avoid uncertainty associated with the condition of the bottom of excavation, since neither manual (e.g., weighted tape, or Ding inspection device) nor visual (Shaft Inspection Device) monitoring can be performed. Consequently, the focus of this research effort concentrated on the development of LRFD resistance factors for side shear.</p> <p>Using the results of instrumented piles, and a segmental numerical analysis for un-instrumented load tests (i.e., no strain gauges embedded in the piles), the nominal side friction for soils (Cohesionless and Cohesive) and rock (Florida Limestone) was assessed for each site. For the calibration, various methods that make use of Standard Penetration Test (SPT) or unconfined compressive strength and splitting tension were analyzed and compared against the load test database. The bias, <math>\lambda</math>, and coefficient of Variation, CV of the measured/predicted side resistances were assessed, and the First Order Second Moment (FOSM) approach was followed to generate resistance factors for each design method. In the case of soils, the FHWA (1999) approaches gave the higher <math>\Phi</math>, and <math>\Phi/\lambda</math> values vs. newer methods. In the case of ACIPs in rock, design methods based on laboratory strength data (Ramos, Herrera, and FDOT) gave the higher <math>\Phi</math>, and <math>\Phi/\lambda</math> values vs. SPT N design methods.</p> <p>Given the limited number of fully instrumented piles, vertical movement of the piles, and distance of boring data from load tests, the report recommends that FDOT perform further static load tests on sites using ACIPs. It is expected that with the addition of more instrumented load tests and nearby boring data, that the LRFD <math>\Phi</math> for ACIPs could be further evaluated with Bayesian updating (Kwak, 2010).</p>					
17. Key Words Auger Cast Piles, LRFD Resistance Factors, Deep Foundations, Cast In situ Piles, ACIP, Design Methods, Florida Case Studies				18. Distribution Statement  No restrictions.	
19. Security Classif. (of this report) Unclassified		20. Security Classif. (of this page) Unclassified		21. No. of Pages: 164	
				22. Price	

**Form DOT F 1700.7 (8-72)**

Reproduction of completed page authorized

## ACKNOWLEDGMENTS

The researchers would like to thank the Florida Department of Transportation (FDOT) for the financial support to carry out this research, as well as the input of the FDOT central office's geotechnical engineers in the collection of site data. They would also like to thank the following firms for providing ACIP load test and boring data: Amec Foster Wheeler, Universal Sciences Engineering Inc., Langan Engineering & Environmental Services, Applied Foundation Tests Inc., DunkelBerger Engineering & Testing, Terracon, and Geosol Testing.

## EXECUTIVE SUMMARY

The focus of this research was the assessment of the Load and Resistance Factor Design (LRFD) resistance factors ( $\Phi$ ) for design methods used for Auger Cast In situ Piles (ACIPs) in Florida. Data from 78 pile load tests from 21 sites, identified by county, were collected in Florida. Sizes based on diameter were: 53-14 inch, 16-16 inch, 6-18 inch, 1-24 inch and 1-30 inch. Most of the piles were between 30 and 80 ft. in length. Forty-four of the test piles were in a layer of limestone with a layer of sand and/or clay above or below. Seven of the test piles were in sand, 4 in clay, 15 piles were in multiple layers of sand, clay or silt and 8 had no borings.

Inspection of the load tests revealed that the maximum pile head displacement was 1.2", but a majority (> 90%) of pile top displacements were in the range of 0.1" to 0.3". Since typical failure (e.g. Davisson, FHWA, etc.) has movements of 0.4" to 0.8" (e.g. FHWA – 5% diameter:  $0.05 \times 14" = 0.75"$ ), most, if not all, the load tests did not reach failure and were generally only loaded to twice the design load (ASTM D1143). Moreover, given the nominal pile head displacements (0.1" to 0.3") as well as typical pile lengths (40 to 60 ft), observed mobilized tip resistance was small compared to applied top load. For example, the maximum mobilized tip was 30% of top load and occurred for a pile embedded in soil with 1" of top movement. Generally, the average tip resistance for the database was less than 10% of the applied top load. For example, in south Florida, e.g. Miami ACIPs were embedded in multiple layers of limestone (Miami and Fort Thompson), had top movements < 0.3" and little if any tip resistance. Therefore, current practice suggests that most if not all ACIP piles are designed for side friction only (i.e. minimal tip). Consequently, the LRFD  $\Phi$  assessment for the project focused only on side friction of ACIPs.

In the case of ACIP installed in soils, the computed LRFD resistance values,  $\Phi$ , for side friction varied by method and soil type:

- For the FHWA (1999) method in sands,  $\Phi = 0.51$  and  $\Phi/\lambda = 0.5$  was found while Zelada (2000) had  $\Phi = 0.64$  and  $\Phi/\lambda = 0.5$ . The higher  $\Phi$  for Zelada vs. FHWA may be attributed to the more conservative predictions of Zelada ( $\lambda = 1.28$ ) vs. FHWA ( $\lambda = 1.03$ ); however both had the same coefficient of variation, CV (0.38), and  $\Phi/\lambda$ .
- Brown's method (2010) original and modified, (Over Consolidation Ratio,  $OCR < 10$ ,  $\phi < 40^\circ$ ) for sand had the lowest  $\Phi$ s for sand: 0.27 and 0.31 (modified) as well as  $\Phi/\lambda$ : 0.30 and 0.31 (modified). The reduced values are due to the high CVs (0.61 and 0.60 - modified) which were attributed to the estimation of OCR and  $\phi$  from multiple borings (mean estimate) at large distances.
- In the case of clays, the FHWA (1999) method had a  $\Phi = 0.83$  and  $\Phi/\lambda = 0.53$ . The high  $\Phi$  may be attributed to the high bias (1.57), suggesting the method is conservative; however the  $\Phi/\lambda$  is similar to the sand methods. Also, the clay dataset considered the Duval Marls (USCS – CH); only a 6% change in results was observed if the data set was removed.

In the case of ACIPs installed in Florida Limestone, the LRFD resistance values,  $\Phi$ , varied by method and rock formation:

- For Miami Limestone, only one method had an LRFD  $\Phi$  above 0.5 (Ramos,  $\Phi = 0.55$ ). In addition, the more efficient methods (i.e., higher  $\Phi/\lambda$ ) were based on laboratory rock strength approaches ( $0.4 < \Phi < 0.55$ , and  $0.40 < \Phi/\lambda < 0.56$ ) versus Standard Penetration Test, SPT, methods ( $0.14 < \Phi < 0.22$ , and  $0.19 < \Phi/\lambda < 0.38$ ).



Besides Ramos method the following other rock strength methods gave reasonable values: Herrera ( $\Phi = 0.48$  and  $\Phi/\lambda = 0.56$ ), FDOT ( $\Phi = 0.47$  and  $\Phi/\lambda = 0.45$ ), Carter ( $\Phi = 0.45$  and  $\Phi/\lambda = 0.42$ ), Reese ( $\Phi = 0.46$  and  $\Phi/\lambda = 0.41$ )

- In the case of Fort Thompson Limestone, one method had an LRFD  $\Phi$  above 0.5 (Carter,  $\Phi = 0.55$ ). Like the Miami Limestone, the more efficient methods for Fort Thompson were based on laboratory rock strength approaches ( $0.40 < \Phi < 0.55$ , and  $0.48 < \Phi/\lambda < 0.66$ ) versus SPT methods ( $0.13 < \Phi < 0.33$ , and  $30 < \Phi/\lambda < 51$ ). Besides Carter's method, the following other rock strength methods gave reasonable values: FDOT ( $\Phi = 0.49$  and  $\Phi/\lambda = 0.58$ ), Herrera ( $\Phi = 0.55$  and  $\Phi/\lambda = 0.55$ ), Horvath ( $\Phi = 0.45$  and  $\Phi/\lambda = 0.48$ ), Reese ( $\Phi = 0.42$  and  $\Phi/\lambda = 0.38$ )

All of the ACIP and site boring data collected was limited by: 1) number of fully instrumented pile load tests, 2) vertical movements of the piles tested, 3) number of rock formations piles were located in and 4) distance of boring, and laboratory data from pile load test. For instance, only 16 piles were monitored along their length, requiring the use of segmental modeling approach to estimate nominal skin friction. In addition, since most borings were greater than 50 ft from the load test, only a site mean for both measured and predicted could be determined. Two rock formations, Miami (with 2 values from Anastasia, similar resistances) and Fort Thompson were evaluated. Four values from North Florida (Ocala) were recorded, but not evaluated (insufficient number). Consequently, it is recommended that static load tests be performed on FDOT projects employing ACIPs to improve current and future designs. The selection of number of load tests should be dependent on site variability. All tested piles should be instrumented along their length to separate out skin and tip resistance.

## TABLE OF CONTENTS

	<u>page</u>
DISCLAIMER.....	ii
SI (MODERN METRIC) CONVERSION FACTORS (from FHWA) .....	iii
EXECUTIVE SUMMARY .....	vii
1 INTRODUCTION .....	1
1.1 Background.....	1
1.2 Objective and Supporting Tasks.....	2
1.2.1 Task 1 – Letter of request for ACIP data .....	2
1.2.2 Task 2 – Review of current design methods for ACIPs .....	3
1.2.3 Task 3 – Evaluation of ACIP Design Methods and LRFD $\Phi$ Assessment .....	3
1.2.4 Task 4 – Recommendations for design and minimum number of load tests.....	4
1.2.5 Task 5 – Final Report and Recommendations.....	5
2 ACIP DATA .....	6
2.1 Request for Data .....	6
2.1.1 Data request letter.....	6
2.1.2 Data request letter recipients .....	7
2.2 General Description of ACIP Data Received.....	10
2.3 Florida Geology by County for ACIPs.....	13
2.3.1 Alachua County .....	13
2.3.3 Broward County .....	14
2.3.4 Hillsborough County .....	15
2.3.5 Nassau County.....	15
2.3.6 Santa Rosa County .....	16
2.3.7 Palm Beach County .....	16
2.3.8 Miami Dade County .....	17
3 ACIP DESIGN METHODS .....	18
3.1 Background.....	18
3.2 Cohesionless Soils .....	18
3.3 Cohesive Soils .....	27
3.4 ACIPs in Weak Rock or IGM.....	31

3.5 ACIPs in Competent Rock and Limestone.....	34
4 ESTIMATION OF NOMINAL RESISTANCE OF ACIPs FROM LOAD TESTS .....	39
4.1 Segmental Approach for Estimating Resistance .....	39
4.2 Estimation of Nominal Resistance of ACIPs with Instrumentation .....	43
4.2.1 Alachua.....	43
4.2.2 Broward .....	50
4.2.3 Hillsborough .....	53
4.2.4 Nassau.....	65
4.2.5 Santa Rosa .....	71
4.3 Estimated Nominal Resistance of Miami Dade ACIPs .....	74
4.4 Estimated Nominal Resistance of All ACIPs in Florida .....	83
5 PREDICTED SIDE FRICTION OF ACIPs IN FLORIDA .....	88
5.1 Background.....	88
5.2 Predicted Ultimate Unit Skin Friction of Limestone.....	92
5.3 Predicted Ultimate Unit Skin Friction for Cohesionless Soils .....	104
5.4 Predicted Ultimate Unit Skin Friction for Cohesive Soils .....	109
6 LRFD RESISTANCE FACTOR ASSESSMENT FOR ACIPs IN FLORIDA.....	112
6.1 Introduction .....	112
6.2 Assessing Segmental Method Uncertainty .....	112
6.3 LRFD Measured/Predicted Bias Assessment .....	116
6.3.1 Granular Soils .....	116
6.3.2 Cohesive Soils .....	116
6.3.3 Miami Limestone (Intermediate GeoMaterial, IGM).....	122
6.3.4 Fort Thompson Limestone .....	124
6.4 LRFD Resistance Factors .....	128
7 RECOMMENDATIONS FOR DESIGN AND SELECTION OF MINIMUM NUMBER OF LOAD TESTS PER SITE.....	134
7.1 Collected Load Test Data and Soil/Rock Data.....	134
7.2 Discussion of Design Methods Evaluated and Their Associated Bias & CVs.....	136
7.3 Discussion of LRFD Resistance Values for ACIPs in Florida.....	139

7.4 Discussion and Recommendations for the Selection of Minimum Number of Load Tests per Site .....	141
REFERENCES .....	143

## LIST OF TABLES

<u>Table</u>	<u>page</u>
Table 2.1 Recipients of the data request letter .....	9
Table 2.2 Summary of ACIP pile load test data .....	11
Table 3.1 ACIP pile design methods for cohesionless soil.....	22
Table 3.2 ACIP pile design methods for cohesive soil.....	29
Table 3.3 Joint modification factors for different RQD (FHWA, 2010) .....	32
Table 3.4 Drilled shaft design methods applicable to ACIP piles in rock or IGM.....	33
Table 3.5 Drilled shaft and ACIP pile design methods for rock.....	35
Table 4.1 Estimated nominal unit skin friction of ACIP piles in Florida.....	86
Table 5.1 Estimated undrained shear strength, $S_u$ , from SPT N (Aggour, 2002) .....	90
Table 5.2. Predicted unit skin friction for Miami Limestone .....	101
Table 5.3 Predicted unit skin friction for Fort Thompson Limestone .....	104
Table 5.4 Predicted unit skin frictions for ACIP piles in cohesionless soils in Florida .....	108
Table 5.5 Predicted unit skin frictions for ACIP piles in cohesive soils in Florida.....	111
Table 6.1 Measured and predicted loads on test pile segments in sand.....	113
Table 6.2 Measured and predicted loads on test pile segments in clay .....	114
Table 6.3 Measured and predicted loads on test pile segments in all soils.....	115
Table 6.4 Bias values of FHWA, Zelada, and Brown methods for ACIPs in granular soils.....	117
Table 6.5 Bias values of FHWA method for ACIP piles in clay .....	121
Table 6.6 Summary statistics of bias for prediction methods using rock strengths for Miami Limestone.....	126
Table 6.7 Summary statistics of bias for prediction methods using SPT N for Miami Limestone.....	126
Table 6.8 Summary statistics of bias for prediction methods using rock strengths for Fort Thompson Limestone.....	127

Table 6.9 Summary statistics of bias for prediction methods using SPT N for Fort Thompson Limestone.....	127
Table 6.10 Resistance factors for ACIP pile methods in sand and clay .....	130
Table 6.11 Resistance factors for ACIP pile methods based on $q_u$ for Miami Limestone .....	131
Table 6.12 Resistance factors for ACIP pile methods based on SPT N for Miami Limestone ...	132
Table 6.13 Resistance factors for ACIP pile methods based on $q_u$ for Fort Thompson Limestone.....	132
Table 6.14 Resistance factors for ACIP pile methods based on SPT N for Fort Thompson Limestone.....	133

## LIST OF FIGURES

<u>Figure</u>	<u>page</u>
Figure 2.1 ACIP piles data request letter .....	8
Figure 3.1 LPC method for unit side resistance for cohesionless soils (FHWA, 2007) .....	21
Figure 3.2 LPC method for unit side resistance for cohesive soils (FHWA, 2007) .....	28
Figure 3.3 $\alpha$ versus $S_u$ for clay (Clemente et al., 2000).....	28
Figure 3.4 $\alpha$ versus $q_u$ for cohesive IGM.....	32
Figure 4.1 Idealized segmental model for ACIP piles.....	40
Figure 4.2 a. Normalized unit skin and tip resistance for sand, FB-Deep (FHWA 1998).....	41
Figure 4.2 b. Normalized unit skin and tip Resistance for clay, FB-Deep (FHWA 1998).....	41
Figure 4.2 c. Normalized unit skin resistance for limestone, FB-Deep (2010) .....	42
Figure 4.2 d. Net unit bearing stress, $q_b$ , for limestone, FB-Deep (FHWA, 2009).....	42
Figure 4.3 Measured and estimated load vs. displacement of Alachua 2 TP-5 .....	44
Figure 4.4 Mobilized unit side and tip resistance for 3 segments of Alachua 2 TP-5 .....	44
Figure 4.5 Distribution of estimated and measured pile forces in Alachua 2 TP-5.....	45
Figure 4.6 Measured and estimated load vs. displacement of Alachua 5 TP-1 .....	46
Figure 4.7 Mobilized unit side and tip resistance for 3 segments of Alachua 5 TP-1 .....	47
Figure 4.8 Distribution of estimated and measured pile forces in Alachua 5 TP-1.....	47
Figure 4.9 Measured and estimated load vs. displacement of Alachua 5 TP-2 .....	48
Figure 4.10 Mobilized unit side and tip resistance for 3 segments of Alachua 5 TP-2 .....	49
Figure 4.11 Distribution of estimated and measured pile forces in Alachua 5 TP-2.....	50
Figure 4.12 Measured and estimated load vs. displacement of Broward 1 TP-1 .....	51
Figure 4.13 Mobilized unit side and tip resistance for 3 segments of Broward 1 TP-1 .....	52
Figure 4.14 Distribution of estimated and measured pile forces in Broward 1 TP-1 .....	53
Figure 4.15 Measured and estimated load vs. displacement of Hillsborough 3 TP2.....	54

Figure 4.16 Mobilized unit side and tip resistance for 3 segments of Hillsborough 3 TP2.....	55
Figure 4.17 Distribution of estimated and measured pile forces in Hillsborough 3 TP2 .....	56
Figure 4.18 Measured and estimated load vs. displacement of Hillsborough 3 TP3.....	57
Figure 4.19 Mobilized unit side and tip resistance for 3 segments of Hillsborough 3 TP3.....	58
Figure 4.20 Distribution of estimated and measured pile forces in Hillsborough 3 TP3 .....	59
Figure 4.21 Measured and estimated load vs. displacement of Hillsborough 3 TP4.....	60
Figure 4.22 Mobilized unit side and tip resistance for 3 segments of Hillsborough 3 TP4.....	61
Figure 4.23 Distribution of estimated and measured pile forces in Hillsborough 3 TP4 .....	62
Figure 4.24 Measured and estimated load vs. displacement of Hillsborough 3 TP5.....	63
Figure 4.25 Mobilized unit side and tip resistance for 3 segments of Hillsborough 3 TP5.....	64
Figure 4.26 Distribution of estimated and measured pile forces in Hillsborough 3 TP5 .....	65
Figure 4.27 Measured and estimated load vs. displacement of Nassau 1 TP14 .....	66
Figure 4.28 Mobilized unit side and tip resistance for 3 segments of Nassau 1 TP14 .....	67
Figure 4.29 Distribution of estimated and measured pile forces in Nassau 1 TP14.....	68
Figure 4.30 Measured and estimated load vs. displacement of Nassau 3 TP-1.....	69
Figure 4.31 Mobilized unit side and tip resistance for 3 segments of Nassau 3 TP-1.....	70
Figure 4.32 Distribution of estimated and measured pile forces in Nassau 3 TP-1.....	71
Figure 4.33 Measured and estimated load vs. displacement of Santa Rosa 1 TP-1 .....	72
Figure 4.34 Mobilized unit side and tip resistance for 3 segments of Santa Rosa 1 TP-1 .....	73
Figure 4.35 Distribution of estimated and measured pile forces in Santa Rosa 1 TP-1 .....	74
Figure 4.36 Measured and estimated load vs. displacement of Miami Dade 6 TP-1 .....	75
Figure 4.37 Mobilized unit side and tip resistance for 3 segments of Miami Dade 6 TP-1 .....	75
Figure 4.38 Measured and estimated load vs. displacement of Miami Dade 6 TP-6 .....	76
Figure 4.39 Mobilized unit side and tip resistance for 3 segments of Miami Dade 6 TP-6 .....	76
Figure 4.40 Measured and estimated load vs. displacement of Miami Dade 6 TP-10 .....	77



Figure 4.41 Mobilized unit side and tip resistance for 3 segments of Miami Dade 6 TP-10 .....	77
Figure 4.42 Measured and estimated load vs. displacement of Miami Dade 6 TP-13 .....	78
Figure 4.43 Mobilized unit side and tip resistance for 3 segments of Miami Dade 6 TP-13 .....	78
Figure 4.44 Measured and estimated load vs. displacement of Miami Dade 6 TP-15 .....	79
Figure 4.45 Mobilized unit side and tip resistance for 3 segments of Miami Dade 6 TP-15 .....	79
Figure 4.46 Measured and estimated load vs. displacement of Miami Dade 6 TP-19 .....	80
Figure 4.47 Mobilized unit side and tip resistance for 3 segments of Miami Dade 6 TP-19 .....	80
Figure 4.48 Measured and estimated load vs. displacement of Miami Dade 6 TP-24 .....	81
Figure 4.49 Mobilized unit side and tip resistance for 3 segments of Miami Dade 6 TP-19 .....	81
Figure 4.50 Measured and estimated load vs. displacement of Miami Dade 6 TP-26 .....	82
Figure 4.51 Mobilized unit side and tip resistance for 3 segments of Miami Dade 6 TP-26 .....	82
Figure 5.1 Undrained shear strength vs. SPT N, Sowers, 1979.....	89
Figure 5.2 SPT N vs. unconfined compressive strength, $q_u$ ( $S_u = q_u / 2$ ) (NAVFAC, 1982).....	90
Figure 5.3 Measured and estimated unconfined compressive strength, $q_u$ ( $S_u = q_u / 2$ ) vs. SPT N.....	91
Figure 5.4 Line sections 1 through 7 of Metro Dade Rapid Transit Project (Law Engineering, 1978).....	93
Figure 5.5 Geological Profile of Miami Stratigraphy (recreated from Prieto, 1981) .....	94
Figure 5.6 Frequency distribution of $q_u$ for Miami Limestone .....	96
Figure 5.7 Frequency distribution of split tension, $q_t$ for Miami Limestone.....	96
Figure 5.8 Frequency distribution of $q_u$ for Fort Thompson Limestone .....	97
Figure 5.9 Frequency distribution of split tension, $q_t$ , for Fort Thompson Limestone.....	98
Figure 5.10 Frequency distribution SPT N values for Miami Limestone.....	99
Figure 5.11 Tamiami Canal Bridge Replacement and Relocation, Geosol Geotechnical Reports (2008, 2014) .....	99
Figure 5.12 Frequency distribution SPT N values for Fort Thompson Limestone .....	100

Figure 5.13 Predicted FHWA unit skin friction Hillsborough-3 using all borings .....	105
Figure 5.14 Predicted Brown unit skin friction Hillsborough-3 using all borings .....	105
Figure 5.15 Predicted FHWA unit skin friction Hillsborough-3, $\pm 2$ standard deviation .....	106
Figure 5.16 Predicted Brown unit skin friction Hillsborough-3, $\pm 2$ standard deviation .....	106
Figure 5.17 Estimated undrained shear strength, $S_u$ , Alachua-2, $\pm 2$ standard deviations.....	109
Figure 5.18 FHWA estimated unit skin friction, Alachua-2, $\pm 2$ standard deviations .....	110
Figure 5.19 FHWA and Zelada sand method bias distributions .....	120
Figure 5.20 FHWA clay model bias distribution.....	120

## CHAPTER 1 INTRODUCTION

### **1.1 Background**

Augercast In Place Piles (ACIP) are deep foundation elements that are drilled with a hollow stem continuous flight auger, and subsequently grouted through the stem from a port at the tip of the auger. A minimum head of grout is injected into the hole and maintained as the rotating auger is removed from the soil. After complete grout placement, steel reinforcement is then lowered into the fluid grout. Under this construction approach, the borehole is never left open as with drilled shafts, eliminating the need for stabilizing slurry or steel casing. This foundation type is particularly well suited for Limestone sockets where it develops a mechanical bond with the rough surface of the drilled hole resulting in significant side shear resistance.

ACIP elements have performed successfully in Florida in the private sector for many years and are used as foundations for of high-rise buildings, elevated rail systems, hospitals and other settlement sensitive structures. Some of the benefits that come from the use of ACIP are typically faster installation time when compared to driven piles and drilled shafts, low noise and minor vibration signatures, as well as the possibility of construction in low headroom areas.

Currently, ACIP are used by the Florida Department of Transportation (FDOT) as foundation elements for sound barrier walls and are designed using allowable stress design methods. Reluctance to implement this foundation type for bridge structures in the past came from the inconsistent practices in installation quality control, where inspection was more of an art than a science, and the lack of resistance factors. The fact that bridge foundations typically consist of a small number of elements, particularly when compared with high-rise structures where ACIP have historically performed well, also worked against its selection for bridge support. With the advent of modern technology for ACIP installation and the ability to monitor

torque, crowd, depth, auger rotational speed, and grout intake into the bored hole, the installation quality control issue can be addressed.

Considering the advancements in monitoring, proven performance, as well as potential benefits to the State (cost savings due to accelerated construction and reduced vibration related claims), it was decided that formal evaluation of ACIP design methods including developing resistance factors for Load and Resistance Factor Design (LRFD) was warranted.

## **1.2 Objective and Supporting Tasks**

The primary objectives of this project were to:

- Collect load test results on ACIP foundations and incorporate them into the deep foundation database;
- Evaluate design methods versus static load test results (e.g. FDOT, alpha, beta, Ramos, Brown, etc.);
- Analyze and reduce the data to obtain the required parameters for calibration of resistance factors;
- Develop resistance factors for various design methods;
- Provide recommendations for design, along with examples for different soil types;
- Provide recommendations for evaluation of the required number of load tests per site.

To accomplish these objectives, the following four tasks with associated deliverables were completed.

### **1.2.1 Task 1 – Letter of request for ACIP data**

At the onset of the project, the researchers in collaboration with FDOT engineers were to distribute to contractors, trade organizations, consultants, and other DOT entities a letter

explaining the need for the project, the benefits to the State and a detailed description of the requested information (e.g. soil borings, installation records, static load test reports, etc.). To protect the anonymity of the owner, contractor, etc. all specific locale information was to be redacted. Prior to the letter dissemination, both the letter and distribution list had to be sent to the FDOT Project Manager for approval.

### **1.2.2 Task 2 – Review of current design methods for ACIPs**

Prior to any design evaluations, a detailed review of existing and new design methods for ACIP was to be undertaken. This included methods for estimating both side friction and end bearing resistance based on in situ tests (SPT, CPT or other) as well as other methods for assessing soil parameters (e.g. undrained shear strength -  $S_u$ , angle of internal friction,  $\phi$ ). The review should consider both the open literature as well as government agencies. For instance, FHWA-HIF-07-03 (GEC No. 8): Design and Construction of Continuous Flight Auger Piles (2007) identified multiple design methods for soil, as well intermediate geomaterials and rock for ACIPs.

Since it is anticipated that data from 40 to 60 load tests and associated soil & laboratory data would be collected, all data had to be digitized (e.g. boring log, load vs. settlement, etc.) and entered into Excel spreadsheets for uploading into the FDOT database. All of the digital data was used by MATLAB codes for design analyses, as well as Load and Resistance Factored Design (LRFD) assessments.

### **1.2.3 Task 3 – Evaluation of ACIP Design Methods and LRFD $\Phi$ Assessment**

Based on the review of the current literature, the design approaches applicable to Florida were to be selected with input from FDOT engineers. For the selection, not only soil and rock types, but methods which employ existing in situ and laboratory data evaluation, as well methods

which distinguish skin vs. tip or total resistance. Summary statistics (mean bias,  $\lambda$  – measured/predicted, standard deviation of bias) and LRFD resistance factors,  $\Phi$ , for individual method as well as their efficiency ( $\Phi/\lambda$  -McVay et al., 2000) were to be evaluated. Note, the efficiency identifies the percentage of measured resistance (e.g.  $R_{\text{measured}}$  – Davisson Capacity) available for design ( $R_{\text{Design}}$ ). The efficiency ( $\Phi/\lambda$ ) is obtained by solving for nominal resistance,  $R_{\text{nominal}}$  (i.e. predicted) from the bias ( $\lambda = \frac{R_{\text{measured}}}{R_{\text{nominal}}}$ ) and substituting it into the LRFD design equation ( $R_{\text{Design}} = \Phi R_{\text{nominal}}$ ) for the nominal resistance (predicted),  $R_{\text{nominal}}$  to obtain design resistance in terms ( $R_{\text{Design}} = \frac{\Phi}{\lambda} R_{\text{measured}}$ ) of the measured resistance (e.g. Davisson).

A number of the methods under consideration were developed for specific soil types (e.g. sand vs. clay), or rock formation (e.g. Miami vs. Fort Thompson Limestone). Many also required the evaluation of soil property/parameters (e.g. soil strength:  $\phi$  and  $S_u$ , unit weight, etc.). Soil and rock property/parameters were either available from laboratory testing or were evaluated from in situ testing.

#### **1.2.4 Task 4 – Recommendations for design and minimum number of load tests**

Using the both the LRFD resistance factors,  $\Phi$ , as well as efficiency ( $\Phi/\lambda$  -McVay et al., 2000), design methods were to be recommended for specific soil and rock types. Impacting the development/evaluation of LRFD resistance factors are location of in situ data relative to the load test as well as specific Florida soils/rocks: cemented soils – e.g. marl, and various rock formations (Miami, Suwannee, Ocala, Anastasia, etc.). In the case of borings greater than 100 ft from the load test, then the mean site predictions based on the whole site boring or laboratory data was compared to the mean measured prediction as suggested in FDOT report BD-545 RPWO#76, Modification of LRFD Resistance Factors Based on Site Variability. Generally, this

results in much higher variability and CVs as well as lower LRFD resistance values than with the use of a number of borings within 50ft of the load test. The task was also to: 1) recommend number of load tests on a site for ACIPs; and 2) methods to improve current and future designs of ACIPs.

### **1.2.5 Task 5 – Final Report and Recommendations**

The final task involves reporting on the data collected for the ACIP design evaluation and LRFD resistance assessment, as well as recommendation on number of load tests per site for ACIPs. For the design method evaluation, identification of all input parameters (e.g. undrained strength,  $S_u$ , angle of internal friction,  $\phi$ ) along with measured and predicted resistances on site by site basis should be identified. For the LRFD assessment, both the mean bias (measured/predicted resistance) and coefficient of variation, CV, of bias will be presented along with LRFD resistance factors for each design method will be identified. Finally, using LRFD  $\phi$  values, and efficiency ( $\Phi/\lambda$  -McVay et al., 2000), comparison of the design methods along with recommendations on future load testing of ACIPs will be presented.

## CHAPTER 2 ACIP DATA

### 2.1 Request for Data

To collect data for the project, a request letter was to be sent to geotechnical engineering consultant firms, deep foundation contractors and department of transportation offices in Florida. The purpose of the letter was to inform the recipient of the Florida Department of Transportation (FDOT) and the University of Florida's (UF) project to develop resistance factors for Load and Resistance Factor Design (LRFD) for Augercast In Place (ACIP) piles, as well as a request all the available data for each site. The letter identified the benefits to the State and as well as a detailed description of the requested information (e.g., soil boring records, pile installation records, load test reports). Specific information about the process of transferring the data and contact persons had to be included as well.

#### 2.1.1 Data request letter

Shown in Figure 2.1 is the final letter that was written with consultation from the FDOT project manager and reviewed by FDOT engineers. The letter is specific in regards to the data that is requested (Figure 2.1). For example, in situ and lab data from the site exploration, the locations of the load test(s) and borings relative to the load test, the methods used to predict the pile capacity and assess measured capacity, load test results in terms of tip, skin or total load displacement measured, pile installation logs, records of pile integrity tests, certification letters, cost estimates (load test and pile), and any pertinent information.

Pile capacity prediction methods use in situ data (e.g., SPT, CPT, etc.) and lab data (e.g., friction angle, undrained strength, etc.). The quality/quantity of this data influences the resistance bias  $\left(i.e. \frac{measured}{predicted}\right)$  and coefficient of variation, CV, which are used to calculate the resistance



factor. The load test results are required in order to assess the measured resistance which is compared to the predicted resistance, i.e. the bias of each pile tested. The locations of the borings relative to the load test are important in estimating the spatial component (spatial variability) of the CV of resistance. Pile installation records provide final diameter and length of the pile which will be used to predict capacity. In some cases where monitoring equipment is used during pile installation, estimates of the torque, crowd, and penetration rate could be useful in making posterior predictions of pile capacity (e.g., increasing pile length).

The letter informs the recipient that the projects will only be identified by county to guarantee that client information is confidential.

Data transfer was addressed in two possible ways: 1) hardcopies could be mailed or retrieved at expense to UF and 2) electronic files (e.g., pdf) could be transferred via a secure FTP site hosted by UF.

The letter closes with the contact information for the Co-PI (Dr. Scott Wasman) and the Project Manager (Mr. Rodrigo Herrera).

### **2.1.2 Data request letter recipients**

Table 2.1 is a list of recipients of the request letter. The list contains 63 consultants and contractors in Florida and 5 from other states (Georgia, Maryland, Oregon, Tennessee, and Texas). Additionally, all 7 district offices of the FDOT received the data request letter as well.



College of Engineering  
Engineering School of Sustainable Infrastructure and Environment

365 Weil Hall  
PO Box 116580  
Gainesville, FL 32611-6580  
352-392-9537 Phone  
352-392-3394 Fax  
[www.essie.ufl.edu](http://www.essie.ufl.edu)

Dear Madam/Sir

The Florida Department of Transportation is partnered with the University of Florida in a study to calibrate geotechnical Load and Resistance Factor Design (LRFD) resistance factors for Auger Cast-In-Place (ACIP) Piles for FDOT design. As part of the project, we are collecting any of the following data from all possible sources for ACIP type foundations:

- 1) Soil exploration data [in-situ (SPT, CPT, etc.), and laboratory results: soil classification and rock strength if available];
- 2) Load test and boring locations relative to pile load tests;
- 3) Pile resistance prediction method, and capacity assessment used (Davisson, 3% diameter, etc.);
- 4) Load test results (static or dynamic) and any tip, skin friction and total load displacement data. Data does not need to be limited to projects in Florida;
- 5) Installation logs for the piles tested;
- 6) Results of any integrity testing of load tested piles;
- 7) Sample certification or acceptance letters;
- 8) Load test and foundation cost estimates;
- 9) Additional pertinent information.

All project sites will be identified by the county and a number; information identifying private owners or exact addresses is not requested and will not be disclosed if included.

Success of the project depends on collecting enough information to develop a statistically significant database from which to calibrate resistance factors. As such, we kindly request the relevant data of projects your office has been involved that used the ACIP pile and where a load test has been performed. In order to transfer the data, a FTP website, hosted by the University of Florida, will be made available for transfer of electronic files. And for hardcopy files, arrangements can be made at no expense to your business.

Following receipt of this letter, either the primary researcher on the project, Scott Wasman, or the project manager, Rodrigo Herrera, will contact you regarding any questions you might have. If you have any questions beforehand, please do not hesitate to contact either one at:

Primary Researcher: Scott Wasman, Ph.D., (352) 273-4609, [swasman@ufl.edu](mailto:swasman@ufl.edu)

Project Manager: Rodrigo Herrera, P.E., (850) 414-4377, [Rodrigo.Herrera@dot.state.fl.us](mailto:Rodrigo.Herrera@dot.state.fl.us)

We greatly appreciate your time and participation.

*The Foundation for The Gator Nation*  
An Equal Opportunity Institution

Figure 2.1 ACIP piles data request letter

Table 2.1 Recipients of the data request letter

Amdrill	Geotechnical & Environmental Consultants
A. H. Beck Foundation Company	Geo-technologies, Inc.
AMEC	GRL
Andreyev Engineering, Inc.	GSE Engineering & Consulting
Antillian Engineering Assoc.	Highway Technologies
Applied Foundation Testing (AFT)	HP Engineering
Ardaman & Associates	Independent Drilling, Inc.
AREHNA Engineering, Inc.	In-situ
AWK	Langan
Bauer Foundations	legacy engineering
Bechtol Engineering	Loadtest
Berkel and Co.	Long and Associates
Blue Marlin	MACTEC
Bob's Barricades	MC2
Cajun USA	Mehta Engineering
Cech Bro Consulting	Meskel and Associates Engineering
Cedar Engineering Consultants, LLC.	Moretrench
Central Testing Laboratory	Nadic Engineering
Clark Foundations	Oregon State University
Dan Brown and Associates	Page One Consultants, Inc.
Ebsary Foundations	Pi Consulting Services, LLC.
ECS	Pragma Consulting, LLC
Elipsis Engineering	PSI
Ellis & Associates	Radise International
FDOT District 1 Office	RS&H CS
FDOT District 2 Office	Saliba Engineering
FDOT District 3 Office	Sunbelt
FDOT District 4 Office	TCP
FDOT District 5 Office	Terracon
FDOT District 6 Office	Test Lab Inc.
FDOT District 7 Office	Tierra
Foundation & Geotechnical Engineering	Tierra South Florida
Fugro Consultants, Inc.	Universal Engineering Sciences
Gannett Fleming	URS
GCI	William Earth Sciences
GCME	Wolf Technologies, Inc.
Geosol	

## **2.2 General Description of ACIP Data Received**

Data of 78 test piles from 21 sites in Florida were collected. Shown in Table 2.2 is the general description of the data. The first column identifies the County, and the second column identifies the individual sites, e.g. Alachua 1, 2, etc., followed by the load test number at each site, e.g. TP-2, TP-3, etc. The next columns identify general soil or rock, pile diameter, embedment length, available instrumentation (i.e. separation of side resistance along length), maximum top displacement of the pile during the static load test, and data provider.

Evident from Table 2.2, the piles diameters varied from 14 to 30 inches (53 - 14 inch piles, 17 - 16 inch piles, 6 - 18 inch piles, 1 - 24 inch pile, and 1 - 30 inch pile). Most of the test piles were between 20 and 68 feet in length, with three piles greater than 100 ft and one pile only 15 feet in length. Forty-four of the test piles were in a layer of limestone with a layer of sand and/or clay above or below. Seven of the test piles were in sand, 4 in clay, 15 piles were in multiple layers of sand, clay or silt and 8 had no borings. Sixteen of the top down compression loaded piles were instrumented along their length from which skin friction distribution measurements as well as T-Z curves were available. In situ and/or lab test data was available for with the exception of nine piles. The in situ data reported was generally SPT blow counts with lab testing for soil classification. One site (Santa Rosa) had conventional CPT sounding, and another Miami site, had dynamic cone data. The Miami sites had limestone with measured rock strength (unconfined compressive strength,  $q_u$ , and split tensile strength,  $q_t$ ) for both the Miami and Fort Thompson formations.

Table 2.2 Summary of ACIP pile load test data

Location	Project Name	Soil Type	Diameter (in)	Embedded Length (ft)	Test Type	Number of Load Test	Water Table Depth (ft)	Instrumentation	Peak Displacement Load Test (in)	Data Provider
Alachua	Alachua-1 TP-2	Clay & IGM	16	64	Static	14	29	Load-Deflection	0.085	Universal Sciences Engineering, Inc.
	Alachua-1 TP-3	Clay & IGM	16	64	Static		31	Load-Deflection	0.125	
	Alachua-1 TP-4	Clay & IGM	16	64	Static		26	Load-Deflection	0.183	
	Alachua-1 TP-5	Clay & IGM	16	64	Static		28	Load-Deflection	0.219	
	Alachua-2 TP-1	Clay	14	42	Static		4.5	Load-Deflection	0.288	
	Alachua-2 TP-2	Clay	14	42	Static		5	Load-Deflection	0.325	
	Alachua-2 TP-3	Clay	14	42	Static		6.5	Load-Deflection	0.295	
	Alachua-2 TP-5	Clay	14	42	Static		5	T-Z & Load-Defl.	0.341	
	Alachua-2 TP-XX-1	No Boring	14	42	Static		None	Load-Deflection	0.777	
	Alachua-2 TP-XX-2	No Boring	14	42	Static		None	Load-Deflection	0.460	
	Alachua-3 TP-1	Clay, Sand & IGM	14	15	Static		12	Load-Deflection	0.549	
	Alachua-5 TP-1	Sand & Clay	14	65	Static		6	T-Z & Load-Defl.	0.600	
	Alachua-5 TP-2	Sand & Clay	14	65	Static		6	T-Z & Load-Defl.	1.000	
	Alachua-5 TP-3	Sand & Clay	14	65	Tension		6	T-Z & Load-Defl.	0.088	
Broward	Broward-1 TP-1	Sand & IGM	18	102	Static	4	5.7	T-Z & Load-Defl.	0.344	Nodarse, A Terracon Company
	Broward-1 TP-2	Sand & IGM	18	102	Tension		5.7	T-Z & Load-Defl.	0.009	
	Broward-1 TP-5	Sand & IGM	30	140	Osterberg		1	O-Cell	0.400	Universal Sciences Engineering, Inc.
	Broward-2 TP-1	Sand & IGM	14	40	Static		None	Load-Deflection	0.350	
Duval	Duval-1 TP 1-2	Sand, Marl & Clay	16	55	Static	4	4.5	Load-Deflection	0.289	Langan Engineering & Environmental Services
	Duval-1 TP 2-2	Sand, Marl & Clay	16	54	Static		4.5	Load-Deflection	0.397	
	Duval-1 TP 3-2	Sand, Marl & Clay	18	54	Tension		4.5	Load-Deflection	0.192	
	Duval-1 TP 3-3	Sand, Marl & Clay	16	54	Static		4.5	Load-Deflection	0.267	
Hollywood	Hollywood-1 TP-1	No Boring	14	50	Static	3	No Boring	Load-Deflection	0.340	DunkelBerger Engineering & Testing
	Hollywood-2 TP-1	No Boring	14	48	Static		No Boring	T-Z & Load-Defl.	0.200	
	Hollywood-2 TP-2	No Boring	14	48	Tension		No Boring	T-Z & Load-Defl.	0.032	
Hillsborough	Hillsborough-2 TP-1	No Boring	14	40	Static	6	None	Load-Deflection	0.079	Applied Foundation Test, Inc.
	Hillsborough-3 TP-1	Sand and Clay	16	60	Static		5.2	T-Z & Load-Defl.	0.548	
	Hillsborough-3 TP-2	Sand and Clay	16	60	Statnamic		5.2	T-Z & Load-Defl.	0.939	
	Hillsborough-3 TP-3	Sand and Clay	16	60	Statnamic		5	T-Z & Load-Defl.	1.176	
	Hillsborough-3 TP-4	Sand and Clay	16	60	Statnamic		5	T-Z & Load-Defl.	0.760	
	Hillsborough-3 TP-5	Sand and Clay	16	67.4	Statnamic		4	T-Z & Load-Defl.	0.653	
Nassau	Nassau-1 TP14	Sand	14	60	Static	3	3.8	T-Z & Load-Defl.	0.385	Amec Foster Wheeler Enviroment & Infrastructure
	Nassau-2 TP-1	Sand	16	39	Static		3	Load-Deflection	0.300	
	Nassua-3 TP-1	Sand	14	65	Static		5	T-Z & Load-Defl.	0.200	
Palm Beach	Palm Beach-1 TP-9	No Boring	16	61	Static	2	None	T-Z & Load-Defl.	0.113	DunkelBerger Engineering & Testing
	Palm Beach-2 TP-8	No Boring	16	61	Static		None	T-Z & Load-Defl.	0.188	
Polk	Polk-1	Clay, Silt & Sand	18	65	Static	1	8.5	Load-Deflection	0.360	Ardaman & Associates, Inc
Santa Rosa	Santa Rosa-1 TP-1	Sand, Cayey Sand	24	47	Static	1	2.5	T-Z & Load-Defl.	0.465	
West Palm	West Palm-1 T2B	Sand	14	40	Tension	3	9	Load-Deflection	0.250	Universal Sciences Engineering, Inc.
	West Palm-1 T8	Sand	14	40	Tension		9	Load-Deflection	0.250	
	West Palm-1 T9B	Sand	14	40	Static		9	Load-Deflection	0.536	

Table 2.2 Summary of ACIP pile load test data (continued)

Location	Project Name	Soil Type	Diameter (in)	Embedded Length (ft)	Test Type	Number of Load Test	Water Table Depth (ft)	Instrumentation	Peak Displacement Load Test (in)	Data Provider
Miami Dade	Miami Dade-1 TP-1	IGM, Sand & FT Limestone	16	43	Static	37	5	Load-Deflection	0.343	Amec Foster Wheeler Enviroment & Infrastructure
	Miami Dade-1 TP-2	Sand & IGM	16	43	Tension		5	Load-Deflection	0.208	
	Miami Dade-5 TP-1	Sand & IGM	14	30	Static		(+) 2.5	Load-Deflection	0.148	
	Miami Dade-5 TP-2	Sand & IGM	14	30	Tension		(+) 2.5	Load-Deflection	0.270	
	Miami Dade-6 TP-1	IGM & Sand	14	25	Static		Not measured	Load-Deflection	0.183	
	Miami Dade-6 TP-2	IGM & Sand	14	40	Static		8	Load-Deflection	0.182	
	Miami Dade-6 TP-3	IGM & Sand	14	40	Static		8	Load-Deflection	0.303	
	Miami Dade-6 TP-5	IGM & Sand	14	40	Static		8	Load-Deflection	0.090	
	Miami Dade-6 TP-6	IGM, Sand & FT Limestone	14	40	Static		4	Load-Deflection	0.206	
	Miami Dade-6 TP-7	IGM & Sand	14	40	Static		Not measured	Load-Deflection	0.060	
	Miami Dade-6 TP-8	IGM & Sand	14	40	Static		Not measured	Load-Deflection	0.093	
	Miami Dade-6 TP-9	IGM & Sand	14	40	Static		Not measured	Load-Deflection	0.142	
	Miami Dade-6 TP-10	IGM & Sand	14	40	Static		Not measured	Load-Deflection	0.572	
	Miami Dade-6 TP-11	IGM & Sand	14	23	Static		5.5	Load-Deflection	0.073	
	Miami Dade-6 TP-12	IGM & Sand	14	23	Static		5.5	Load-Deflection	0.346	
	Miami Dade-6 TP-13	IGM, Sand & FT Limestone	14	50	Static		Not measured	Load-Deflection	0.072	
	Miami Dade-6 TP-14	IGM & Sand	14	58	Static		8	Load-Deflection	0.182	
	Miami Dade-6 TP-15	IGM & Sand	14	45	Static		7.5	Load-Deflection	0.119	
	Miami Dade-6 TP-16	IGM & Sand	14	25	Static		5.5	Load-Deflection	0.115	
	Miami Dade-6 TP-17	IGM & Sand	14	25	Static		5.5	Load-Deflection	0.135	
	Miami Dade-6 TP-18	Sand & IGM	14	20	Static		4	Load-Deflection	0.115	
	Miami Dade-6 TP-19	IGM, Sand & FT Limestone	14	55	Static		8	Load-Deflection	0.192	
	Miami Dade-6 TP-20	IGM & Sand	14	30	Static		9	Load-Deflection	0.091	
	Miami Dade-6 TP-21	IGM & Sand	14	46	Static		12	Load-Deflection	0.110	
	Miami Dade-6 TP-22	IGM & Sand	14	41	Static		12	Load-Deflection	0.058	
	Miami Dade-6 TP-23	Sand	14	58.5	Static		10.5	Load-Deflection	0.560	
	Miami Dade-6 TP-24	IGM & Sand	14	47	Static		4	Load-Deflection	0.182	
	Miami Dade-6 TP-25	IGM & Sand	14	56	Static		10	Load-Deflection	0.095	
	Miami Dade-6 TP-26	IGM, Sand & FT Limestone	14	57	Static		10	Load-Deflection	0.296	
	Miami Dade-6 TP-27	IGM, Sand & FT Limestone	14	47	Static		11	Load-Deflection	0.053	
	Miami Dade-6 TP-28	IGM, Sand & FT Limestone	14	65	Static		8	Load-Deflection	0.408	
	Miami Dade-6 TP-29	IGM, Sand & FT Limestone	14	56	Static		9	Load-Deflection	0.107	
	Miami Dade-6 TP-30	IGM, Sand & FT Limestone	14	56	Static		9	Load-Deflection	0.107	
	Miami Dade-6 TP-31	No Boring	14	44	Static		None	Load-Deflection	0.432	
	Miami Dade-7 TP-1	Sand & IGM	18	41	Static		4	Load-Deflection	0.064	
	Miami Dade-7 TP-2	Sand & IGM	18	41	Static		4	Load-Deflection	0.069	
	Miami Dade-8 TP-1	Sand & IGM	14	52	Static		1	Load-Deflection	0.300	
Total # of Test Piles						78	Total T-Z Curve	16		

## **2.3 Florida Geology by County for ACIPs**

A description of the geology of Florida by county or city where the piles are located is presented followed by general descriptions. Of interest are types of soil and rock as well as its vertical and horizontal variability.

### **2.3.1 Alachua County**

Alachua County is separated geomorphically into the Northern Highlands (Gainesville, Alachua, Santa Fe), Western Valley (Archer), Alachua Lake Cross Valley, Fairfield Hills, Central Valley and Brooksville Ridge (White 1970). The Northern Highlands (i.e. Gainesville, Alachua, etc.) is composed of siliciclastic sediments belonging to the Hawthorn Group (Miocene epoch), Cypresshead Formation (Pliocene epoch) and undifferentiated siliciclastic sediments (Pleistocene and Holocene epochs) that are often residuum from older sediments. The Miocene Hawthorn Group is a complex unit of interbedded and intermixed carbonates and siliciclastic, containing widely varying percentages of phosphate grains (Scott, 1988). The percentages of quartz sand, silt, clay, and carbonate exhibit a high degree of variability often over short distances both horizontally and vertically. The Hawthorn Group lies unconformably on the Ocala Limestone (Eocene) or, in rare instances, on isolated outliers of Suwannee Limestone (Oligocene). The phosphatic, clayey sediments of the Hawthorn Group occur under the Northern Highlands and the central valley in Alachua County. Throughout much of the area, it is covered by less than 20 feet of undifferentiated siliciclastic sediments. The Ocala Limestone which is white to buff colored, is very fossiliferous, karstic and ranges from poorly to well indurated packstone to grainstone material.

### **2.3.2 Duval County**

Jacksonville covers a large percentage of the county and is part of the Atlantic Coastal Plain physiographic province which encompasses a series of ancient marine terraces. The

natural sandy overburden soils of the Pleistocene epoch consist of interbedded layers of very loose to dense brown, brown and gray fine sands (USCS – SP), slightly clayey fine sands (SP-SC), and clayey fine sands (SC) which are associated with marine and estuarine deposits (Wolf 2004). Beneath the overburden soil deposits, a calcareous limestone formation (Pliocene and upper Miocene) of various depths is found. This limestone formation is typically highly variable in composition and cementation, containing zones of tan gray and brown calcareous clay, silt, and clayey fine sand as well as cemented sandy fossiliferous limestone. Standard Penetration Test N values range from single digits to well over 100 blows per foot. Beneath the limestone formation, the Hawthorn formation (locally termed Marl) of the Miocene Epoch is found with thickness ranging from 50 to 300 ft. Atterberg Limits testing of Marl indicates that it is classified as high plasticity clay (CH), Wolf 2004. SPT N values with the Marl range from upper 20's to well over 100 blows per foot. Beneath the Hawthorn formation resides the Ocala Limestone formation (Eocene Epoch) with deposits exceeding 350 ft thick, composed primarily of light colored, granular fossiliferous marine limestone.

### **2.3.3 Broward County**

Causaras (1985) reports a number of transects of Broward County's geology. Starting in the West (Everglades) traveling East along I-75 and then I-595 (Port Everglades Expressway) to the east coast (5 miles south of Fort Lauderdale), Causaras reports approximately 5 to 8 ft of fill, underlain by the Fort Thompson Formation with consists of layers of sand and limestone inclined (east to west) from 30ft to 60 until I-75 turns south (junction with I-595). East of I-75 and I-595 junction, the Fort Thompson formation is interfingered with the Anastasia formation (sand & limestone layers) until US 441. East of US 441 mostly Anastasia formation (sand and limestone layers) is encountered until I-95 (depths from 10 to 120 ft) with Pamlico Sand at the surface (5 - 15ft thick). On the same transect (I-595) east of I-95, the Anastasia formation is replaced by the



Miami formation (sand and limestone (10ft to 35ft depth), underlain by intersfingered Key Largo and Anastasia formations. Beneath the Fort Thompson and Anastasia Formations (east – west transect) is the Tamiami Formation which varies in depth from 120 ft to 240 ft.

#### **2.3.4 Hillsborough County**

The cities of Tampa and St. Petersburg are situated on the Gulf Coastal Lowlands (White 1970) or Pleistocene age terraces formed from dune fields. The terrace deposits were developed on sediments of the Peace River Formation in southern Hillsborough County, while in the northern part of the county, the terraces were developed on clayey residuum of the Hawthorn Group or locally directly on limestone of the Tampa Member of the Arcadia Formation. A large portion of the northwestern Hillsborough County is riddled with sinkholes due to the absence or thinning of the clayey residuum of the Hawthorn Group. In northeast part of the county, Suwannee Limestone is exposed at the surface (e.g. Hillsborough River bed). In all other parts of the county, the Suwannee is overlain by the Tampa Member of the Arcadia formation. The Arcadia Formation (Scott, 1984) consists in ascending order the Nocatee Member, The Tampa Member and unnamed upper member. The Nocatee Member consists of Tampa sand and clay unit and extends into southern and eastern Hillsborough County

#### **2.3.5 Nassau County**

Nassau County is located in north Florida is at the border between Georgia and Florida with towns of Boulogne, Callahan and Fernandina Beach. As identified by Watts (1991), Nassau County is covered with undifferentiated surficial material consisting of clay and sand layers that vary from 10 to 70 ft thickness. Beneath the surficial material are shell beds that vary from 10 to 50 ft, and then the Hawthorn Group (300 to 500 ft thick) consisting of interbedded sand, clay and carbonates. Throughout the Hawthorn Group sand-size grains of phosphate are common except in the some areas where the very top of the group consists of relatively thin clay and carbonate

beds that are non phosphatic to sparsely phosphatic. Underlying the Hawthorn Group is the Ocala Group consisting of predominately pure white limestone made up of shells of microscopic single celled animals (foraminifera) which are poorly cemented and very crumbly to well cemented and hard. The Ocala Group is approximately 300 ft thick over the whole county.

### **2.3.6 Santa Rosa County**

Santa Rosa County, located in northwest Florida is overlain with Pleistocene Terrace Deposits composed of light tan fine to coarse sand (less than 20ft thick). Underlying the terrace deposits is the Pleistocene Citronelle Formation (100ft thick) consisting of light yellowish brown to reddish brown poorly sorted sand with thick layers of clay and gravel. Logs and carbonates are present in pockets in the Citronelle Formation with fossils extremely scarce except near the coast where shell beds may be present. Underlying the Citronelle Formation is the Pensacola Clay (200 ft thick) and Chickasawhay Limestone Formation.

### **2.3.7 Palm Beach County**

Lithography, the county is underlain by the following formations: Pamlico Formation (Pleistocene), Anastasia Formation (Pleistocene), Fort Thompson Formation (Pleistocene), Caloosahatchee Formation (Pliocene-Pleistocene) and Tamiami Formation (Pliocene) (Miller, 1987). The Pamlico occurs at or near the surface throughout the county. It is generally quartz sand with shell occurring in bedded layers or disseminated throughout the sand. Other less common constituents include silts, clays and organic debris. The Anastasia Formation varies in composition from pure coquina to mixtures of sand, sandy limestone, sandstone and shell. Lateral changes in lithology are difficult to predict while vertical changes in lithology tend to follow a downward progression from unconsolidated sand and shell to calcareous sandstone to biogenic limestone and coquina (Shine et al, 1989). The upper part of the Anastasia Formation is contemporaneous with the Miami Limestone. The contact between these two formations is

gradational and occurs near the Palm Beach/Broward county border (Shine et al, 1989). The Fort Thompson formation is composed of sand, marl, shell marl, sandstone and limestone of fresh-water and marine origin (USGS). Both the Fort Thompson and Tamiami Formations are related to fluctuations of the water table accompanied by cementation with calcium carbonate (USGS). The lower part of the Anastasia is contemporaneous with the Fort Thompson Formation. This contact is also gradational and occurs in the south and western part of Palm Beach County.

### **2.3.8 Miami Dade County**

The highest elevation in the county is the Atlantic Coastal Ridge which runs from Homestead (south) to Miami in the north (Fish and Stewart, 1991). The ridge is 2 to 10 miles in width and ranges from 8 to 15 ft above sea level and consists of fine sand with moderate natural drainage. West of Miami and the Atlantic Coastal Ridge are marl and fine sand followed by peat and muck (Everglades) at border of Collier County. Beneath the peat and muck of the Everglades (Collier County) is the Fort Thompson Formation (20ft thick) which gets thicker and transitions below the Miami Limestone westward (towards Miami). The Miami Limestone typically varies from 5ft to 15ft thick while the Fort Thompson Formation increases from 15 ft (Collier) to 70ft in depth and then transitions to the Anastasia Formation on the West Coast (Miami Limestone above) (Fish and Stewart, 1991). Beneath the Fort Thompson is the Tamiami Formation which varies in depths from 80 to 140ft. Stretching south and then west from present Miami to the Dry Tortugas is the Key Largo Limestone which is exposed on the surface from Soldier Key to the southeast portion of Big Pine Key. With depths (> 150' – Big Pine Key), the Key Largo (Pleistocene) Limestone consisting of hermatypic corals with interbedded calcarenitic (matrix) of limestone and thin beds of quartz sand. The upper part of the formation consists of boundstones, grainstones, and packstones (Shinn 1989).

## CHAPTER 3 ACIP DESIGN METHODS

### 3.1 Background

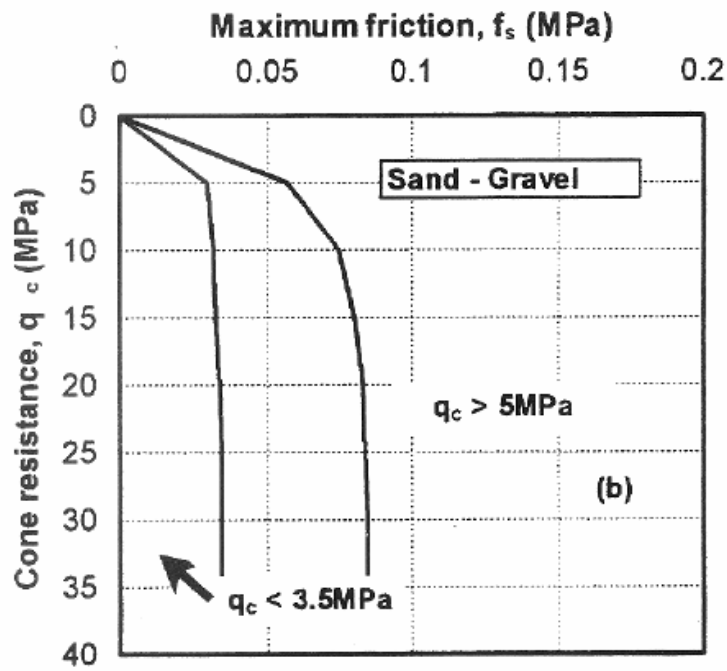
As part of scope of services (task 2), a review of estimation methods for nominal side and tip resistance of ACIPs in government manuals and published literature was required. The majority of the methods have been reported in a recent FHWA review of ACIP pile design and published in GEC 8 (Brown et al, 2007). More recent methods in the literature have been found based on CPT in-situ testing. All the methods have been developed for piles in cohesionless soil, cohesive soil, mixed soil, and limestone. Furthermore, the methods are based on either soil properties ( $S_u$ ,  $\phi$ ), rock properties ( $q_u$ ,  $q_t$ , RQD), or in-situ tests (SPT-N, CPT- $q_c$ ), and a few of the methods are based on both soil properties and in-situ test results. All of the methods presented estimate the nominal (ultimate) unit skin and/or tip resistance of ACIPs. A discussion follows.

### 3.2 Cohesionless Soils

Table 3.1 lists the methods identified for design of ACIP piles in cohesionless soil. The Wright and Reese (1979) method for unit side resistance is a function of the average vertical effective stress, the lateral earth pressure coefficient, and the angle of internal friction of the sand. The  $\phi$  is a weighted average of each sand layer along the length of the pile. The unit tip resistance is a function of the SPT blow count,  $N$ , near the pile tip elevation. The LPC method (Bustamante and GIANESELLI, 1981 and 1982) is recommended by the Brown (2007) where CPT cone bearing resistance ( $q_c$ ) is to be used to estimate capacity. The unit side resistance for sand and gravel is estimated from a graph of maximum side resistance  $f_s$  (MPa) versus  $q_c$  (MPa), as

shown in Figure 3.1. For cone tip resistance,  $q_c$  in the range of 3.5 MPa to 5 MPa, the unit side resistance should be interpolated based on the average  $q_c$  along the length of pile or pile segment in cohesionless soil. The unit tip resistance is shown in Table 3.1 as a coefficient times the  $q_c$  (MPa). Douglas (1983) method was developed based on 28 full scale load tests of ACIP piles in multiple Europe countries. The unit side resistance is function of the vertical effective stress, lateral earth pressure coefficient, and the angle of internal friction of the sand. The lateral earth pressure coefficient is assumed to be 1 and the vertical effective stress is limited for piles in loose and medium dense sand (Table 3.1). In the load tests, the unit tip resistance was defined as the end bearing occurring at a pile tip displacement of 30 mm (1.2 in) and is estimated as 25% of  $q_c$  at the pile tip elevation. The Rizkalla (1988) method is a function of  $q_c$  and was developed based on a database of load test performed on ACIP piles. For piles in cohesionless soils, the unit side resistance is estimated as 0.8% of  $q_c$  and the unit tip resistance is 12% of the  $q_c$  plus 0.1 and limited to 25 MPa (Table 3.1). The Neely (1991) method is based on a data base of 66 load test on ACIP piles in sandy soils. The unit side resistance is a function of the vertical effective stress, the lateral earth pressure coefficient, and the friction angle at the pile-soil interface,  $\delta$ . A  $\beta$  factor represents  $K \cdot \tan(\delta)$  in the equation. Here, the vertical effective stress is computed at the mid depth of the pile length and  $\beta$  is limited to  $\geq 0.2$ . The unit tip resistance is correlated to the measured SPT N-values near the pile tip elevation and limited to 75 tsf (Table 3.1). Viggiani (1993) developed methods for unit side and unit tip resistance based on load tests on ACIP piles in Italy, in volcanic soils (Table 3.1). The unit side resistance is a function of a coefficient  $\alpha$  and the  $q_c$ , where  $\alpha$  is function of  $q_c$ . The unit tip resistance is obtained by average  $q_c$  4 pile diameters above and below the pile tip elevation. O'Neill and Reese (1999) developed methods for unit side and unit tip resistance based on SPT N-values corrected for 60% hammer efficiency,

$N_{60}$ . The methods are commonly referred to as the FHWA 1999 method and are presented in Table 3.1 for cohesionless soil. The unit side resistance is a function of the lateral earth pressure coefficient, the vertical effective stress, and the angle of internal friction. A  $\beta$  factor represents  $K \cdot \tan(\phi)$  in the equation and is estimated based on  $N_{60}$  (Table 3.1). Similarly, the unit tip resistance is estimated from equations depending on the  $N_{60}$  near the pile tip elevation, where  $N_{60}$  is taken as the average over 1 pile diameter above and 2 or 3 pile diameters below the pile tip elevation. Brown (2010) uses both  $K_o \cdot \tan(\delta)$  to represent  $\beta$  and uses  $N_{60}$  to estimate OCR and  $K_o$ ; Zelada and Stephenson (2000) studied 43 compression load tests and 10 tension load tests of ACIP piles in cohesionless soil and modified the FHWA 1999 methods for unit side and unit tip resistance (Table 3.1). Coleman and Arcement (2002) recommended a modified  $\beta$  for ACIP piles based on load tests performed in Mississippi and Louisiana mixed soils. Equations for  $\beta$  as a function of depth for sands and silts (that exhibited drained behavior, nonplastic) are shown in Table 3. Note, the Coleman and Arcement (2002) equations are only valid for  $\beta$  between 0.2 and 2.5. Stuedlein and Gurtowski (2013) proposed a power curve trend line to estimate the unit side resistance of ACIP piles in cohesionless soil. The method is a function of SPT N-values and pile head displacements normalized by pile diameter,  $B$ .



Source: Bustamante and Gianselli, (1982)

Figure 3.1 LPC method for unit side resistance for cohesionless soils (FHWA, 2007)

Table 3.1 ACIP pile design methods for cohesionless soil

Authors	Design Methodology	Note	Comment
Wright and Reese (1978)	Unit Skin Friction: $f_s = K_s \tan \phi \cdot \sigma'_v < 1.6 \text{ tsf (150 kPa)}$ Unit End Bearing: $q_{0.05d} = \frac{2}{3} \cdot N < 40 \text{ tsf (3.8MPa)}$	$K_s$ = lateral earth pressure coefficient; $\sigma'_v$ = average effective stress at the midpoint of the pile length; $\phi$ = internal friction angle of the soil; N = SPT N-value at the tip of the pile.	Ultimate pile capacity is assumed to be reached at a settlement equal to 5% pile diameter.
Bustamante & Gianeselli (LPC) (1981)	Unit End Bearing: $q_p = 0.375 \cdot q_c$	$q_c$ = cone tip resistance.	
Douglas (1983)	Unit Skin Friction: $f_s = \sigma'_v \cdot K_o \cdot \tan \phi$ Unit End Bearing: $q_p = 0.25 \cdot q_c$	$\sigma'_v$ = vertical effective stress; $K_o$ = lateral earth pressure coefficient; $\phi$ = angle of internal friction; $q_c$ = cone tip resistance.	$K_o = 1$ , B=diameter $\sigma'_v$ is limited for depths greater than 6B for piles in loose sand and 10 B for piles in medium dense sand.



Brown (2010)	Unit Skin Friction: $f_s = \sigma'_v \cdot K_o \cdot \tan \delta$ $K_o = (1 - \sin \phi) \cdot OCR^{\sin \phi} \leq K_p$ $OCR = \frac{\sigma'_p}{\sigma'_v} ; \frac{\sigma'_p}{P_a} \approx 0.47(N_{60})^m$	$K_o$ = at-rest lateral earth pressure coefficient; $\delta$ = angle of friction at soil-shaft interface $\phi$ = angle of internal friction; $\sigma'_p$ = the maximum past vertical effective stress (Mayne 2007); m=0.6 for clean quartzitic sands and m=0.8 for silty sands	$K_p$ is Rankine's earth pressure coefficient In FHWA GEC 10 examples, $\delta = \phi$ $P_a$ =atmospheric pressure
Rizkalla (1988)	Unit Skin Friction: $f_s = 0.008 \cdot q_c$ (MPa) Unit End Bearing: $q_p = 0.12 \cdot q_c + 0.1$ (MPa) for $q_c \leq 25$ MPa	$q_c$ = cone tip resistance.	
Neely (1991)	Unit Skin Friction: $f_s = \beta \cdot \sigma'_v \leq 1.4$ tsf	$\sigma'_v$ = average effective vertical stress at the along pile length; $\beta$ = friction factor correlated to pile length;	

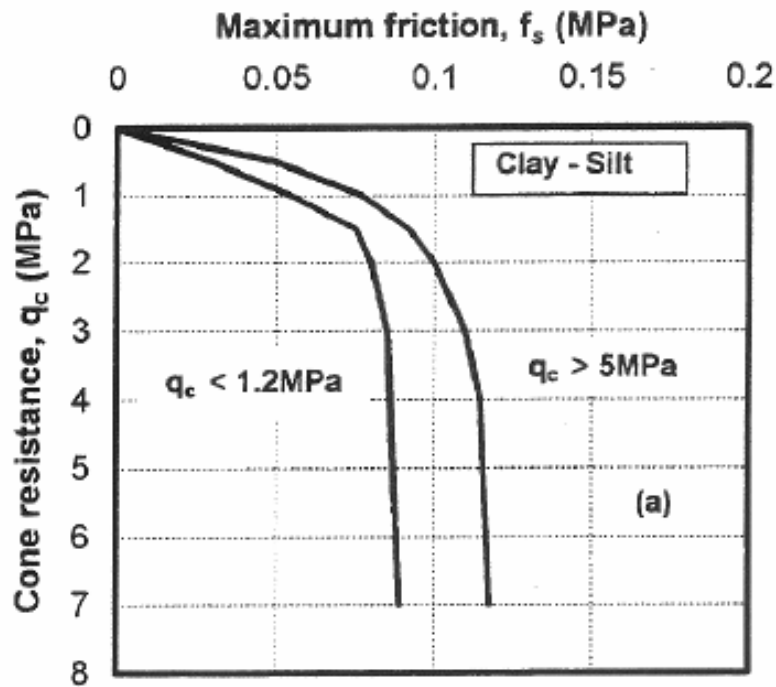
	Unit End Bearing:  $q_p = 1.9 \cdot N \leq 75 \text{ tsf}$	$N = \text{SPT value near the tip of pile.}$	
Viggiani (1993)	Unit Skin Friction:  $f_s = \alpha \cdot q_c \text{ (MPa)}$  $\alpha = \frac{6.6 + 0.32 \cdot q_c}{300 + 60 \cdot q_c}$  Unit End Bearing:  $q_p = q_{c(ave)} \text{ (MPa)}$	$q_c = \text{cone tip resistance;}$  $q_{c(ave)} = \text{average cone tip resistance 4 pile diameters above and below the pile tip.}$	
FHWA 1999  (O'Neill and Reese,1999)	Unit Skin Friction:  $f_s = \beta \cdot \sigma'_v < 2.0 \text{ tsf}$  $\beta = 1.5 - 0.135 \cdot Z^{0.5} \quad N_{60} \geq 15$  $\beta = \frac{N_{60}}{15} (1.5 - 0.135 \cdot Z^{0.5}) \quad N_{60} < 15$	$\sigma'_v = \text{average vertical effective stress on segment/layer;}$  $\beta = \text{friction factor;}$  $Z = \text{depth to mid-layer in feet;}$  $N_{60} = \text{SPT-}N \text{ value at 60\% of hammer efficiency;}$	

FHWA 1999  (O'Neill and Reese,1999)	Unit End Bearing:  $q_p = 0.6 \cdot N_{60}$ , for $0 \leq N_{60} \leq 75$  $q_p = 4.3 \text{ MPa (45 tsf)}$ , for $N_{60} > 75$	$N_{60}$ = SPT- $N$ value at 60% of hammer efficiency averaging approximately 1 B above and 2B to 3B below the pile tip	B = pile diameter
Zelada and Stephenson (2000)	Unit Skin Friction:  $f_s = \beta \cdot \sigma'_v < 1.6 \text{ tsf}$  $\beta = 1.2 - 0.11 \cdot Z^{0.5} \quad N_{60} \geq 15$  $\beta = \frac{N_{60}}{15} (1.2 - 0.11 \cdot Z^{0.5}) \quad N_{60} < 15$	$\sigma'_v$ = average vertical effective stress on segment or layer;  $\beta$ = friction factor  $Z$ = depth to middle of layer in feet;  $N_{60}$ = SPT- $N$ value at 60% of hammer efficiency;	
Zelada and Stephenson (2000)	Unit End Bearing:  $q_p = 1.7 \cdot N_{60} \leq 75 \text{ tsf}$	$N_{60}$ = SPT- $N$ value at 60% of hammer efficiency averaging approximately 1B above and 2B to 3B below the pile tip.	B = pile diameter
Coleman and Arcement (2002)	Unit Skin Friction:  $f_s = \beta \cdot \sigma'_v \leq 200 \text{ kPa (2.0 tsf)}$  $\beta = 2.27 \cdot Z_m^{-0.67}$ for silty soils	$Z_m$ = depth (meters) from the ground surface to the middle of a given soil layer or pile segment.	

	$\beta = 10.72 \cdot Z_m^{-1.3}$ for sandy soils where $0.2 \leq \beta \leq 2.5$		
Stuedlein, A. and Gurtowski, T. (2013)	Unit Skin Friction: $f_s = \left(1.23 \cdot \frac{\delta}{B} + 1.65\right) \cdot N^{0.82} \text{ (kPa)}$	N = SPT N-value; $\delta$ = pile head displacement; B = pile diameter.	

### 3.3 Cohesive Soils

Table 3.2 lists the methods identified for design of ACIP piles in cohesive soil. The LPC method (Bustamante and Gianeselli, 1981 and 1982) is recommended by the Brown (2007) where CPT cone bearing resistance ( $q_c$ ) is to be used to estimate capacity. The unit side resistance for clay and silt is estimated from a graph of maximum side resistance (MPa) versus  $q_c$  (MPa), as shown in Figure 3.2. For cone tip resistance,  $q_c$  in the range between 1.2 MPa and 5 MPa, the unit side resistance should be interpolated based on the average  $q_c$  along the length of pile in the cohesive soil. The unit tip resistance is shown in Table 3.2 and is 15% of the  $q_c$  (MPa), where  $q_c$  is the lesser of the average  $q_c$  two or three pile diameters below the pile tip elevation. O'Neill and Reese (1999) developed methods for unit side and unit tip resistance based on the soil's undrained shear strength,  $S_u$ . The method for the unit skin friction is an alpha method where a reduction factor,  $\alpha$ , is applied to the  $S_u$  for the layer obtained from its representation ( $S_u/P_a$ ). The unit tip resistance applies a bearing capacity factor,  $N_c$ , to  $S_u$  and is recommended based on  $S_u$ . These methods are commonly referred to as the FHWA 1999 methods and are presented in Table 3.2 for cohesive soil. The Clemente et al (2000) method recommends reduction factors,  $\alpha$ , back calculated from skin friction measurements on ACIP piles installed in clays in Louisiana, Mississippi, and Texas. The reduction factors can be selected from a graph based on the  $S_u$  as shown in Figure 3.3. Coleman and Arcement (2002) recommended a modified  $\alpha$  for ACIP piles based on 32 load tests in clays and silts (that exhibited undrained behavior). The unit side resistance is a function of the average  $S_u$  and the modified  $\alpha$  in Table 3.2, which is only valid for  $S_u$  between 0.25 and 1.5 tsf.



Source: Bustamante and Gianselli (1982)

Figure 3.2 LPC method for unit side resistance for cohesive soils (FHWA, 2007)

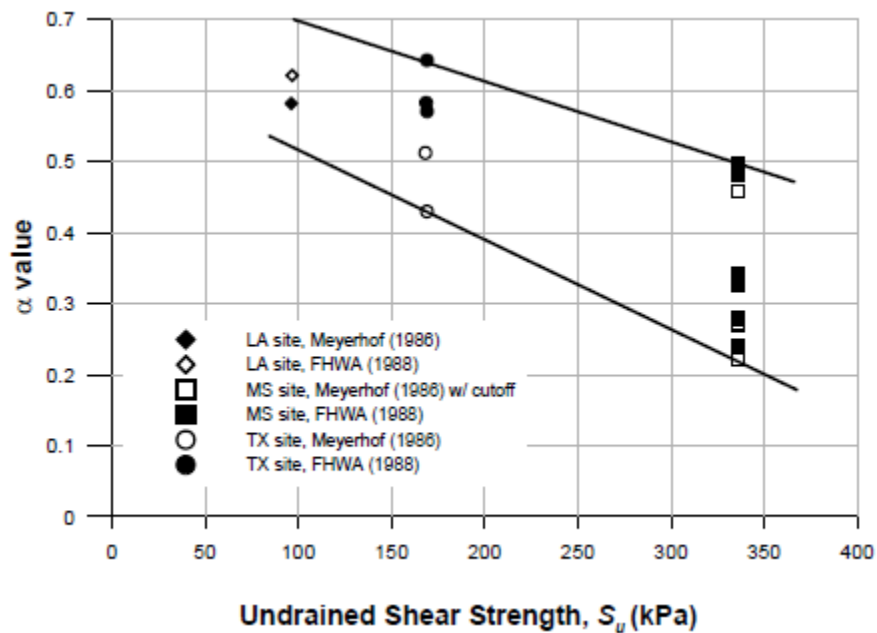


Figure 3.3  $\alpha$  versus  $S_u$  for clay (Clemente et al., 2000)

Table 3.2 ACIP pile design methods for cohesive soil

Authors	Design Methodology	Note	Comment
Bustamante & Gianeselli (LPC) (1981)	<p>Unit Skin Friction:</p> <p>Graphical method (Figure 3).</p> <p>Unit End Bearing:</p> $q_p = 0.15 \cdot q_c$	$q_c$ = cone tip resistance.	
Reese and O'Neill (FHWA, 1999)	<p>Unit Skin Friction:</p> $f_s = \alpha \cdot S_u$ $\alpha = 0.55 \text{ for } \frac{S_u}{P_a} \leq 1.5$ $\alpha = 0.55 \text{ to } 0.45 \text{ for } 1.5 \leq \frac{S_u}{P_a} \leq 2.5$	$S_u$ = undrained shear strength of the soil at the pile segment location; $\alpha$ = reduction factor; $P_a$ = standard atmospheric pressure.	
Reese and O'Neill (FHWA, 1999)	<p>Unit End Bearing:</p> $q_p = N_c^* \cdot S_u$ $N_c^* = 9 \text{ for}$ $200 \text{ kPa (2 tsf)} \leq S_u \leq 250 \text{ kPa (2.6 tsf)}$	$S_u$ = undrained shear strength of the soil 2B below the tip; $N_c^*$ = bearing capacity factor; $I_r$ = rigidity index;	$E_s$ is best determined from triaxial testing or insitu tests (e.g. PMT). When $E_s$ cannot be measured, $I_r$ can be estimated

	$N_c^* = \frac{4}{3} [\ln I_r + 1] \text{ for}$ $S_u \leq 200 \text{ kPa (2 tsf)}$ $I_r = \frac{E_s}{3S_u}$	$E_s$ = undrained Young's modulus of soil below pile tip.	based on Table 5.1 from Brown (2007).
Clemente et al. (2000)	Unit Skin Friction:  Graphical method (Figure 4). Back calculated $\alpha$ , from pile side shear tests in very stiff to hard clay in Louisiana, Mississippi, and Texas, plotted versus $S_u$ ( $100 \text{ kPa} \leq S_u \leq 340 \text{ kPa}$ )		
Coleman and Arcement (2002)	Unit Skin Friction:  $f_s = \alpha \cdot S_u$ $\alpha = \frac{0.56}{S_u} \text{ (tsf)}$ $\alpha = \frac{56.2}{S_u} \text{ (kPa)}$ $0.25 \text{ tsf (25 kPa)} \leq S_u \leq 1.5 \text{ tsf (150 kPa)}$	$S_u$ = undrained shear strength;  $\alpha$ = reduction factor.	



### 3.4 ACIPs in Weak Rock or IGM

In addition to methods to estimate the pile resistance in cohesionless soil, cohesive soil, and rock are those for ACIP piles in intermediate geotechnical material (IGM). IGMs are defined as materials with strengths between those of soil and rock (O'Neill et al., 1996). Cohesionless IGMs are dense granular materials with  $N_{60}$  between 50 and 100 blows/ft (Brown 2010). Cohesive IGMs (e.g. CH-marls) are those that exhibit  $q_u$  values between 10 ksf and 100 ksf ( $S_u$  between 5 ksf and 50 ksf) (Brown, 2010). Brown groups methods to estimate pile resistance in cohesionless IGMs in the “cohesionless” methods. Table 3.3 lists methods to estimate the unit skin friction and unit tip resistance of ACIP piles in IGM with  $q_u$  between 10 ksf and 100 ksf.

FHWA recommends a method by O'Neill et al. (1996) and Hassan et al. (1997) to estimate the unit side resistance of a shaft in cohesive IGM. The method was developed based on load tests, lab and field tests, and modeling. The unit side resistance is a function of  $q_u$ , a correction factor to account for jointing,  $\phi$  (Table 3.4), and an empirical factor,  $\alpha$ , that can be estimated from Figure 3.4. Note, to use Figure 3.4, the modulus of the rock mass,  $E_m$ , the fluid pressure exerted by the concrete at the time of the placement,  $\sigma_n$ , the atmospheric pressure  $\sigma_p$ , and the total vertical displacement required for mobilization of the side resistance (assumed to be 1 inch) must be known. The joint correction,  $\alpha$ , (FHWA, 2010) is based on open or closed and/or gouge filled joints as well as Rock Quality Designation (RQD - %). Crapps (1992) recommended a method to estimate the unit side resistance of a shaft in IGM (Table 3.4) based on a load test in Marl (mudstone). Crapps (1992) method is a function of the vertical effective stress,  $\sigma'_v$ , and the SPT blow count,  $N$  (blows/ft). AASHTO recommends O'Neill and Reese's

(1999) method to estimate the unit tip resistance of a shaft as a function of  $q_u$ . AASHTO recommends the method for IGM and rock (AASHTO, 2014).

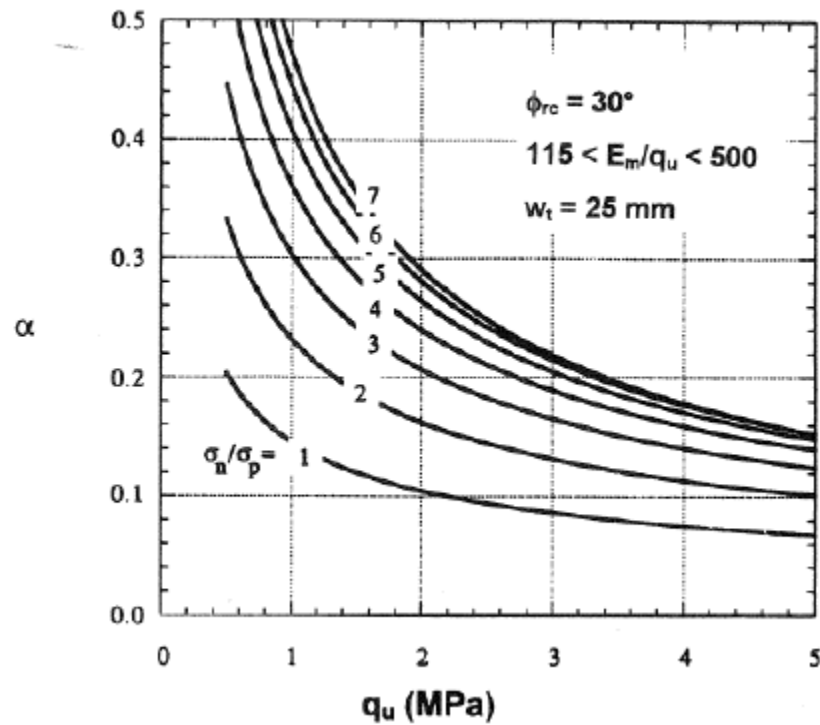


Figure 3.4  $\alpha$  versus  $q_u$  for cohesive IGM

Table 3.3 Joint modification factors for different RQD (Brown, 2010)

RQD (%)	Joint Modification Factor, $\phi$	
	Closed joints	Open or gouge-filled joints
100	1.00	0.85
70	0.85	0.55
50	0.60	0.55
30	0.50	0.50
20	0.45	0.45

Table 3.4 Drilled shaft design methods applicable to ACIP piles in rock or IGM

Authors	Design Methodology	Note	Comment
FHWA (Brown 2010)	Unit Skin Friction: $f_s = \alpha \cdot \varphi \cdot q_u$ (ksf)	$\alpha$ = reduction factor for IGM; $\varphi$ = correction factor to account for the degree of jointing; $q_u$ = unconfined compressive strength (ksf).	$\alpha$ values obtained from Figure 3.4, the interface friction angle, $\phi_{rc}$ , is assumed to be $30^\circ$ . Where $\phi_{rc} \neq 30^\circ$ , $\alpha = \alpha_{Figure\ 3.4} \frac{\tan \phi_{rc}}{\tan 30^\circ}$
Crapps (IGM)	Unit Skin Friction: $f_s = \sigma'_v \cdot [e^{0.0646(N-13.6)}]$ (ksf)	$\sigma'_v$ = vertical effective stress (ksf) $N$ = blow count (blows/ft).	
AASHTO (2014) (Rock/IGM)	Unit End Bearing: $q_p = 2.5 \cdot q_u$ (ksf)	$q_u$ = unconfined compressive strength (ksf).	

### 3.5 ACIPs in Competent Rock and Limestone

Table 3.5 lists methods to estimate the unit side resistance of ACIP piles installed in competent rock (limestone). Methods listed include ones to estimate unit side resistance for drilled shafts (Horvath and Kenney, 1979; Williams et al., 1980; Reynolds and Kaderabeck, 1980; Gupton and Logan, 1984; Crapps, 1986; Reese and O'Neill, 1987; Rowe and Armitage, 1987; Carter and Kulhaway, 1988; McVay et al., 1992; Ramos et al., 1994; Lai, 1998; Kulhaway et al., 2005) and to estimate unit side resistance for ACIP piles (Ramos et al., 1994; Frizzi and Meyer, 2000). With the exception of Crapps (1986), one method by Ramos et al. (1994), and Frizzi and Meyer (2000), the methods in Table 3.5 are a variant of a function of  $q_u$  of the limestone. McVay et al. (1992) compared most of the methods that are a function of  $q_u$  against a database of 14 load tests of rock socketed drilled shafts. McVay et al. (1992) showed that using the laboratory measured  $q_u$  and the split tension strength,  $q_t$ , better describes the unit side resistance. Furthermore, McVay et al. (1992) showed that methods based on SPT blow count (e.g., Crapps, 1986), did not predict the measured unit side resistance very well. In this project, methods based on SPT blow count (Crapps, 1986, Ramos et al., 1994; and Frizzi and Meyer, 2000), were also evaluated.

Table 3.5 Drilled shaft and ACIP pile design methods for rock

Authors	Design Methodology	Note	Comment
Horvath and Kenney (1979)	Unit Skin Friction: $f_s = 0.67 \cdot \sqrt{q_u}$ (tsf)	$q_u$ = unconfined compressive strength (tsf).	
Williams et al. (1980)	Unit Skin Friction: $f_s = 1.842 \cdot q_u^{0.367}$ (tsf)	$q_u$ = unconfined compressive strength (tsf).	
Reynolds and Kaderabek (1980)	Unit Skin Friction: $f_s = 0.3 \cdot q_u$ (tsf)	$q_u$ = unconfined compressive strength (tsf).	Miami Limestone
Gupton and Logan (1984)	Unit Skin Friction: $f_s = 0.2 \cdot q_u$ (tsf)	$q_u$ = unconfined compressive strength (tsf).	Key Largo, Anastasia, Fort Thompson and Miami limestone formations

Reese and O'Neill (1987)	Unit Skin Friction: $f_s = 0.15 \cdot q_u$ (tsf)	$q_u$ = unconfined compressive strength (tsf).	
Crapps (1986)	Unit Skin Friction: $f_s = 0.01 \cdot N$ (tsf)	N = SPT N - value (blows/ ft);	
Rowe and Armitage (1987)	Unit Skin Friction: $f_s = 1.45 \cdot \sqrt{q_u}$ (tsf) (clean sockets) $f_s = 1.94 \cdot \sqrt{q_u}$ (tsf) (rough sockets)	$q_u$ = unconfined compressive strength (tsf).	
Carter and Kulhawy (1988)	Unit Skin Friction: $f_s = 0.63 \cdot \sqrt{q_u}$ (tsf)	$q_u$ = unconfined compressive strength (tsf).	
McVay et al. (1992)	Unit Skin Friction: $f_s = \frac{1}{2} \cdot \sqrt{q_u} \cdot \sqrt{q_t}$ (tsf)	$q_u$ = unconfined compressive strength (tsf); $q_t$ = split tensile strength (tsf).	

Ramos et al. (1994)	Unit Skin Friction:  for $q_u \leq 1800 \text{ kPa}$ (36 ksf)  $f_s = 0.5 \cdot q_u$ (kPa or ksf)  $f_s = 0.35 \cdot q_u$ (kPa or ksf) (lower bound)  for $q_u > 1800 \text{ kPa}$ (36 ksf)  $f_s = 0.12 \cdot q_u$ (kPa or ksf)	$q_u$ = unconfined compressive strength (kPa or ksf);	
Ramos et al. (1994)	Unit Skin Friction:  for $5 \leq N \leq 60$ blows/ft  $f_s = 19.2 \cdot N + 192$ (kPa)  $f_s = 0.4 \cdot N + 4$ (ksf)  for $N > 60$ blows/ft  $f_s = 9.6 \cdot N + 768$ (kPa)  $f_s = 0.2 \cdot N + 16$ (ksf)	N = SPT N – value (blows/ft).	N = SPT N-value (blows/ft) is used in both US and SI equations

Lai (1998)	Unit Skin Friction: $f_s = \frac{1}{2} \cdot \sqrt{q_u} \cdot \sqrt{q_t} \cdot REC \text{ (tsf)}$	$q_u$ = unconfined compressive strength (tsf); $q_t$ = split tensile strength (tsf); $REC$ = average recovery of rock core.	
Frizzi & Meyer (2000)	Unit Skin Friction: $f_s = 0.35 \cdot N_{60} - 1.5 \text{ (tsf) (1)}$ $f_s = 0.14 \cdot N_{60} + 1 \text{ (tsf) (2)}$	$N_{60}$ = SPT- $N$ value at 60% of hammer efficiency (blows/ foot).	(1) Miami limestone formation; (2) Ft. Thompson limestone formation.
Kulhawy et al. (2005)	Unit Skin Friction: $f_s = C \cdot \sqrt{\frac{q_u}{P_a}} \cdot P_a \text{ (ksf)}$	$C$ = coefficient taken as 1 for normal rock socket conditions. $q_u$ = unconfined compressive strength (ksf); $P_a$ = standard atmospheric pressure (ksf).	



## CHAPTER 4

### ESTIMATION OF NOMINAL RESISTANCE OF ACIPs FROM LOAD TESTS

#### 4.1 Segmental Approach for Estimating Resistance

As identified in Table 2.2, 16 piles were top down static compression with instrumentation, 2 were uplift (tension) with instrumentation and 1 was an Osterberg with instrumentation which separated side from tip resistance. Unfortunately, 4 of the 19 instrumented piles were missing boring information (e.g. Hollywood and Palm Beach), and an additional 2 tests had top displacements less 0.1". This left 13 piles with multiple sets of instrumentation (i.e. separate out sand, clay, and rock), but insufficient number for assessment of LRFD resistance,  $\Phi$ , especially for specific rock formations (i.e. Miami and Fort Thompson).

To obtain an estimate of measured resistance for all soil or rock types along the piles, it was decided to use a segmental top model (Figure 4.1) representing the pile and surrounding soil to model the measured load vs. displacement of the pile. For the analysis, each pile was divided into 1ft segments with a nonlinear spring (Figure 4.1) at its center representing side friction alongside the pile on each segment and a tip spring at the bottom of the pile representing end bearing. The multiple pile segments were contained in either a soil or layer. Each nonlinear spring was characterized by normalized T-Z (side) and Q-Z (tip) curve (Figure 4.2) with the only unknown being nominal (ultimate) side resistance of each layer and ultimate tip resistance of the bearing layer. For the analyses of any pile, the soil/rock layering would first be identified (Figure 4.1), next the appropriate normalized side and tip resistance model was selected (Figure 4.2, e.g. Sand, Clay, Rock), a displacement was applied to the top of the pile, and then the algorithm (MatLab) was run to optimize the ultimate or nominal unit side friction and end bearing until the estimated forces matched the measured load at the top of the pile for all load

steps. Due to the elastic nature of the pile, as well as the analysis being performed from the top down, specific layer nominal unit side resistances controlled specific portions of the load vs. deformation response of the pile. For instance, skin friction of top layers are mobilized prior to bottom layers, and tip resistance after mobilization of side resistance of the pile.

For validation of the MatLab code, the algorithm was applied to all sites where load distribution was available as a function of depth (sections 4.2 & 4.3). User input was the load displacement response of the top of the pile as well as layering (sand, clay, rock). The algorithm iterated on ultimate skin and tip resistance of the layer materials to obtain the closest match (least squares) between measured and estimated pile top response. Estimated and measured force distribution along each pile is presented for comparison in section 4.2. Section 4.3 provides results for Miami Dade which does not have instrumentation along the pile only conventional top down load test results. Presented are the match between measured and estimated load vs.

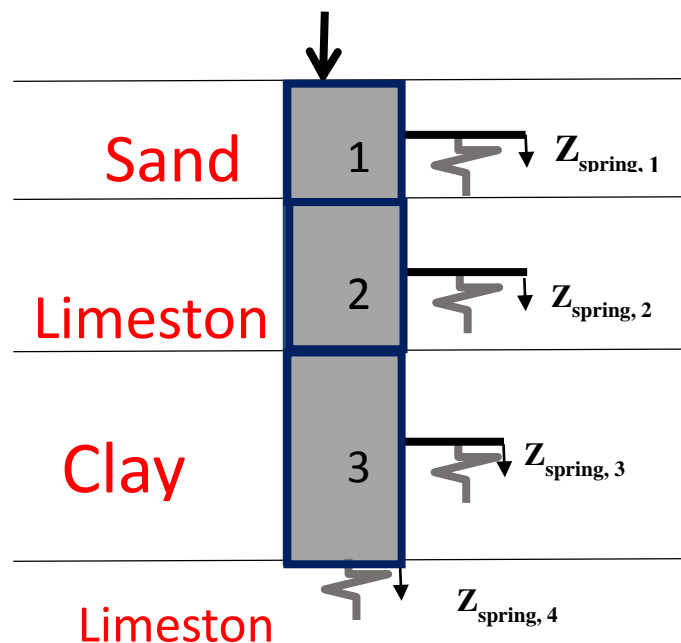


Figure 4.1 Idealized segmental model for ACIP piles

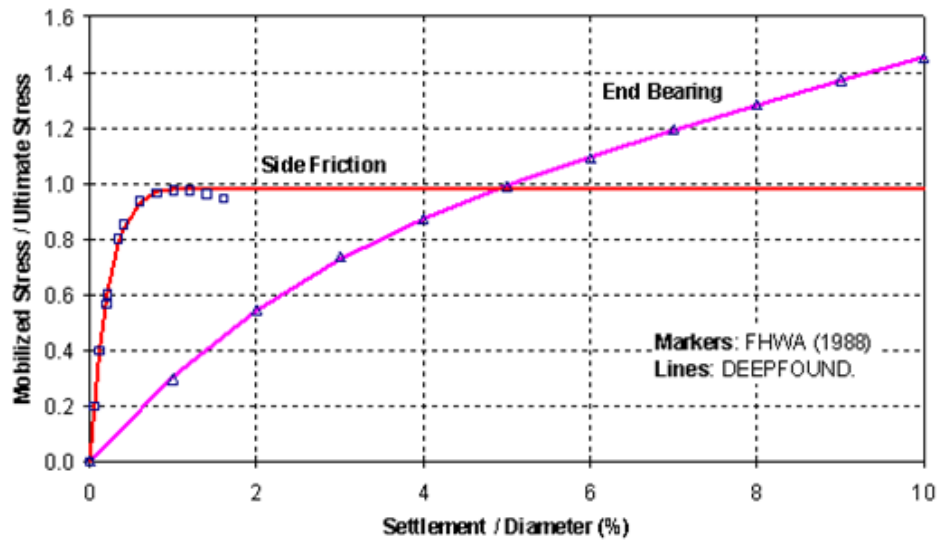


Figure 4.2 a. Normalized unit skin and tip resistance for sand, FB-Deep (O'Neill 1999)

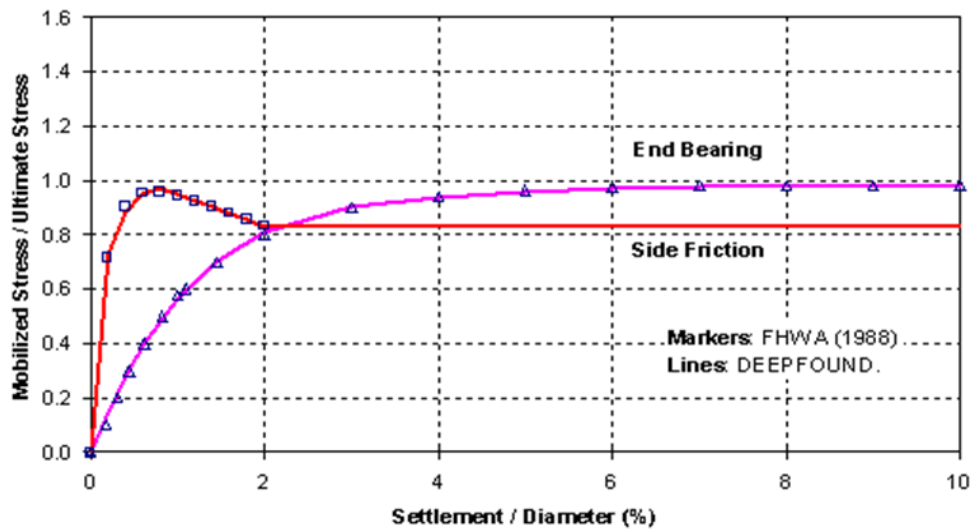
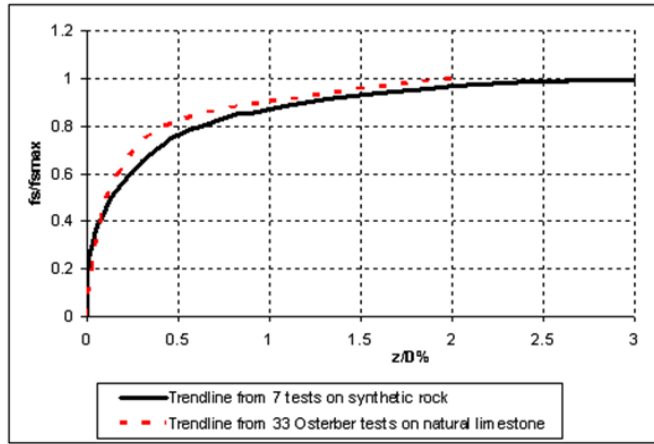


Figure 4.2 b. Normalized unit skin and tip resistance for clay, FB-Deep (O'Neill 1999)



$$\frac{f_z}{f_{smax}} = 0.96R^{0.33} \quad 0 = R = 0.5$$

$$\frac{f_z}{f_{smax}} = 0.86R^{0.16} \quad 0.5 = R = 3$$

$$\frac{f_z}{f_{smax}} = 1 \quad 3 = R$$

where:  $R = z/D \times 100$ .  
 $f_s$  = skin friction  
 $f_{smax}$  = ultimate unit skin friction

Figure 4.2 c. Normalized unit skin resistance for limestone, FB-Deep

$$q_b = \Lambda W_t^{0.67}$$

Where  $\Lambda$ (Lambda) = Elastic compressibility parameter;

$W_t$  = Displacement at top of shaft

$$\Lambda = 0.0134 E_m \left( \frac{L}{D} + 1 \right) \left\{ \frac{200 \left[ \left( \frac{L}{D} \right)^{0.5} - \Omega \right] \left[ \frac{L}{D} + 1 \right]}{\pi L \Gamma} \right\}^{0.67}$$

$E_c$  = concrete modulus  
 $E_m$  = rock mass modulus

$$\Gamma = 0.37 \left( \frac{L}{D} \right)^{0.5} - 0.15 \left[ \left( \frac{L}{D} \right)^{0.5} - 1 \right] \log_{10} \left( \frac{E_c}{E_m} \right) + 0.13 \quad \begin{array}{l} L = \text{Length of Shaft} \\ D = \text{Diameter of Shaft} \end{array}$$

$$\Omega = 1.14 \left( \frac{L}{D} \right)^{0.5} - 0.05 \left[ \left( \frac{L}{D} \right)^{0.5} - 1 \right] \log_{10} \left( \frac{E_c}{E_m} \right) - 0.44$$

Figure 4.2 d. Net unit bearing stress,  $q_b$ , for limestone, FB-Deep (O'Neill, 1999)

displacement at the top of the pile, estimated ultimate skin frictions along the pile, as well as mobilization of side resistance along the pile and tip resistance as function of pile head

displacements. In assessing LRFD resistance factors,  $\Phi$ , the segmental unit skin friction values will be converted to the measured unit skin frictions (i.e. T-z) and compared to the predicted values in chapter 5.

## **4.2 Estimation of Nominal Resistance of ACIPs with Instrumentation**

### **4.2.1 Alachua**

As identified in Table 2.2, 3 of the Alachua ACIP piles had soil boring information, load deformation and load distribution along their lengths (Alachua 2-TP5, Alachua 5-TP1, and Alachua 5-TP2). Soil stratigraphy of the Alachua site (Table 2.2) was clays, sands, and soft Limestone (IGM).

Shown in Figures 4.3 to 4.5 are the algorithm's evaluation of Alachua 2-TP5 (sandy clay over clay). The layering: layer 1 - 15 ft thick sandy clay, layer 2 – 15ft thick clay and layer 3 – 12ft thick clay layer. The back calculated unit skin frictions (insert in Figure 4.3) were 0.597 tsf – sandy clay, 1.2 tsf – clay, and 1.2 tsf –clay.

Presented in Figure 4.4, is the mobilized side and tip resistance of each segment (layer) as function of displacement and applied top load (Figure 4.3). A review of Figure 4.4 shows the layer 1 (sandy clay) reaches peak at 0.12 inches of movements. Layers 2 (clay) and 3 (clay) reach their peak resistances at displacements of 0.2 inches and contribute little if any additional resistance to further loading of the pile. Only the pile tip, clay, continues to mobilize pile resistance with movements beyond 0.2 inches.

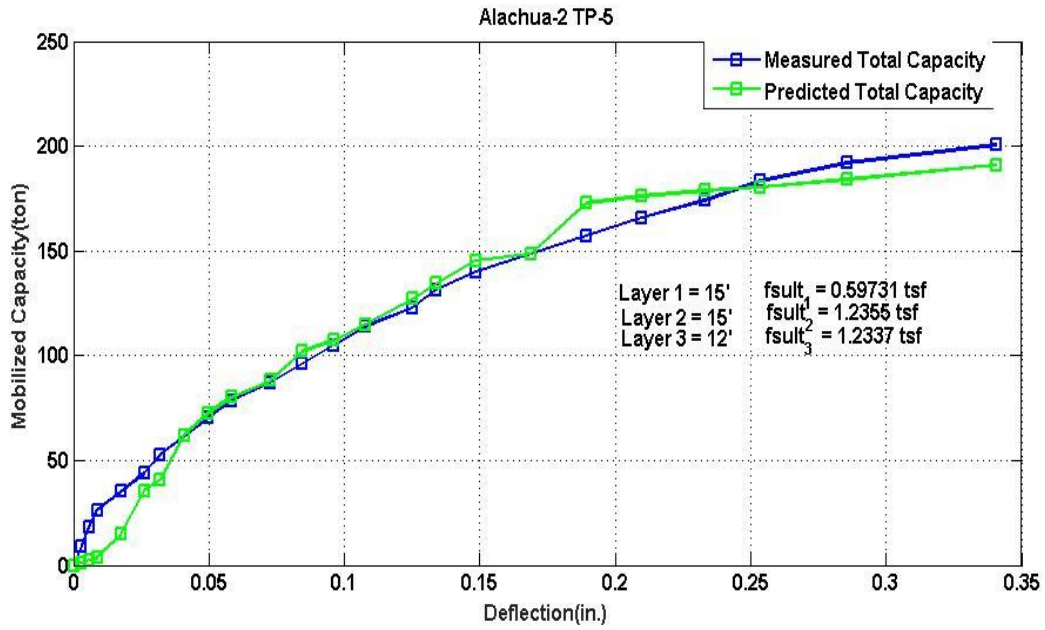


Figure 4.3 Measured and estimated load vs. displacement of Alachua 2 TP-5

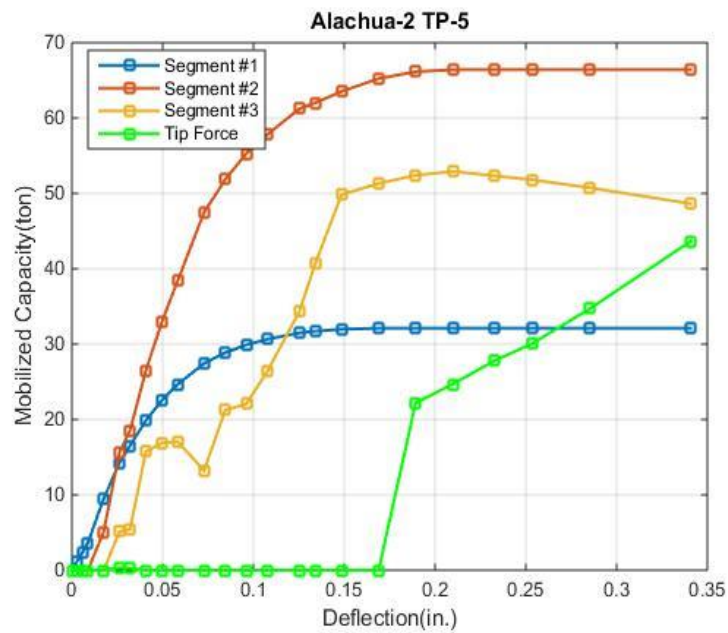


Figure 4.4 Mobilized unit side and tip resistance for 3 segments of Alachua 2 TP-5

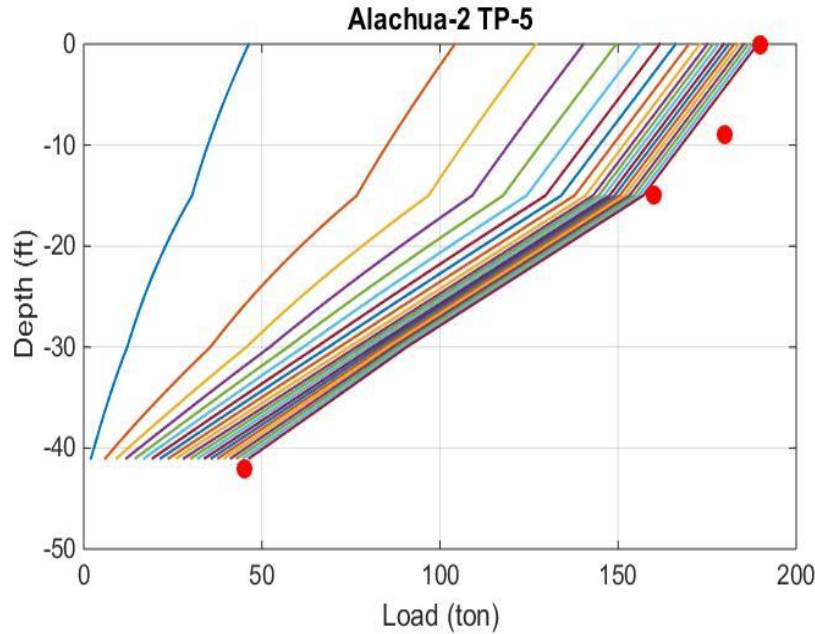


Figure 4.5 Distribution of estimated and measured pile forces in Alachua 2 TP-5

Presented in Figure 4.5 is the associated pile forces with depth for Alachua-2 TP-5 pile using the back calculated ultimate unit side and tip resistances (Figure 4.3) with prescribed tip displacements and mobilized side and top forces. Shown for the final estimated forces are the reported measured values (red dots) along the pile. The measured and estimate load transfers agree within 15% at final load step. Note, layer 2 and 3 had almost identical unit skin frictions (Figure 4.3)

Shown in Figures 4.6 to 4.8 are the algorithm's evaluation of Alachua 5-TP1. Soil stratigraphy for this pile was sand and multiple clay layers. Shown in Figure 4.6, is the layering: layer 1 – 27 ft thick sand layer, layer 2 – 18 ft thick clay layer and layer 3 – 20ft thick clay layer along with the back calculated ultimate unit skin frictions (0.498 tsf – sand, 1.398 tsf – clay, and 1.498 tsf –clay).

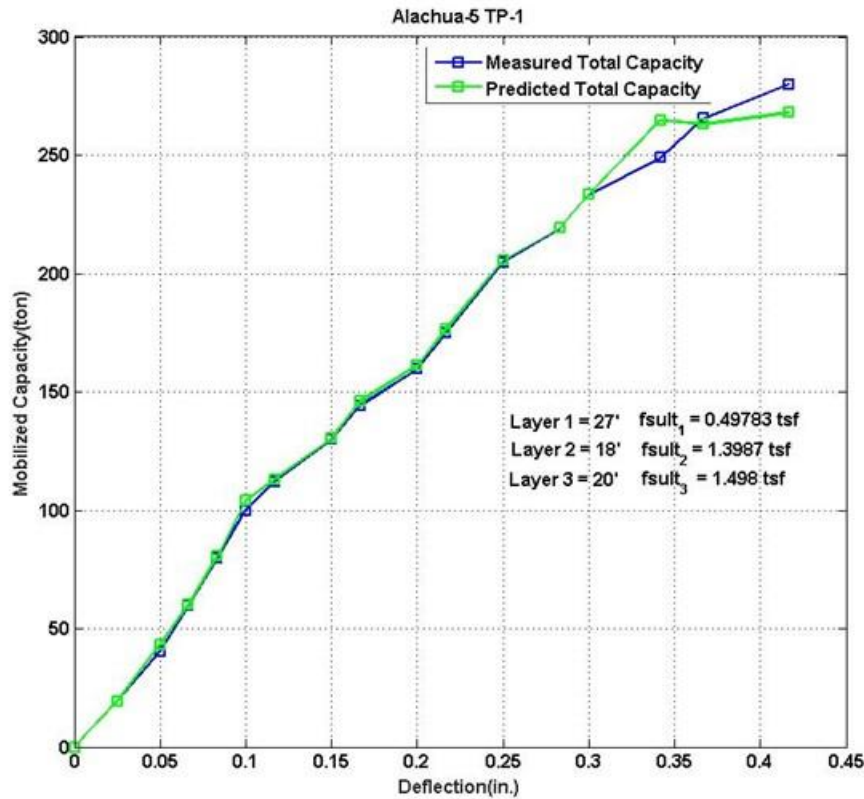


Figure 4.6 Measured and estimated load vs. displacement of Alachua 5 TP-1

Presented in Figure 4.7, is the mobilized side and tip resistance of each segment (layer) as function of displacement and applied top load (Figure 4.6). A review of Figure 4.7 shows the layer 1 (sand) reaches its peak resistance at 0.15 inch and layer 2 (clay) reach its' peak resistances at a displacement less than 0.25 inches and resistance drops with further movement due to trend line (Figure 4.2b). The second clay layer, segment 3, reaches peak resistance at 0.4'' of displacement. At 0.3'' of top movement, the pile begins to mobilize tip resistance. Evident from Figure 4.6, the match between the measured and estimated load displacement response of the pile is quite good.



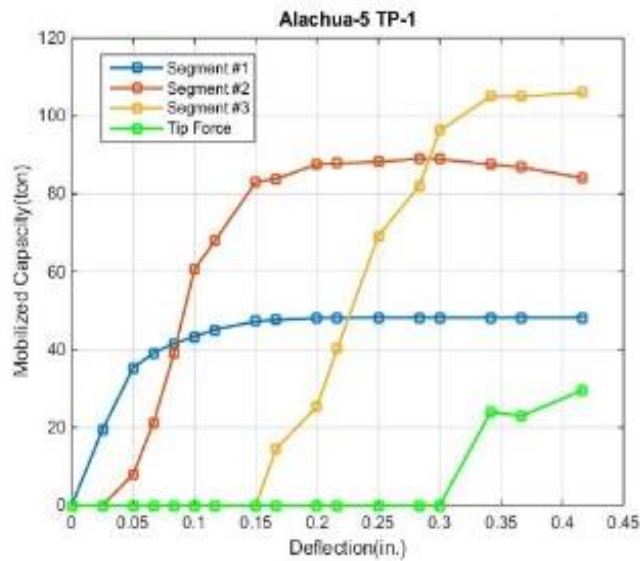


Figure 4.7 Mobilized unit side and tip resistance for 3 segments of Alachua 5 TP-1

Given in Figure 4.8 is the associated pile forces with depth for Alachua-5 TP-1 pile using the back calculated ultimate unit side and tip resistances (Figure 4.6) vs. the reported measured values for the final load step. Again the measured and estimate load transfer with depth agrees within 15%.

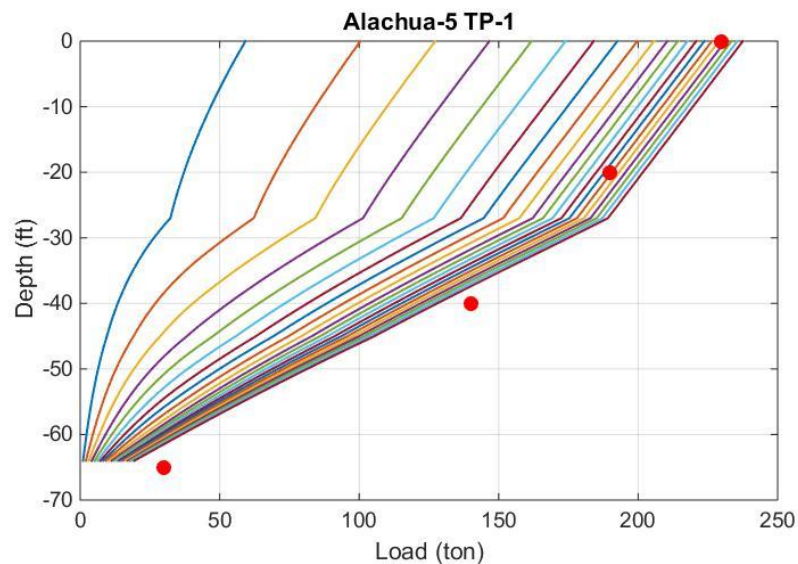


Figure 4.8 Distribution of estimated and measured pile forces in Alachua 5 TP-1

Presented in Figures 4.9 to 4.11 are the algorithm's evaluation of Alachua 5-TP2. Soil stratigraphy for this pile was sand, underlain by multiple clay layers. Shown in Figure 4.9, is the layering: layer 1– 15 ft thick sand, layer 2 – 25 ft thick clay, and layer 3 – 10ft thick clay along with the back calculated ultimate unit skin frictions (0.50 tsf – sand, 1.45 tsf – clay, and 3.0 tsf – clay) and estimated vs. measured load – displacement response of the pile.

Figure 4.10 is the mobilized side and tip resistance of each segment (layer) as function of displacement and applied top load (Figure 4.9). Layers 1 (sand) and 2 (clay) reach their peak resistances at displacements less than 0.40” of top movement. In the first clay layer (segment 2), the resistance drops with further movement based on trend line (Figure 4.2b). Only segment 3 (i.e., deeper stiff clay layer) contributes to the increased resistance of the pile beyond 0.4” movement. As pile top head movements increases beyond 0.4” pile tip resistance is mobilized. The match between the measured and estimated load displacement response of the pile, Figure 4.9 is quite good up to 1” of movement.

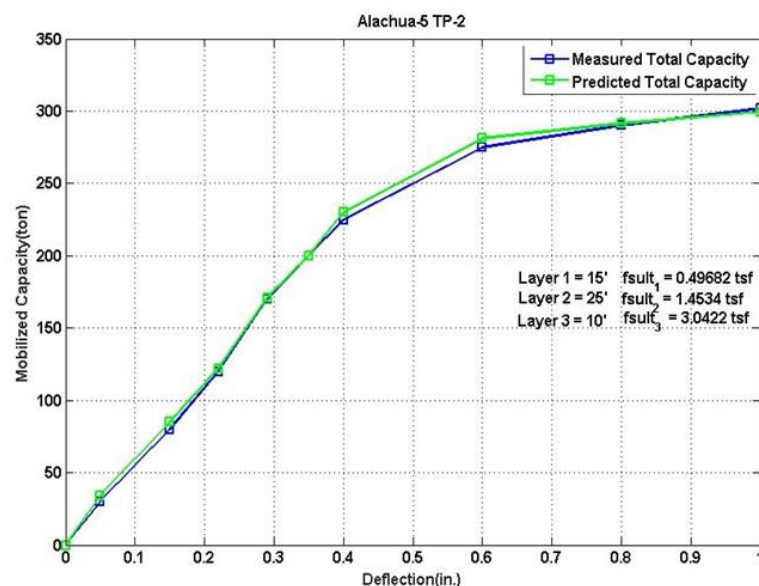


Figure 4.9 Measured and estimated load vs. displacement of Alachua 5 TP-2

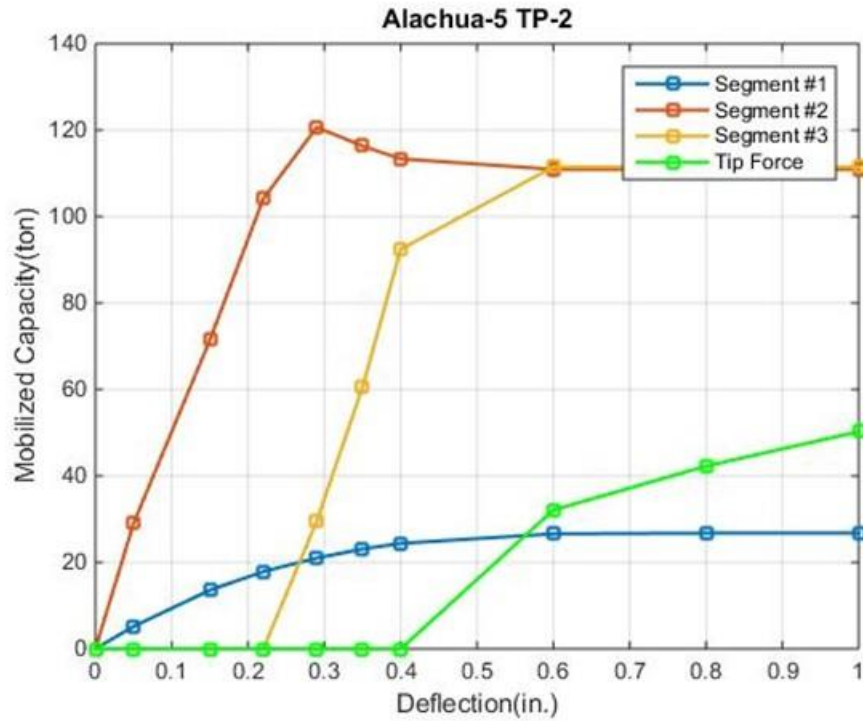


Figure 4.10 Mobilized unit side and tip resistance for 3 segments of Alachua 5 TP-2

Presented in Figure 4.11 is the associated pile forces with depth for Alachua-5 TP-2 pile using the back calculated ultimate unit side and tip resistances for multiple load steps on the pile. Shown in Figure 4.11 for the final estimated top load are the reported measured pile forces (red dots) along the pile. Again the measured and estimate load transfer with depth agrees within 10 to 15%.

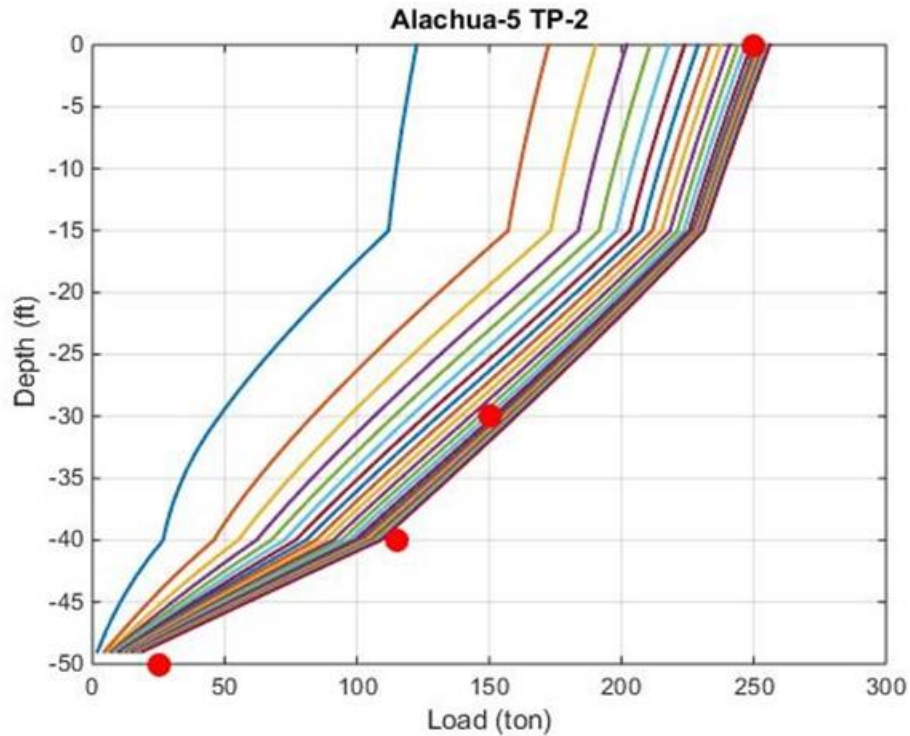


Figure 4.11 Distribution of estimated and measured pile forces in Alachua 5 TP-2

Note, there were 2 other piles in Alachua which had both load vs. deformation response of the pile (Table 2.2). Unfortunately, neither pile has available soil boring information; multiple requests to contractor and engineers did not result in the information.

#### 4.2.2 Broward

The next site evaluated with load distribution was in Broward County, Broward 1 TP-1 which had a top down static load test with load distribution and soil boring information. Broward 1 TP-2 which had a tension test which was not modeled since it had very small deformations (0.009 inches) and not fully mobilized.

Shown in Figures 4.12 to 4.14 are the algorithm's evaluation of Broward 1-TP1. Soil stratigraphy for this pile was sand, limestone, and another sand layer. Shown in Figure 4.11, is the layering: layer 1 – 15 ft thick sand, layer 2– 33 ft thick limestone and layer 3– 72ft thick

sand layer along with the back calculated ultimate unit skin frictions (0.36 tsf – sand, 2.4 tsf – limestone, and 0.48 tsf – sand) and estimated vs. measured load – displacement response of the pile.

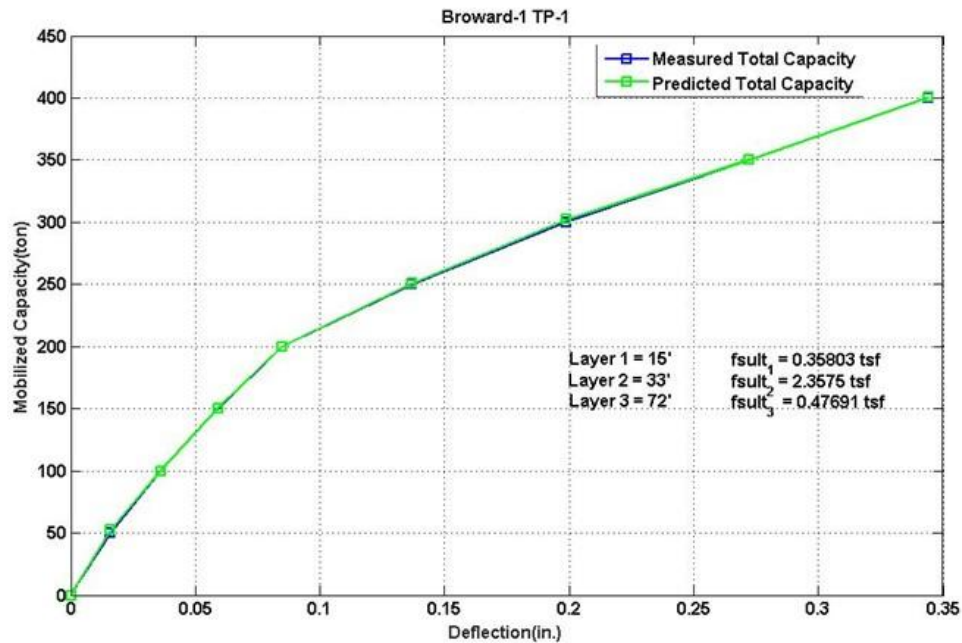


Figure 4.12 Measured and estimated load vs. displacement of Broward 1 TP-1

Shown in Figure 4.13, is the mobilized side and tip resistance of each segment (layer) as function of displacement and applied top load (Figure 4.12). A review of Figure 4.13 shows the layers 1 (sand) is fully mobilized at displacements less than 0.10 inches and contribute little if any additional resistance to further loading of the pile. Layer 2, contributes significantly to the pile's resistance up to a top head movement of 0.25"; larger pile head movements, i.e. > 0.25" result in the mobilization of side resistance in the bottom sand layer. However, with only a top head movement of 0.35", significant side resistance of bottom sand layer was not mobilized. Also, little if any tip resistance was mobilized on the pile. Notice the match between the

measured and estimated load displacement response of the pile, Figure 4.12 is quite good up to 0.35" of movement.

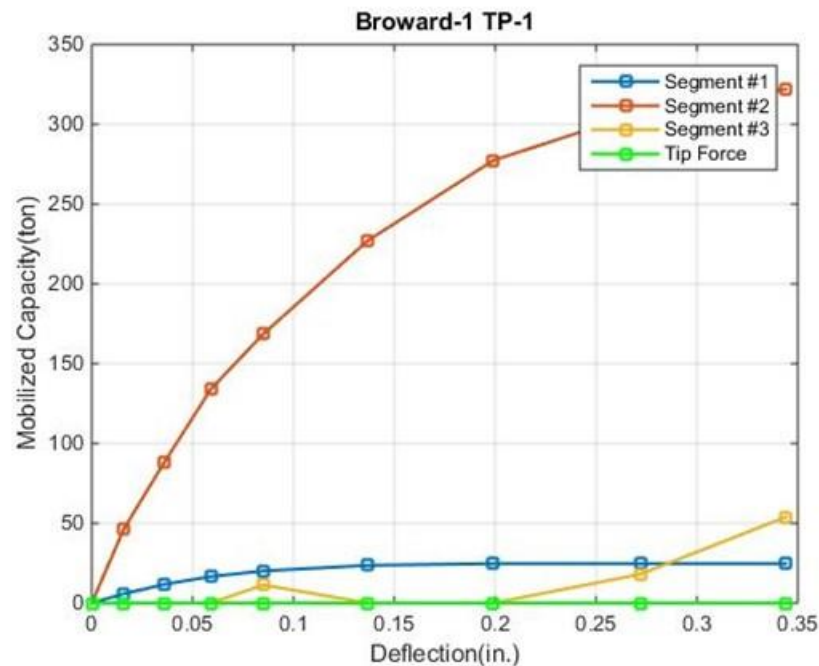


Figure 4.13 Mobilized unit side and tip resistance for 3 segments of Broward 1 TP-1

Presented in Figure 4.14 is the associated pile forces with depth for Broward 1 TP-1 pile using the back calculated ultimate unit side (Figure 4.12) and tip resistances for multiple load steps on the pile. Shown in Figure 4.14 for the final estimated top load is the reported measured values (red dots) along the pile. As identified in Figure 4.13, for maximum top head displacement (0.35"), little if any load has been transmitted into segment or layer 3 (i.e. no load beneath 80 ft – pile is 120 ft long). Again the measured and estimate load transfer with depth agrees within 10 to 15%.

Also at this site, Broward 1 TP-5, had the Osterberg cell located within the pile (i.e. 15 ft of pile beneath the cell) and would require significant effort to model with the MatLab algorithm. Specifically, load would have to be applied to 2 separate sections of pile (Figure 4.1) in different

directions (up and down) to model the test. This wasn't done since the ultimate unit skin frictions were monitored and reported by the contractor. However, the Osterberg results (nominal layer unit skin frictions) were estimated (Section 4.4) and used in evaluating LRFD resistance, chapter 5.

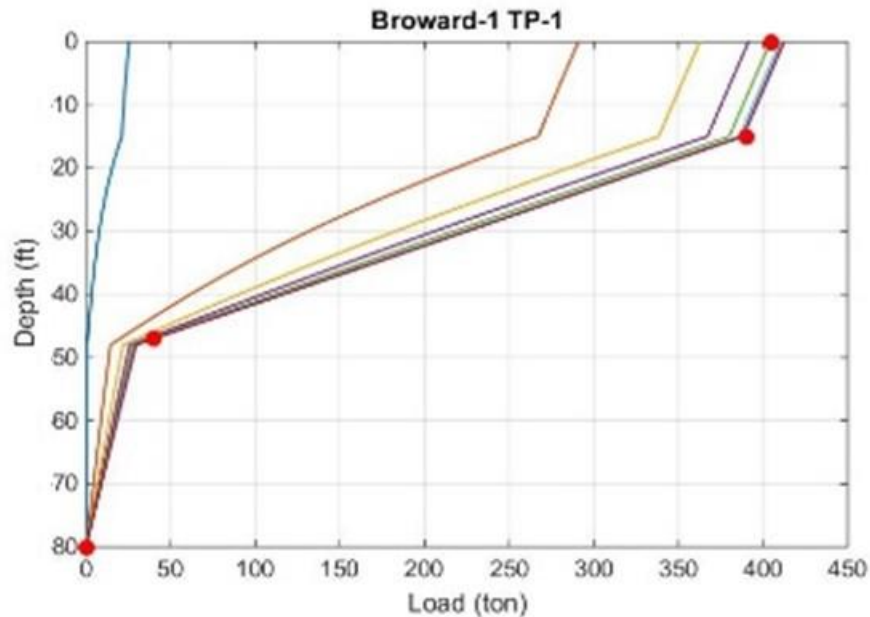


Figure 4.14 Distribution of estimated and measured pile forces in Broward 1 TP-1

### 4.2.3 Hillsborough

The next site presented was in Hillsborough County (Hillsborough 3 TP2, TP3, TP 4 and TP 5) which had static load test load distribution from Statnamic testing along with soil boring information. Soil stratigraphy for this site was thick sand layer underlain by variable stiff clay.

Shown in Figures 4.15 to 4.17 are the algorithm's evaluation of Hillsborough 3 TP2. Shown in Figure 4.15, is the layering: layer 1– 25 ft thick sand layer, layer 2 – 20 ft thick sand layer and layer 3 – 15ft thick clay layer along with the back calculated ultimate unit skin frictions



(1.35 tsf – sand, 1.0 tsf – sand, and 1.4 tsf – stiff clay) and estimated vs. measured load – displacement response of the pile.

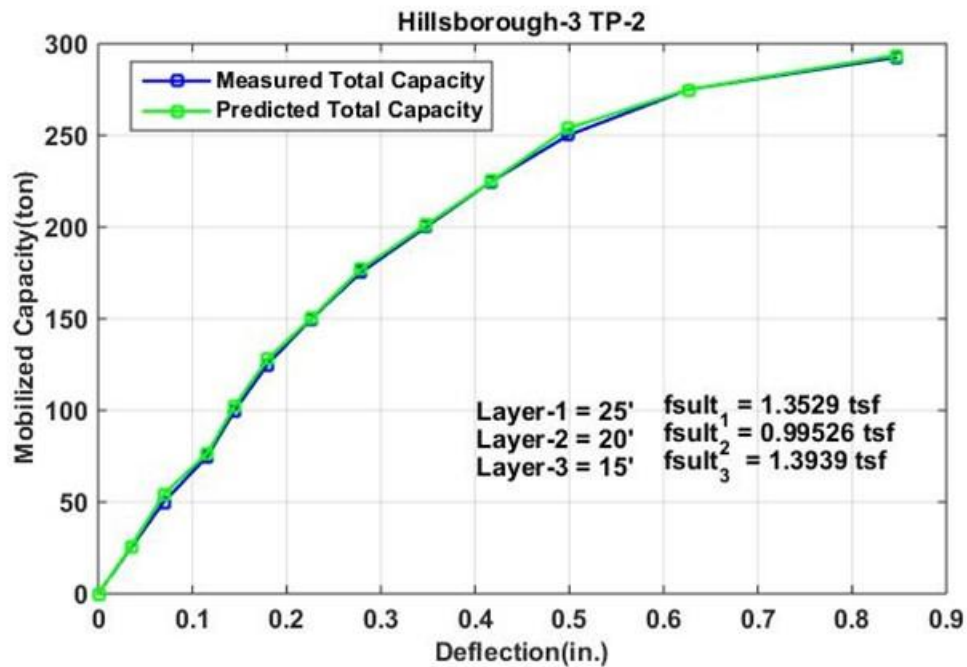


Figure 4.15 Measured and estimated load vs. displacement of Hillsborough 3 TP2

Presented in Figure 4.16, is the mobilized side and tip resistance of each segment (layer) as function of displacement and applied top load (Figure 4.15). A review of Figure 4.16 shows the layers 1 (sand) is fully mobilized at displacements less than 0.25 inches and contribute little if any additional resistance to further loading of the pile. Layer 2 contributes to the pile's resistance from pile head top movement of 0.2" to 0.4"; for larger pile head movements, i.e. > 0.4" segment 3, the stiff clay layer is being mobilized, and the clay layer has lost some unit skin friction (see Figure 4.16). At top head movement of 0.8", approximately 70 tons from the clay layer is mobilized. Notice the match between the measured and estimated load displacement response of the pile, Figure 4.15 is quite good up to 0.85" of movement.



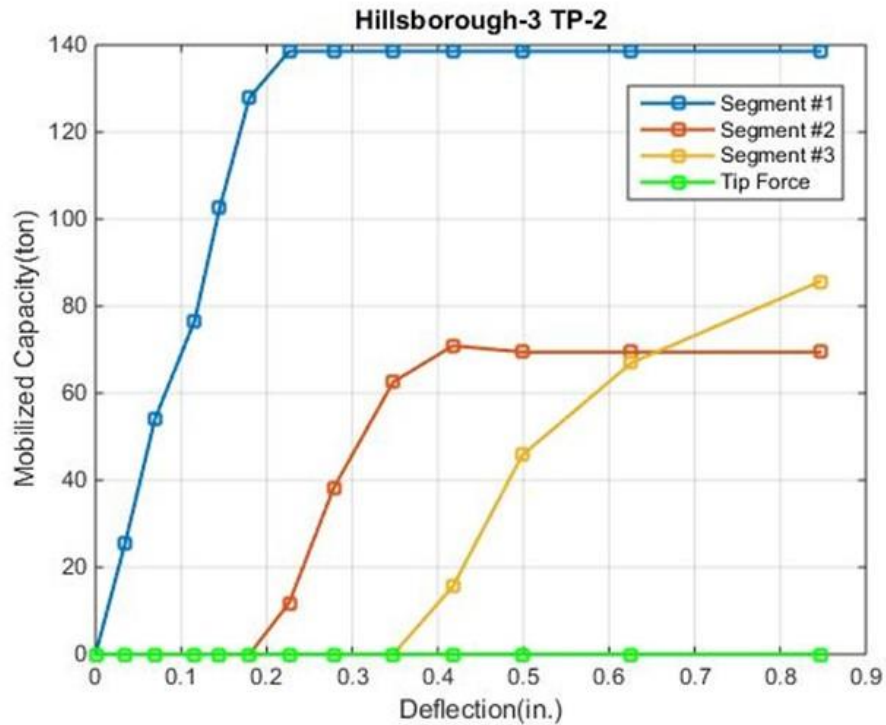


Figure 4.16 Mobilized unit side and tip resistance for 3 segments of Hillsborough 3 TP2

Plotted in Figure 4.17 is the associated pile forces with depth for Hillsborough 3 TP2 pile using the back calculated ultimate unit side and tip resistances (Figure 4.15) for multiple load step vs. the reported measured values along the pile (red dots) for the final load step. As identified in Figure 4.16, for maximum top head displacement (0.8”), not all of the unit skin friction has been mobilized in the bottom layer. However, the upper 2 layers skin friction has been fully mobilized (sand and clay layers). Again the measured and estimate load transfer with depth agrees within 15%.

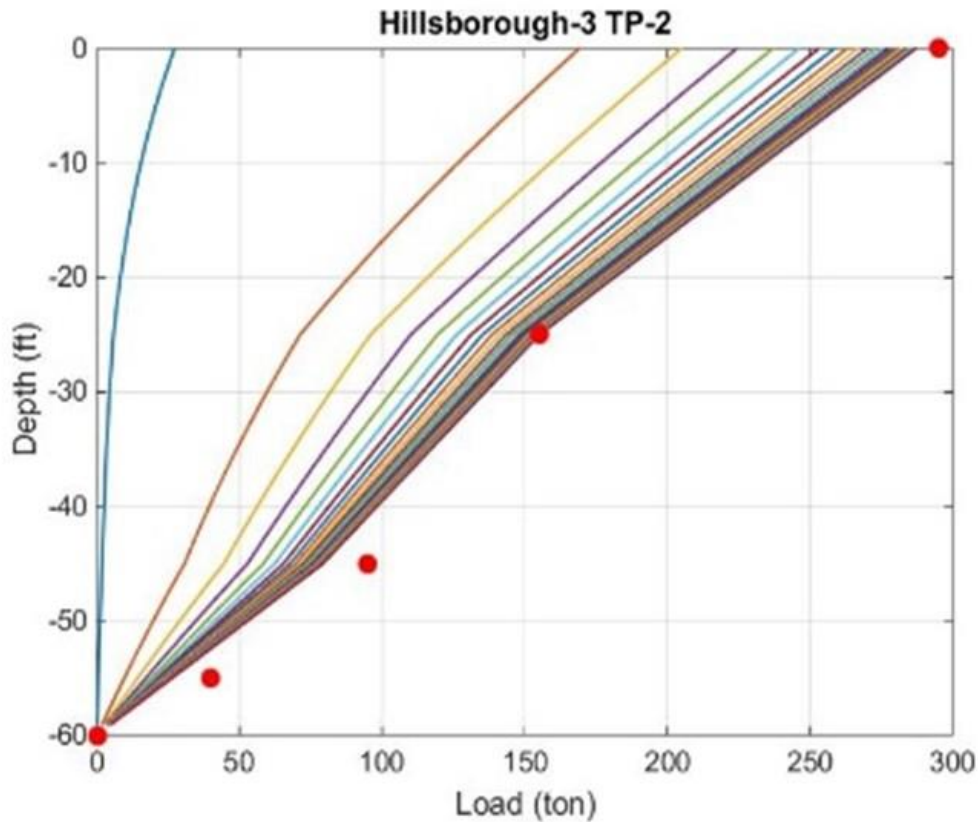


Figure 4.17 Distribution of estimated and measured pile forces in Hillsborough 3 TP2

Presented in Figures 4.18 to 4.20 are the algorithm's evaluation of Hillsborough 3 TP3. Soil stratigraphy for this pile was sand, and clay. Shown in Figure 4.18, is the layering: layer 1 – 25 ft thick sand layer, layer 2 – 20 ft thick sand layer and layer 3 – 15ft thick clay layer along with the back calculated ultimate unit skin frictions (0.47 tsf – sand, 0.47 tsf – sand, and 2.31 tsf – clay) and estimated vs. measured load – displacement response of the pile. Evident from the figure, the measured and estimated deflections match up to 0.5", slightly differ at 0.6" and then agree at larger displacements. This difference ( $>0.5"$ ) is attributed to the difference of measured and estimated tip model of the pile. The general clay (FHWA) tip model was used for the material, which appears to be mobilized too quickly.

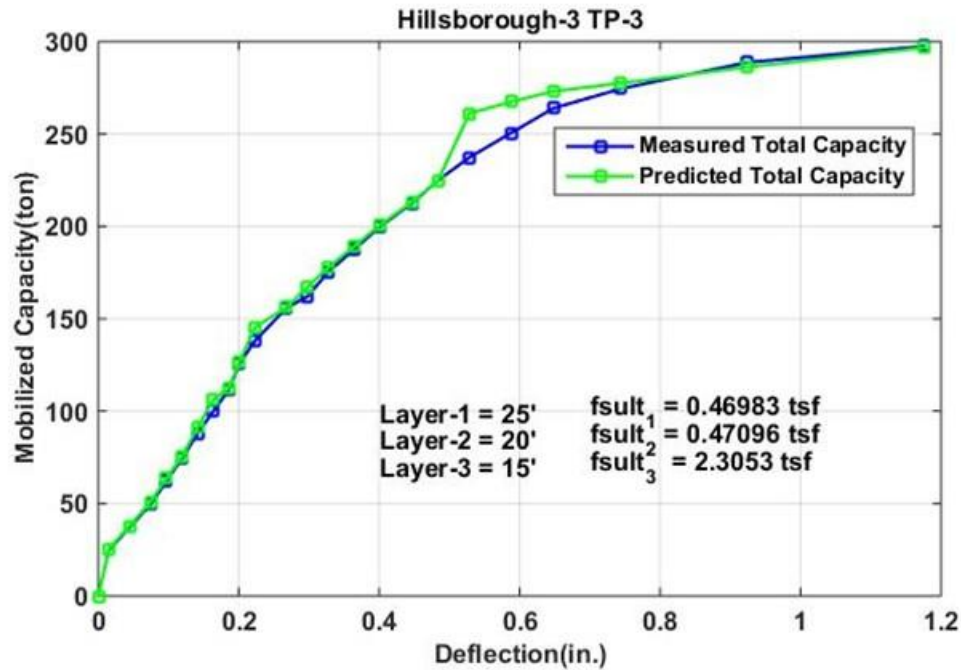


Figure 4.18 Measured and estimated load vs. displacement of Hillsborough 3 TP3

Shown in Figure 4.19, is the mobilized side and tip resistance of each segment (layer) as function of displacement and applied top load (Figure 4.18). A review of Figure 4.19 shows the layers 1 and 2 (sand) are fully mobilized at displacements less than 0.20 inches and contribute little if any additional resistance to further loading of the pile. Layer 3 (clay) contributes to the pile's resistance for top movements from 0.1" to 0.6"; for larger pile head movements, i.e. > 0.5" the clay tip model is being mobilized. The maximum unit skin friction occurs in the 15ft thick clay layer – 145 tons. The sand layers contributed 85 tons of side resistance and the tip contributed 70 tons at the maximum test load. Note, the clay (segment 3) shows a peak and a small drop in side friction due to shape of trend line (Figure 4.2b). Movements up to 1.2 inches were estimated for the 60 ft pile.

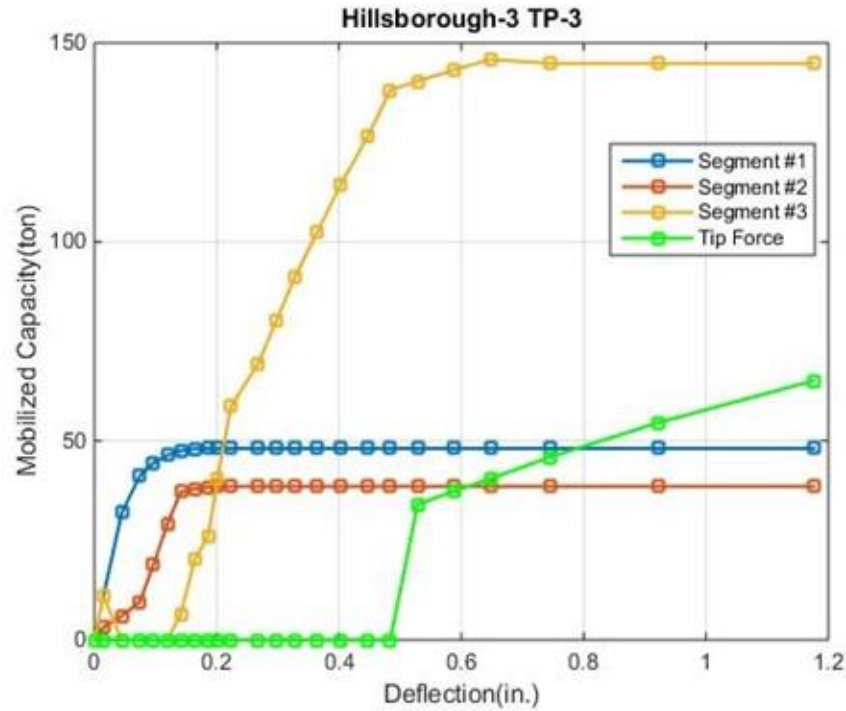


Figure 4.19 Mobilized unit side and tip resistance for 3 segments of Hillsborough 3 TP3

Presented in Figure 4.20 is the associated pile forces with depth for Hillsborough 3 TP3 pile using the back calculated ultimate unit side and tip resistances (Figure 4.18) for multiple load step vs. the reported measured values along the pile (red dots) for an applied load of approximately 300 tons. As identified in Figure 4.19, the ultimate unit skin friction has been mobilized for all three layers. Note, since layers 1 and 2 have the same unit skin friction, the slope of load transfer is constant to a depth of 45 ft. Again the measured and estimate load transfer with depth agrees within 15%.

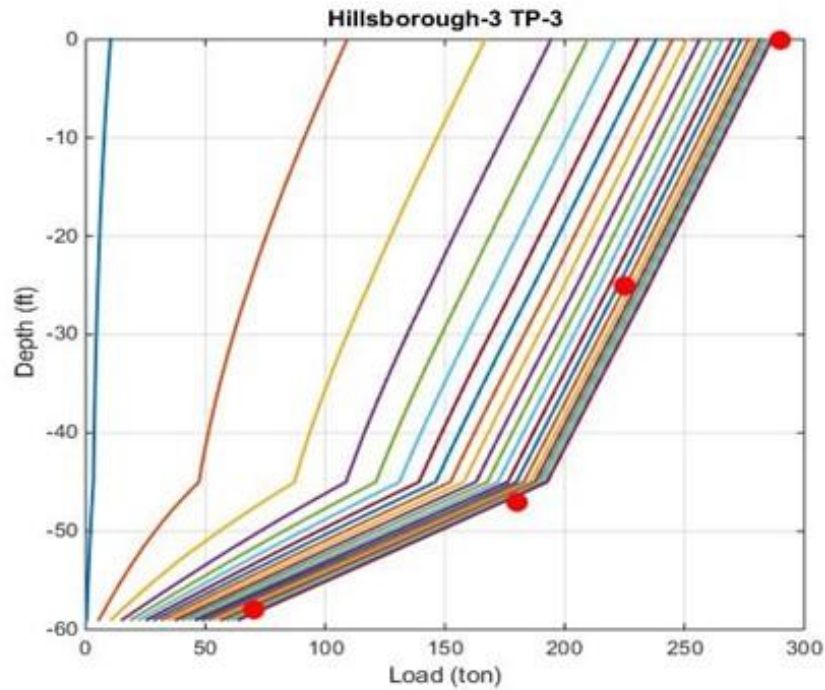


Figure 4.20 Distribution of estimated and measured pile forces in Hillsborough 3 TP3

Shown in Figures 4.21 to 4.23 are the algorithm's evaluation of Hillsborough 3 TP4. Soil stratigraphy for this pile was silty sand underlain by stiff clay. Shown in Figure 4.21, is the layering: layer 1 – 43 ft thick sand layer, layer 2 – 15ft thick sand layer and layer 3– 2ft thick stiff clay layer along with the back calculated ultimate unit skin frictions (0.77 tsf – sand, 0.63 tsf – sand, and 4.65 tsf – stiff clay) and estimated vs. measured load – displacement response of the pile. Evident from the figure, the measured and estimated match up to 0.3” and then differ. This difference (e.g. 0.35”) is attributed to the tip model of the pile. The general clay (FHWA) tip model was used for the material, which appears to mobilize too fast. Note, only 2’ of pile was embedded into the stiff clay, resulting in development of end bearing.

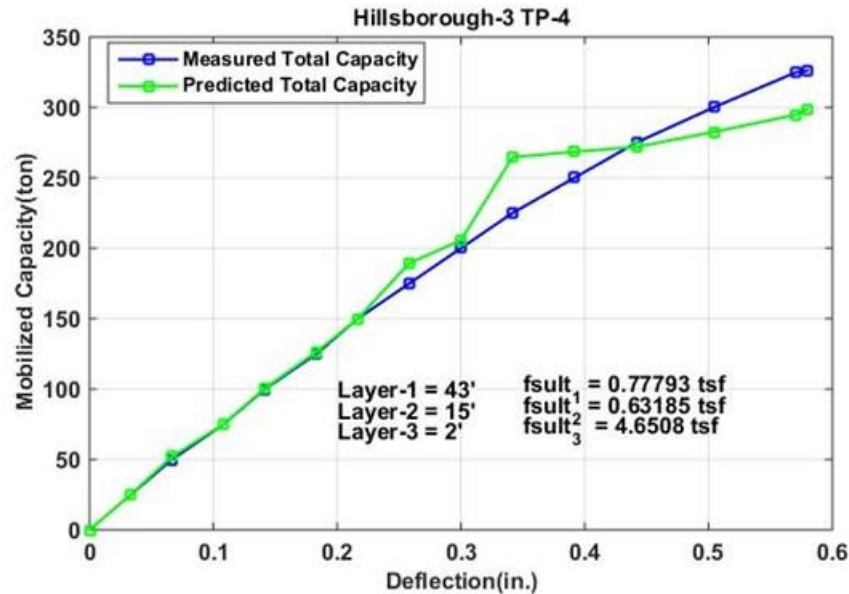


Figure 4.21 Measured and estimated load vs. displacement of Hillsborough 3 TP4

Presented in Figure 4.22, is the mobilized side and tip resistance of each segment (layer) as function of displacement and applied top load (Figure 4.21). A review of Figure 4.22 shows the layers 1 (sand) is fully mobilized at displacements less than 0.25 inches and contribute little if any additional resistance to further loading of the pile. The second sand layer 2 contributes to the pile's resistance from pile head top movement of 0.2" to 0.3"; for larger pile head movements, i.e. > 0.2" segment 3, the clay is being mobilized. At top head movement of 0.58", approximately 35 tons of skin friction is mobilized along the 2 ft section of the pile. The match between the measured and estimated load displacement response of the pile, Figure 4.18 is good up to 0.3" of movement, and difference after is attributed to the tip model.

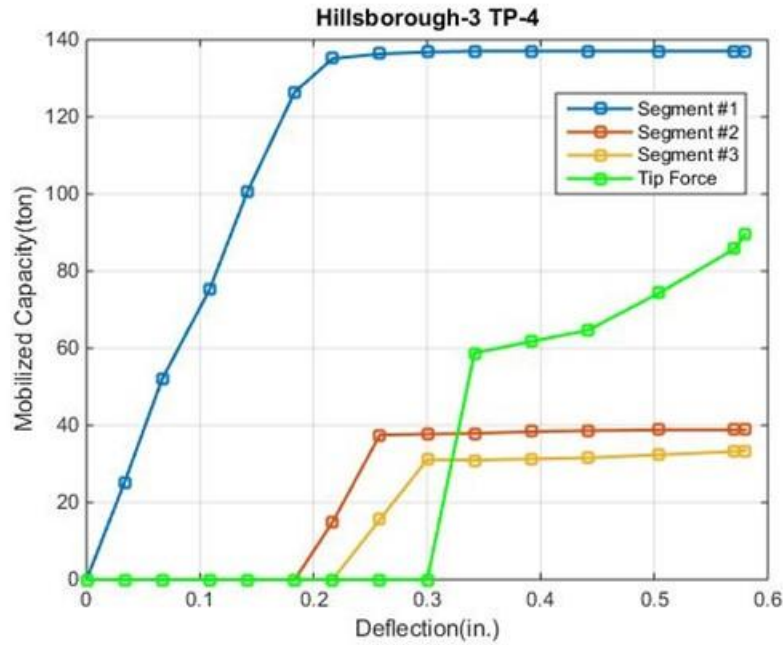


Figure 4.22 Mobilized unit side and tip resistance for 3 segments of Hillsborough 3 TP4

Plotted in Figure 4.23 is the associated pile forces with depth for Hillsborough 3 TP4 pile using the back calculated ultimate unit side and tip resistances (Figure 4.21) vs. the reported measured values for an applied load of 300 tons. As identified in Figure 4.22, the ultimate unit skin friction has been mobilized for all three layers. Also note, the location of the bottom strain gage (Figure 4.23) was approximately 2 ft from bottom of shaft (Saint Venant Principle), and doesn't identify the load transfer from the bottom clay layer. Again the measured and estimate load transfer with depth agrees within 10 to 15%.



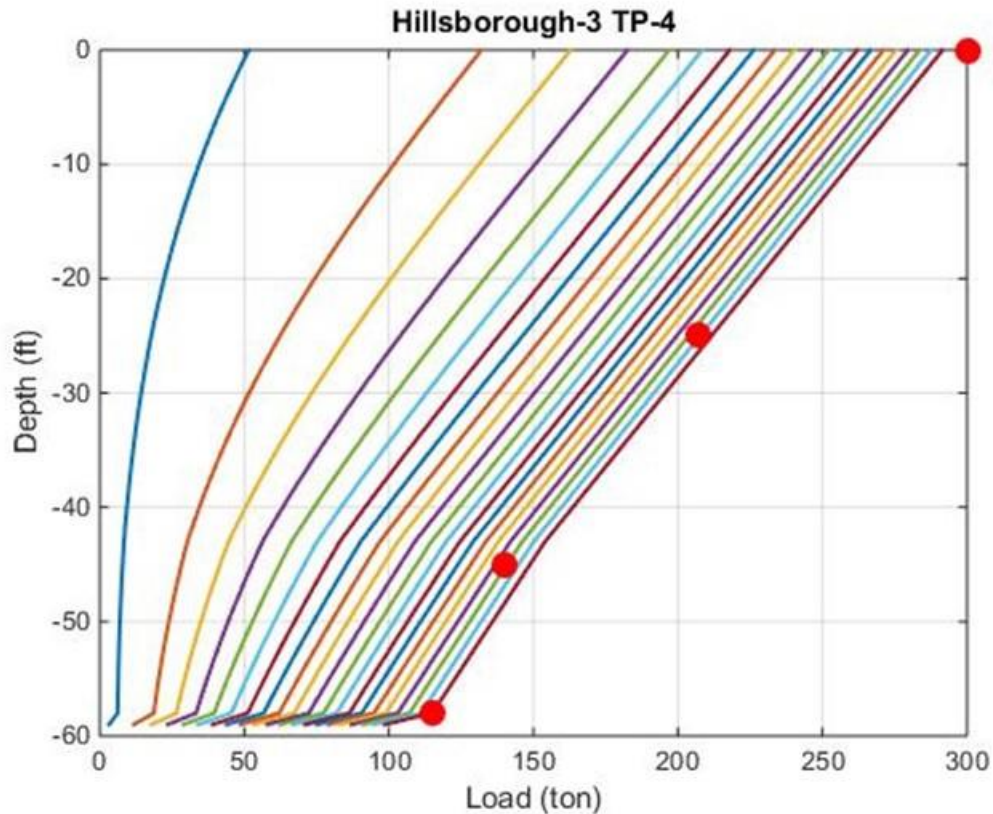


Figure 4.23 Distribution of estimated and measured pile forces in Hillsborough 3 TP4

The final pile analyzed in Hillsborough was Hillsborough 3 TP5. Again, soil stratigraphy for this pile was sand, over a stiff clay layer. Shown in Figure 4.24, is the layering: layer 1 – 30 ft thick sand layer, layer 2 – 20 ft thick sand layer and layer 3 – 19 ft thick clay layer along with the back calculated ultimate unit skin frictions (0.73 tsf – sand, 0.47 tsf – sand, and 3.42 tsf – stiff clay) and estimated vs. measured load – displacement response of the pile. Evident from the figure, the measured and estimated match up to 0.65 inches. Also, since the pile was embedded 19 ft into the stiff clay layer (predominately side friction), little if any end bearing developed, resulting in the good match.



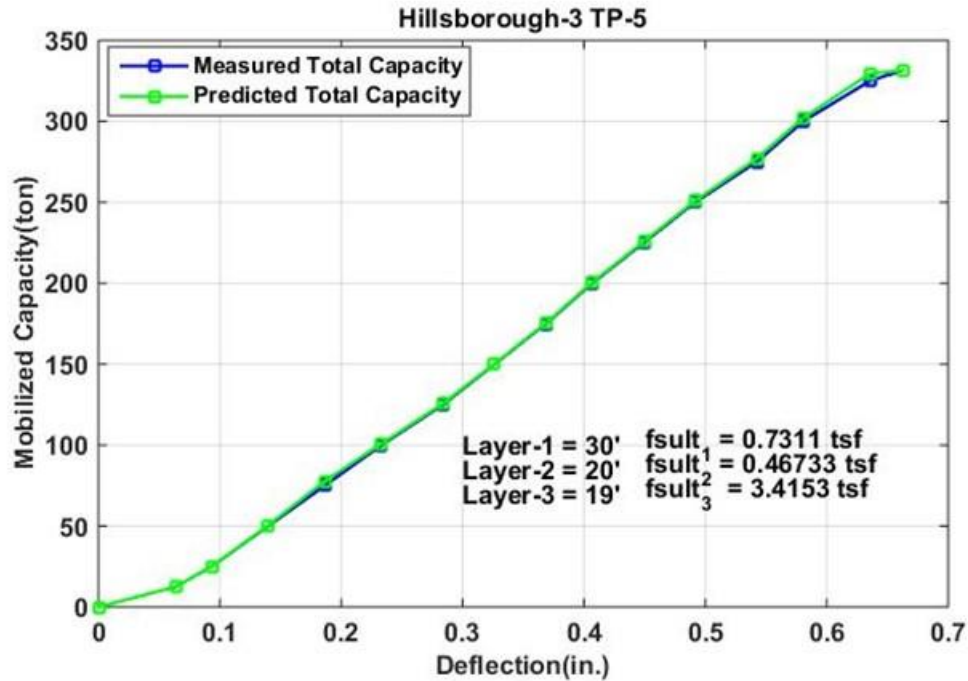


Figure 4.24 Measured and estimated load vs. displacement of Hillsborough 3 TP5

Presented in Figure 4.25, is the mobilized side and tip resistance of each segment (layer) as function of displacement and applied top load (Figure 4.24). A review of Figure 4.25 shows the layers 1 (sand) is fully mobilized at displacements less than 0.25 inches and contribute little if any additional resistance to further loading of the pile. The next sand layer contributes to the pile's resistance from pile head top movement of 0.2" to 0.3"; for larger pile head movements, i.e. > 0.3" segment 3, the stiff clay is being mobilized. At top head movement of 0.6", approximately 200 tons of skin friction is mobilized in the 19 ft section of the pile in the clay layer. The match between the measured and estimated load displacement response of the pile, Figure 4.24 is good up to 0.65" of movement, with little if any tip resistance mobilized (Figure 4.25).

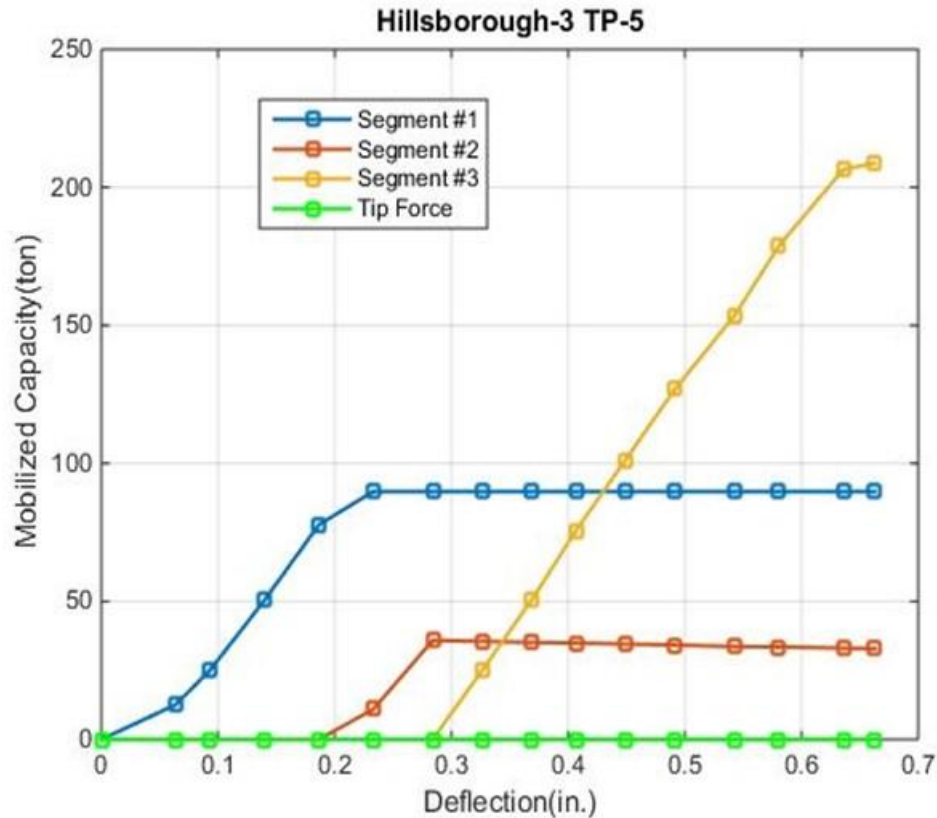


Figure 4.25 Mobilized unit side and tip resistance for 3 segments of Hillsborough 3 TP5

Plotted in Figure 4.26 is the associated pile forces with depth for Hillsborough 3 TP5 pile using the back calculated ultimate unit side and tip resistances (Figure 4.24) for multiple load steps vs. the reported measured values along the pile (red dots) for an applied load of 345 tons. As seen in Figure 4.26, the ultimate unit skin friction has been fully mobilized in the upper 2 layers, but not the bottom layer. This is evident from load distribution within the pile, Figure 4.26; note there was no tip resistance mobilized on the pile. As identified in Figure 4.25, the side friction on the bottom clay layer is nearing ultimate skin friction. Again the measured and estimate load transfer with depth agrees within 10 to 15%.

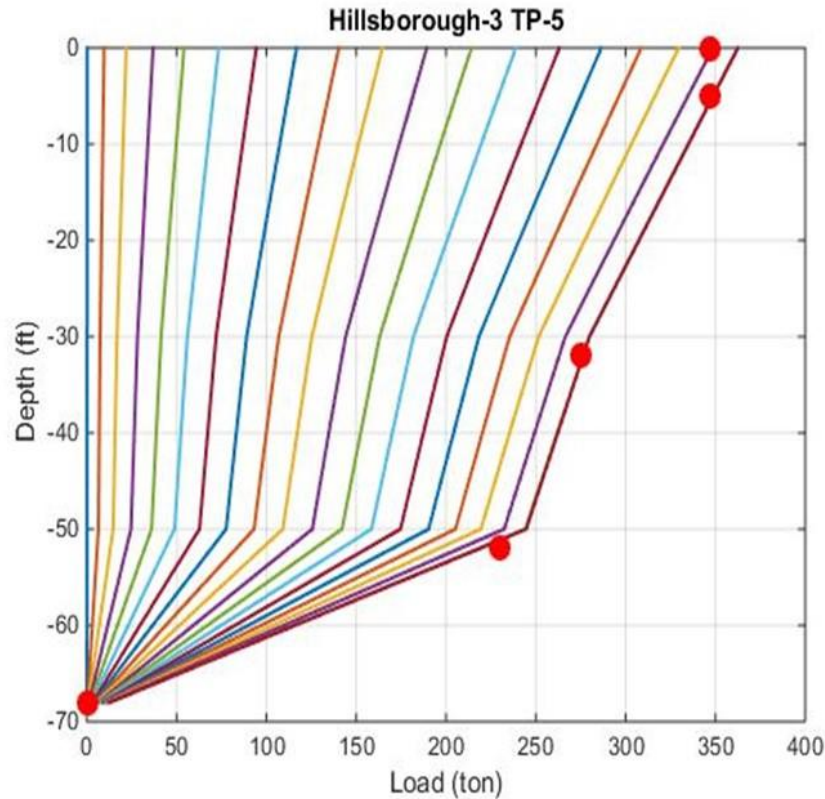


Figure 4.26 Distribution of estimated and measured pile forces in Hillsborough 3 TP5

#### 4.2.4 Nassau

The next site evaluated was in northeast Florida (Nassau 1 TP14, and Nassau 3 TP1) which had static load tests as well as load distribution (instrumentation) along with soil boring information. Nassau 1 TP14 had loose sand overlying dense sand, followed by a shelly sand. Nassau 3 TP1 had dense sand underlain by loose sand, followed by silty fine sand.

Shown in Figure 4.27, is the layering for Nassau 1 TP14 (layer 1 – 10 ft thick sand layer, layer 2 – 40 ft thick dense sand layer and layer 3 – 10 ft thick shelly sand layer) along with the back calculated ultimate unit skin frictions (0.50 tsf – loose sand, 1.38 tsf – dense sand, and 1.31 tsf – shelly sand) and estimated vs. measured load – displacement response of the pile. Evident from the figure, the measured and estimated match up to 0.4 inches.

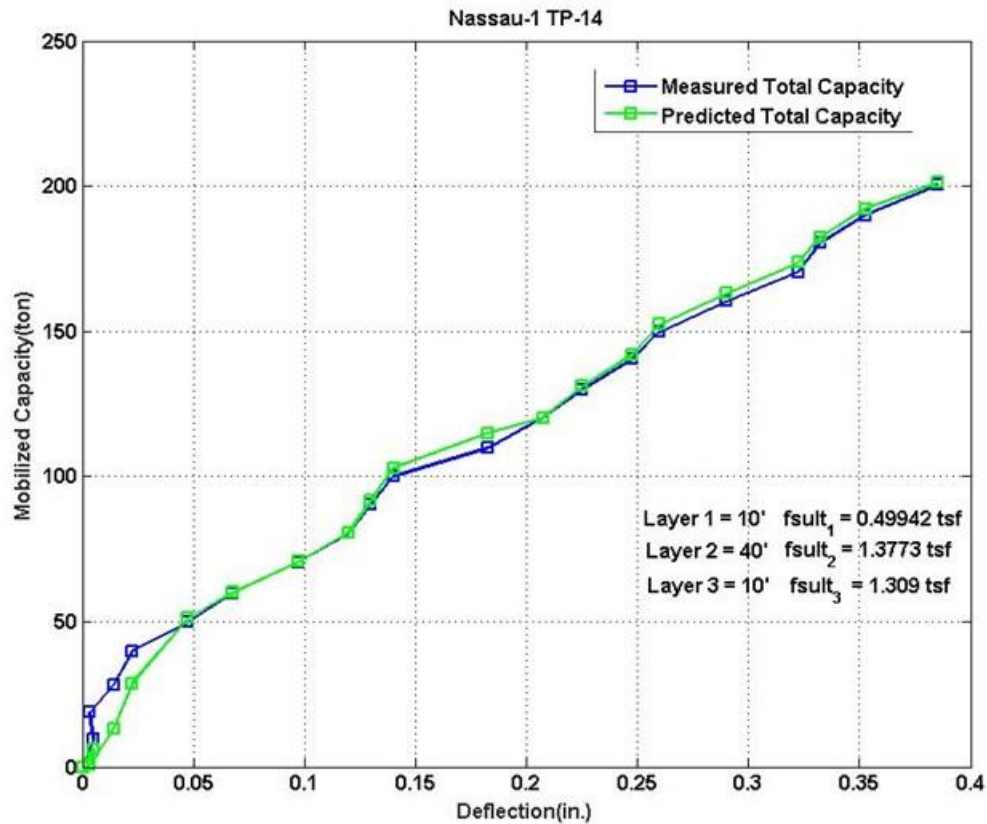


Figure 4.27 Measured and estimated load vs. displacement of Nassau 1 TP14

Plotted in Figure 4.28, is the mobilized side and tip resistance of each segment (layer) as function of displacement and applied top load (Figure 4.27). A review of Figure 4.28 shows the layers 1 (loose sand) is fully mobilized at displacements less than 0.10 inches and contribute little if any additional resistance to further loading of the pile. Layer 2 (dense sand) contributes to the pile's resistance from pile head top movement of 0.01" to 0.39"; for movements < 0.39" segment 3, the shelly sand has not been mobilized, but the segmental model has estimated the ultimate skin friction as 1.31tsf. The match between the measured and estimated load displacement response of the pile, Figure 4.27 is good up to 0.4" of movement, with little if any tip resistance mobilized (Figure 4.28).

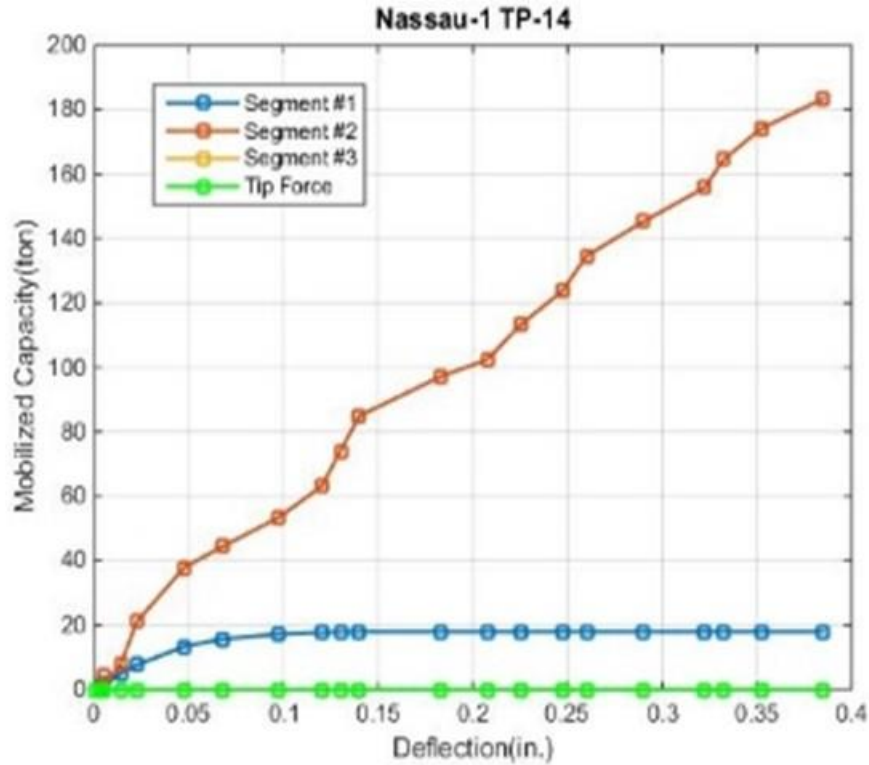


Figure 4.28 Mobilized unit side and tip resistance for 3 segments of Nassau 1 TP14

Presented in Figure 4.29 is the associated pile forces using the back calculated ultimate unit side and tip resistances (Figure 4.27) using a bottom up model with multiple load steps vs. the reported measured values along the pile (red dots) for an applied load of 200 tons. As identified in Figure 4.28, the ultimate unit skin friction has been mobilized for the first 2 layers. Also note, the location of the bottom strain gage (Figure 4.29) was approximately at the bottom of shaft. Again the measured and estimate load transfer with depth agrees within 10 to 15%.

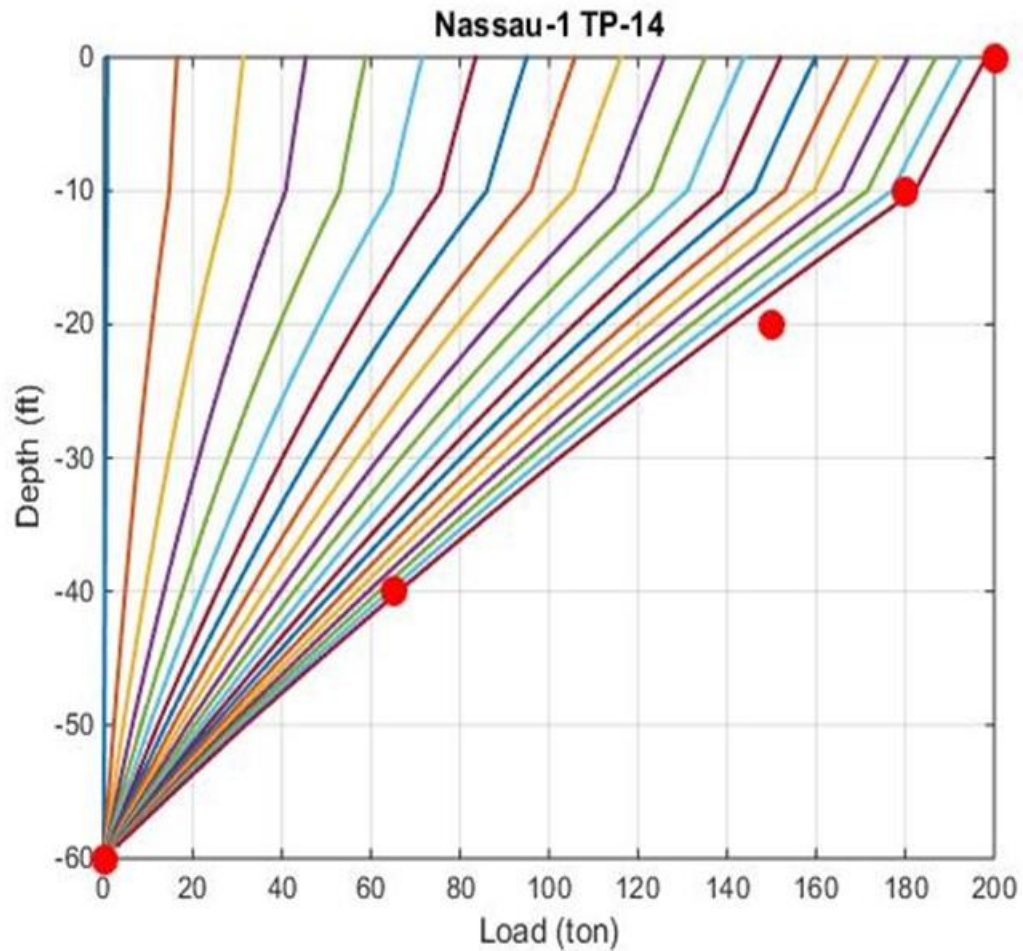


Figure 4.29 Distribution of estimated and measured pile forces in Nassau 1 TP14

Shown in Figure 4.30, is the layering for Nassau 3 TP-1 (layer 1 –10 ft thick sand layer, layer 2 – 40 ft thick sand layer and layer 3 – 10 ft thick sand layer) along with the back calculated ultimate unit skin frictions (0.84 tsf –sand, 0.268 tsf – sand, and 0.838 tsf –silty sand) and estimated vs. measured load – displacement response of the pile. Evident from the figure, the measured and estimated match up to 0.2 inches.

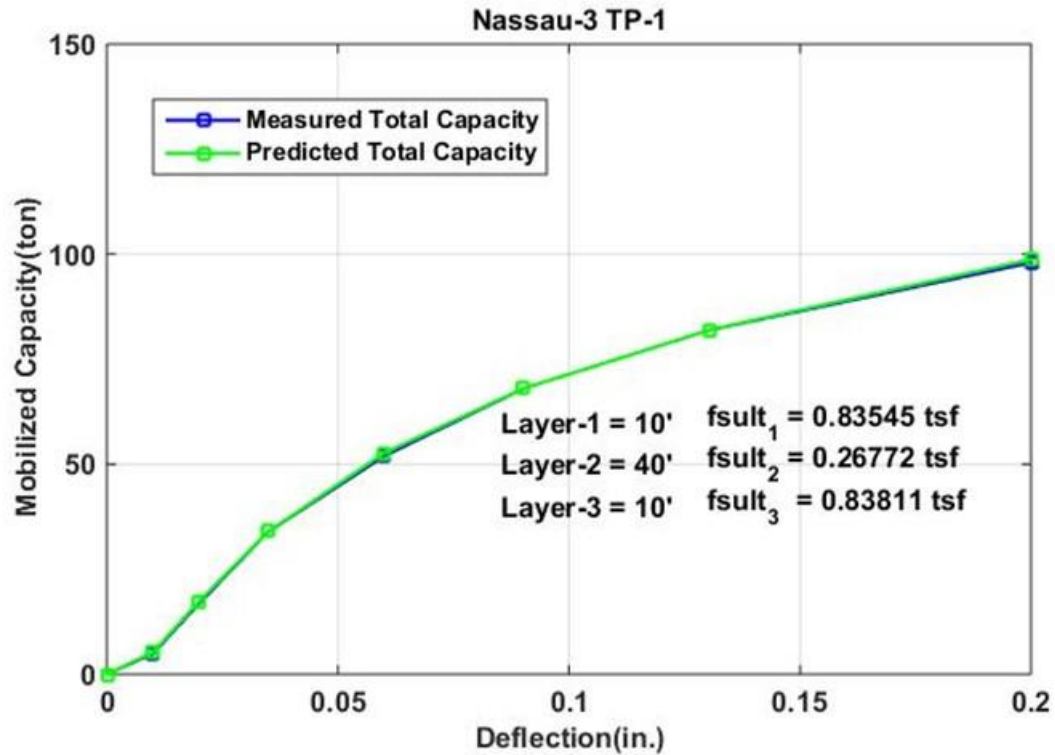


Figure 4.30 Measured and estimated load vs. displacement of Nassau 3 TP-1

Presented in Figure 4.31, is the mobilized side and tip resistance of each segment (layer) as function of displacement and applied top load (Figure 4.30). A review of Figure 4.31 shows that layer 1 (sand) is fully mobilized at displacements less than 0.1 inches and contribute little if any additional resistance to further loading of the pile. The second sand layer 2 contributes to the pile's resistance from pile head top movement of 0.02" to 0.14"; for larger pile head movements, i.e. > 0.1" the bottom sand layer, segment 3, is being mobilized. At top head movement of 0.2", approximately 100 tons of skin friction is mobilized along the full length of the pile. Little if any tip resistance is mobilized at the bottom of the pile for 0.2" of movement. The match between the measured and estimated load displacement response of the pile, Figure 4.30 is good up to 0.2" of movement, with little if any tip resistance mobilized.



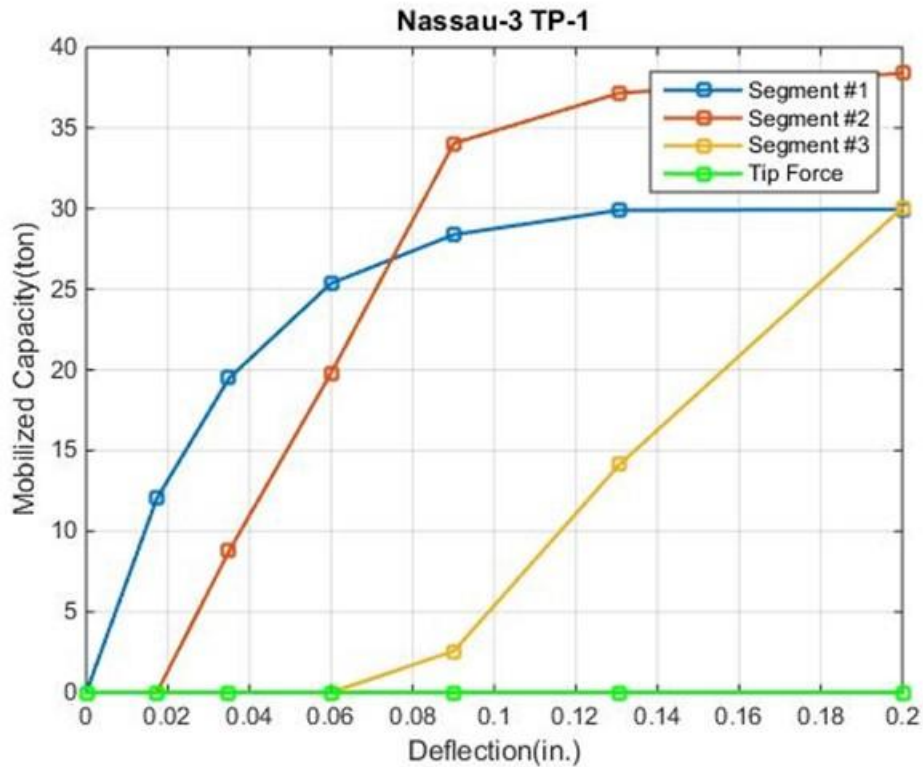


Figure 4.31 Mobilized unit side and tip resistance for 3 segments of Nassau 3 TP-1

Given in Figure 4.32 is the associated pile forces with depth for Nassau 3 TP1 pile using the back calculated ultimate unit side and tip resistances (Figure 4.30) vs. the reported measured values for an applied load of 100 tons. As identified in Figure 4.31, the ultimate unit skin friction has been mobilized for the first 2 layers. It should be noted that the top 10ft segment of pile has much higher skin friction than underlying 40 ft. It is not known if this due to enlarged diameter at the top of the pile or the dense sand layer. However, the engineer/contractor placed strain gage along the shaft to monitor soil-pile resistance (suggesting stiff layer). Again the measured and estimate load transfer with depth agrees within 10 to 15%.



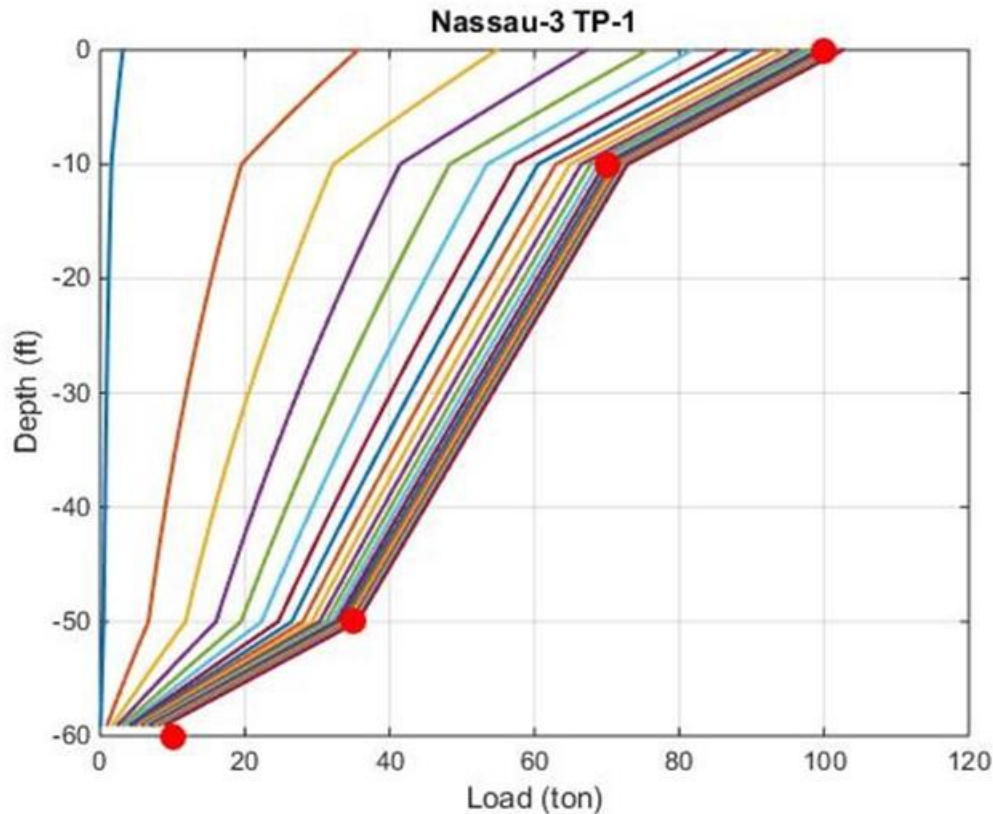


Figure 4.32 Distribution of estimated and measured pile forces in Nassau 3 TP-1

#### 4.2.5 Santa Rosa

The final site presented is in northwest Florida (Santa Rosa 1 TP-1) which had static load tests as well as load distribution (instrumentation) along with soil boring information. Santa Rosa 1 TP-1 had a sand layer underlain by a sandy clay layer.

Shown in Figure 4.33, is the layering for Santa Rosa 1 TP-1 (layer 1 – 15 ft thick sand layer, layer 2 – 14 ft thick sand layer and layer 3 – 15ft thick sandy clay layer) along with the back calculated ultimate unit skin frictions (0.83 tsf –sand, 0.83 tsf – sand, and 0.185 tsf –sandy clay) and estimated vs. measured load – displacement response of the pile. Evident from the figure, the measured and estimated match up to 0.3 inches. After 0.3 inches the estimated

diverges from the measured due to mobilization of tip resistance which was modeled with FHWA's normalized clay model.

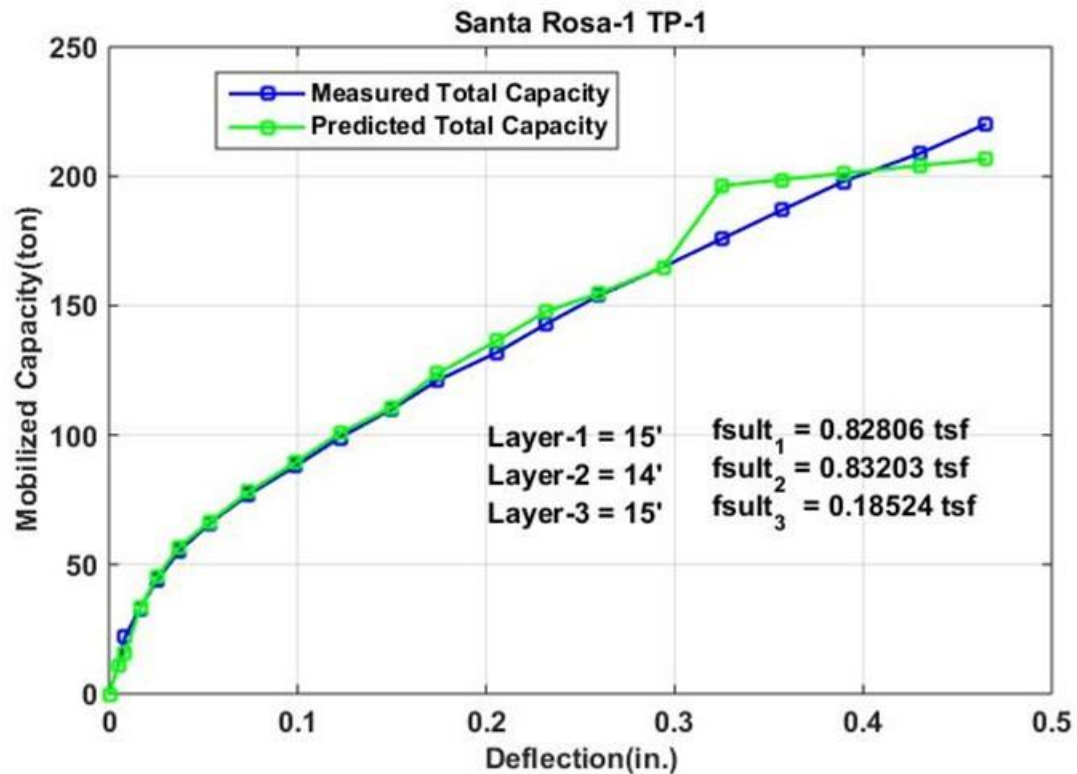


Figure 4.33 Measured and estimated load vs. displacement of Santa Rosa 1 TP-1

Plotted in Figure 4.34, is the mobilized side and tip resistance of each segment (layer) as function of displacement and applied top load (Figure 4.33). A review of Figure 4.34 shows that layer 1 and 2 (both sand) are fully mobilized at displacements less than 0.25 inches and contribute little if any additional resistance to further loading of the pile. Note, both contribute almost the same resistance (70-75 tons). Layer 3 (sandy clay) contributes to the pile resistance from pile head top movement of 0.22" to 0.3"; for larger pile head movements, i.e. top displacements > 0.3" the load is being mobilized at the tip of the auger cast pile. Evident from Figures 4.33 and 4.34, the tip is being mobilized quickly with little change from 0.35" to 0.45".

Due to its match (Figure 4.33) and shape (Figure 4.34), a more gradual increasing tip resistance with displacement may be more representative for stiff clays. The match between the measured and estimated load displacement response of the pile, Figure 4.33 is good up to 0.3” when the tip model was mobilized.

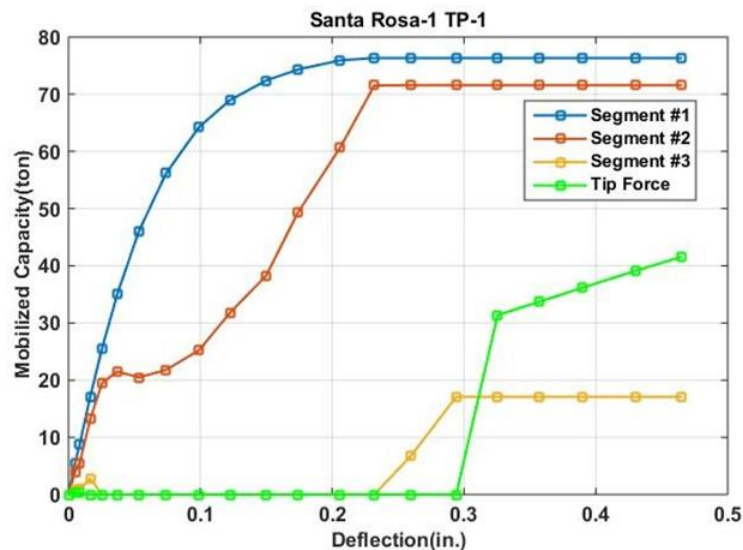


Figure 4.34 Mobilized unit side and tip resistance for 3 segments of Santa Rosa 1 TP-1

Presented in Figure 4.35 is the associated pile forces with depth for Santa Rosa 1 TP1 pile using the back calculated ultimate unit side and tip resistances (Figure 4.33) for multiple load steps vs. the reported measured values along the pile (red dots) for an applied load of 200 tons. As identified in Figure 4.34 and 4.35, the ultimate unit skin friction has been mobilized for all 3 layers. Again the measured and estimate load transfer with depth agrees within 10 to 15%.

A comparison between estimated unit skin frictions from the segmental approach and the measured unit skin frictions from field instrumentation are presented in chapter 6. The bias (measured/estimated), and coefficient of variation (standard deviation / mean) of the bias will be found and used when assessing the LRFD phi for each method.

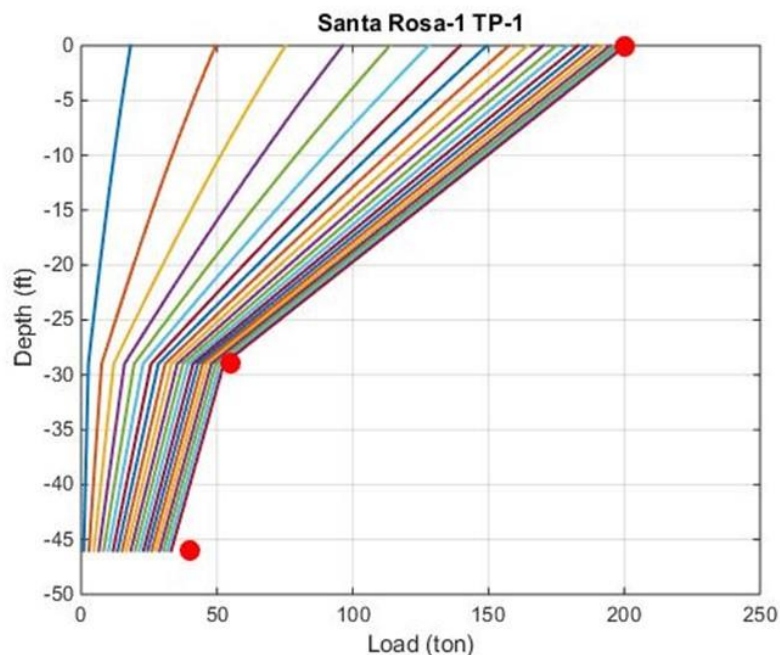


Figure 4.35 Distribution of estimated and measured pile forces in Santa Rosa 1 TP-1

#### 4.3 Estimated Nominal Resistance of Miami Dade ACIPs

As identified in Table 2.2, approximately 30 ACIPs were collected in the Miami Dade area. Even though no load distributions were available, the site was predominately sand underlain by Miami Limestone followed by another sand layer and then the Fort Thompson Formation. Both borings and laboratory rock strength data were available (provided by AMEC) for subsequent evaluation of design methods. Approximately 28 tests have been characterized with the segmental Matlab algorithm. Generally, the predominate resistance of the pile was provided by the upper layer (Miami Limestone) which had a range of back calculated unit skin friction from 3 tsf to 6.5 tsf and the bottom Fort Thompson formation with back calculated unit skin friction ranging from 4 tsf to 7 tsf. A number of plots (estimated & measured load vs. displacement, and unit skin friction vs. deflection) are presented for comparison below.

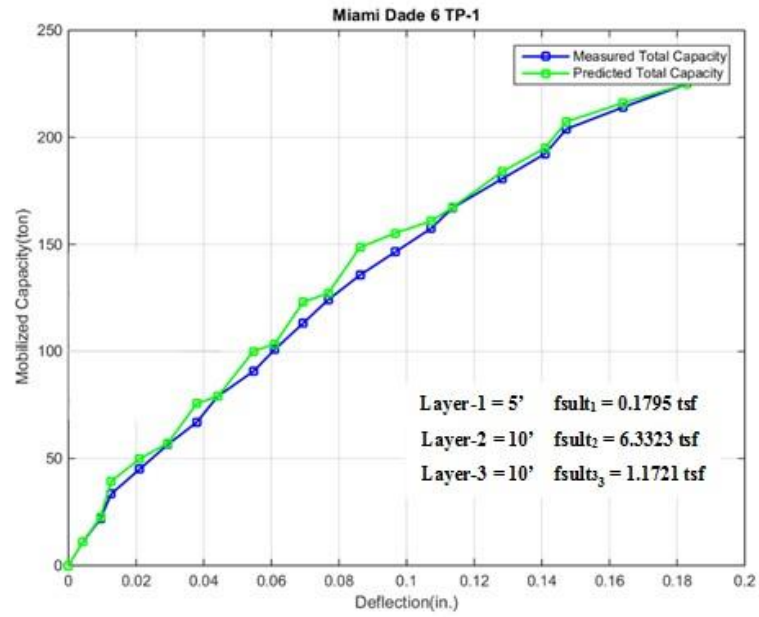


Figure 4.36 Measured and estimated load vs. displacement of Miami Dade 6 TP-1

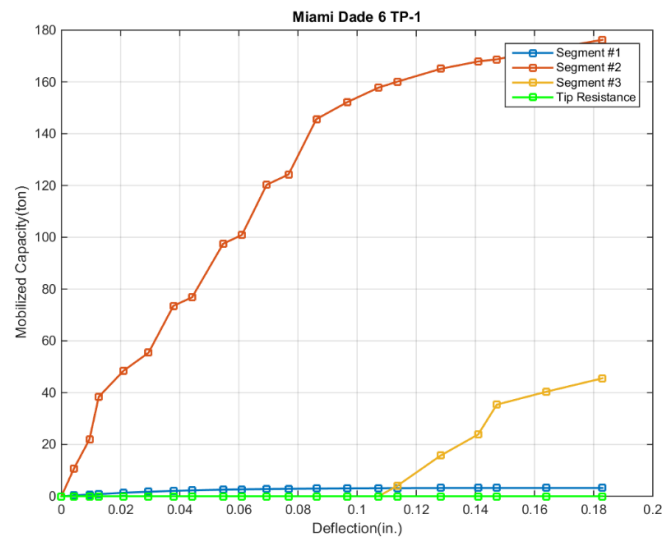


Figure 4.37 Mobilized unit side and tip resistance for 3 segments of Miami Dade 6 TP-1

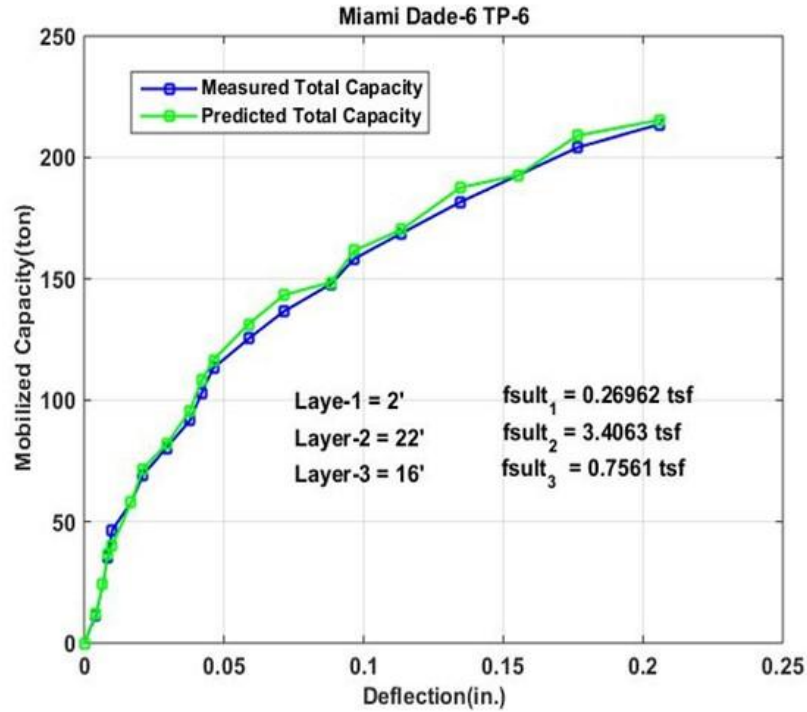


Figure 4.38 Measured and estimated load vs. displacement of Miami Dade 6 TP-6

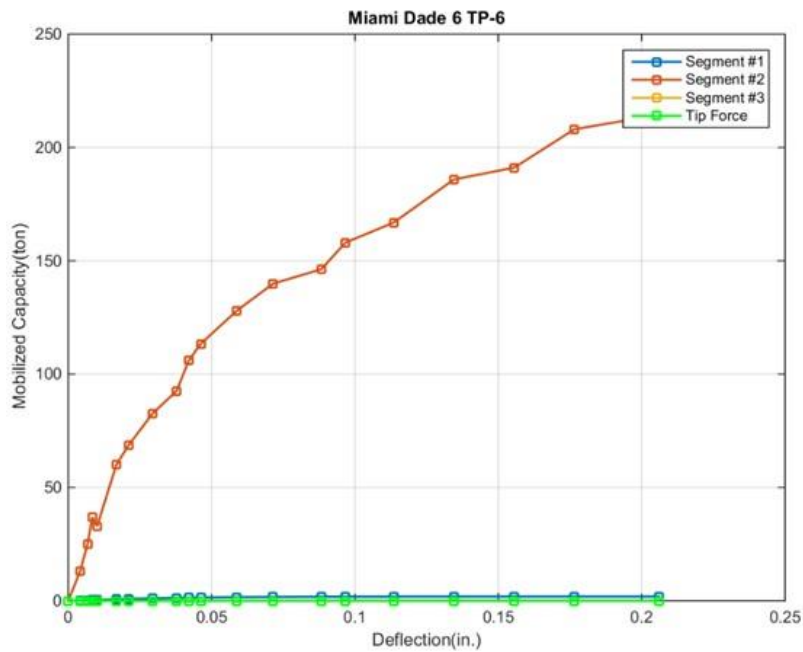


Figure 4.39 Mobilized unit side and tip resistance for 3 segments of Miami Dade 6 TP-6

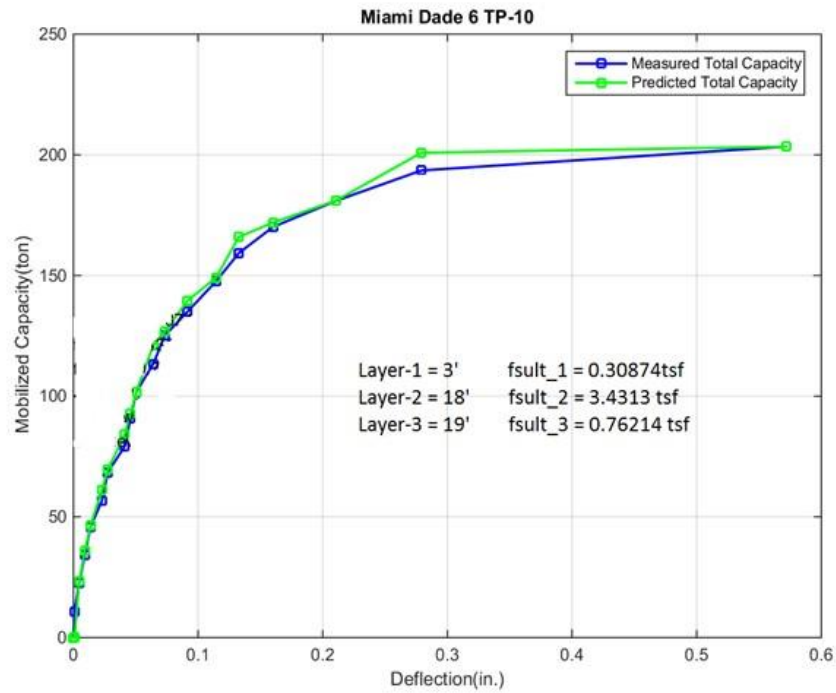


Figure 4.40 Measured and estimated load vs. displacement of Miami Dade 6 TP-10

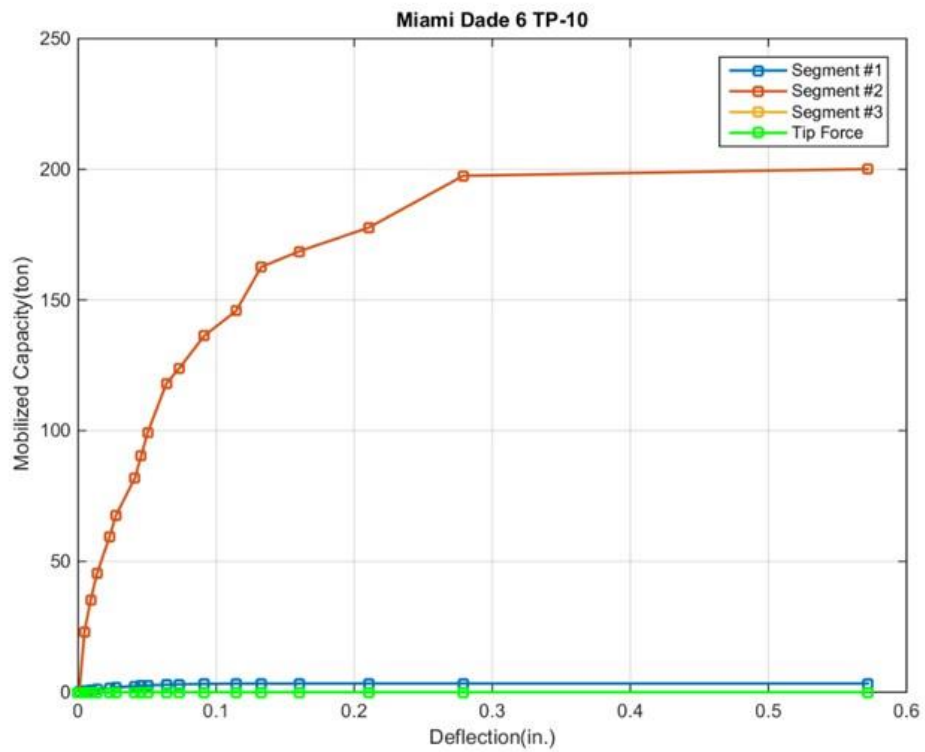


Figure 4.41 Mobilized unit side and tip resistance for 3 segments of Miami Dade 6 TP-10

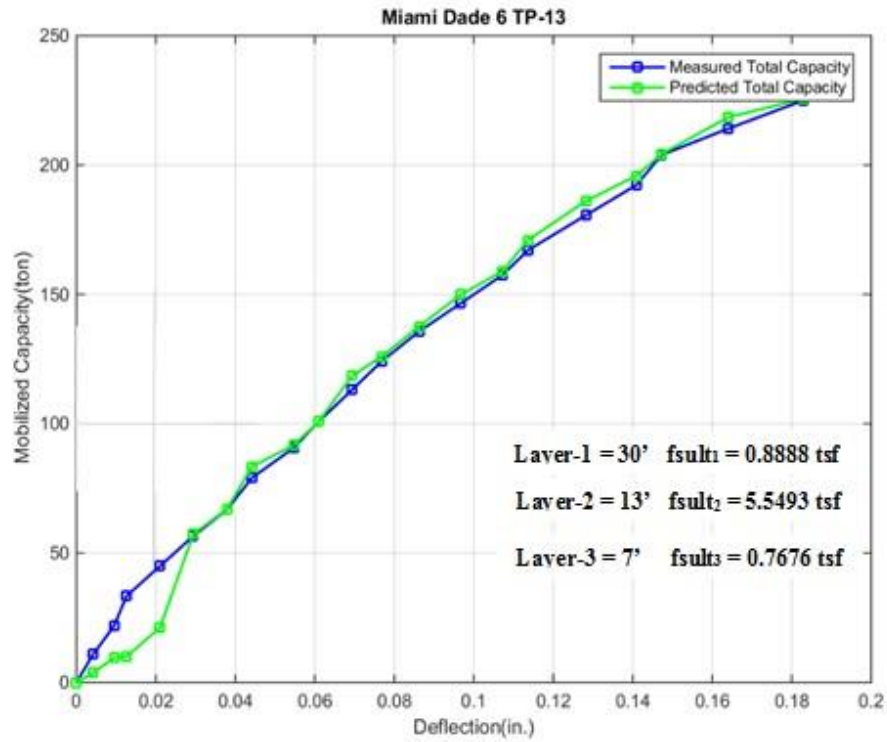


Figure 4.42 Measured and estimated load vs. displacement of Miami Dade 6 TP-13

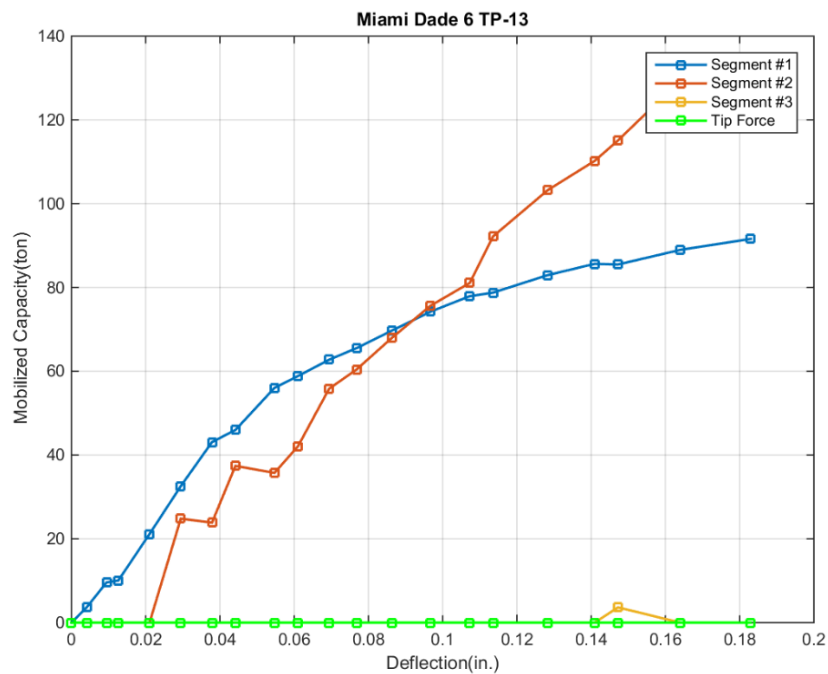


Figure 4.43 Mobilized unit side and tip resistance for 3 segments of Miami Dade 6 TP-13



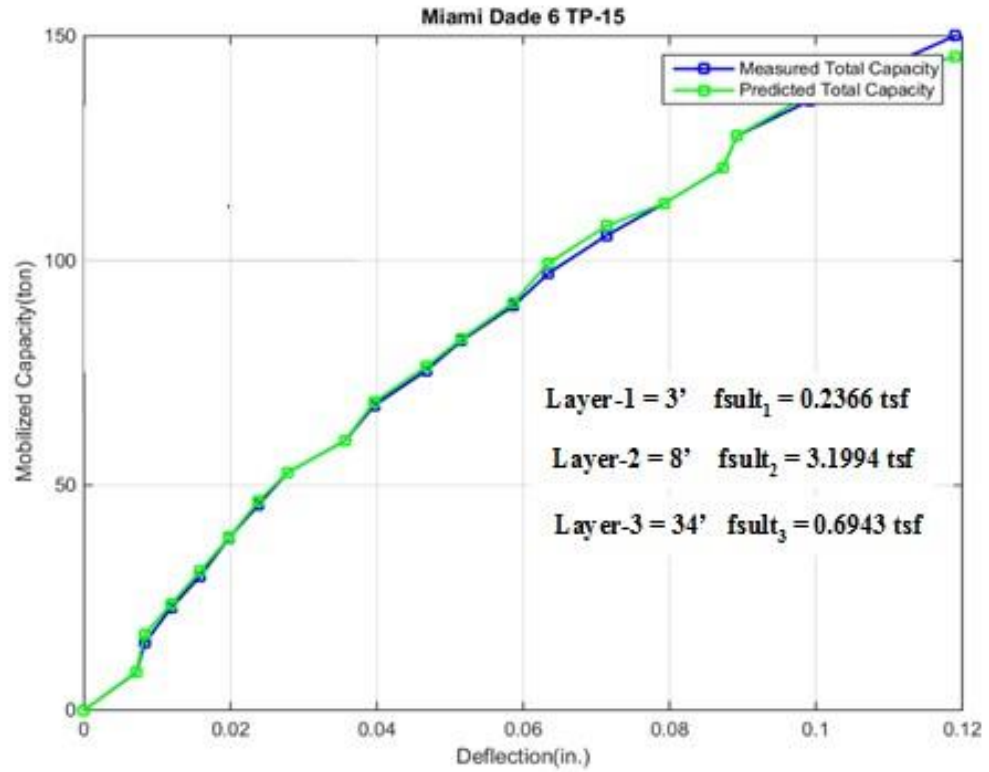


Figure 4.44 Measured and estimated load vs. displacement of Miami Dade 6 TP-15

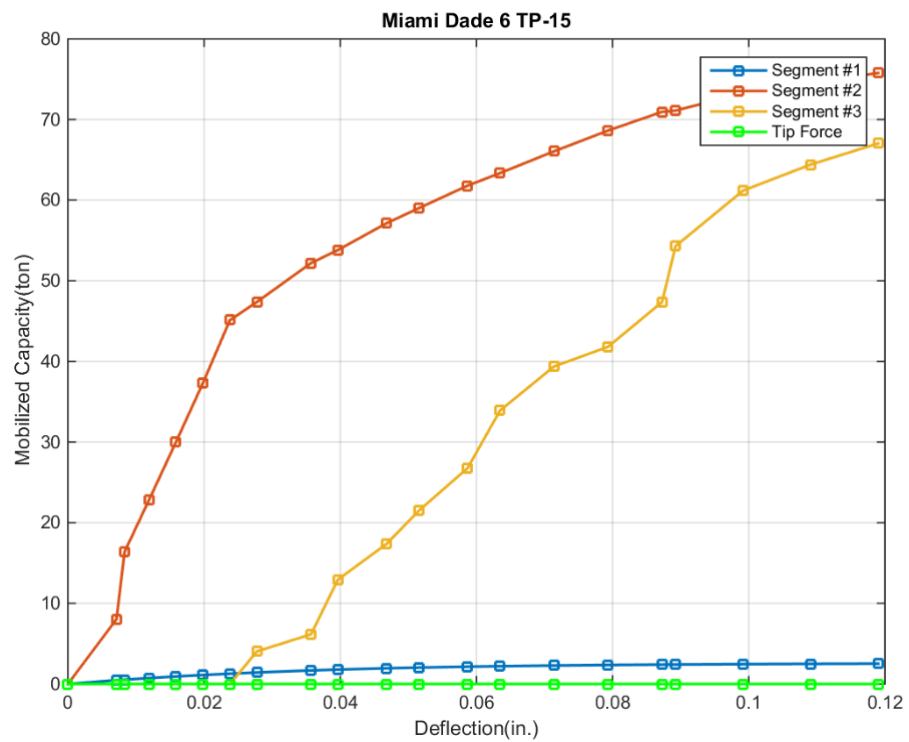


Figure 4.45 Mobilized unit side and tip resistance for 3 segments of Miami Dade 6 TP-15

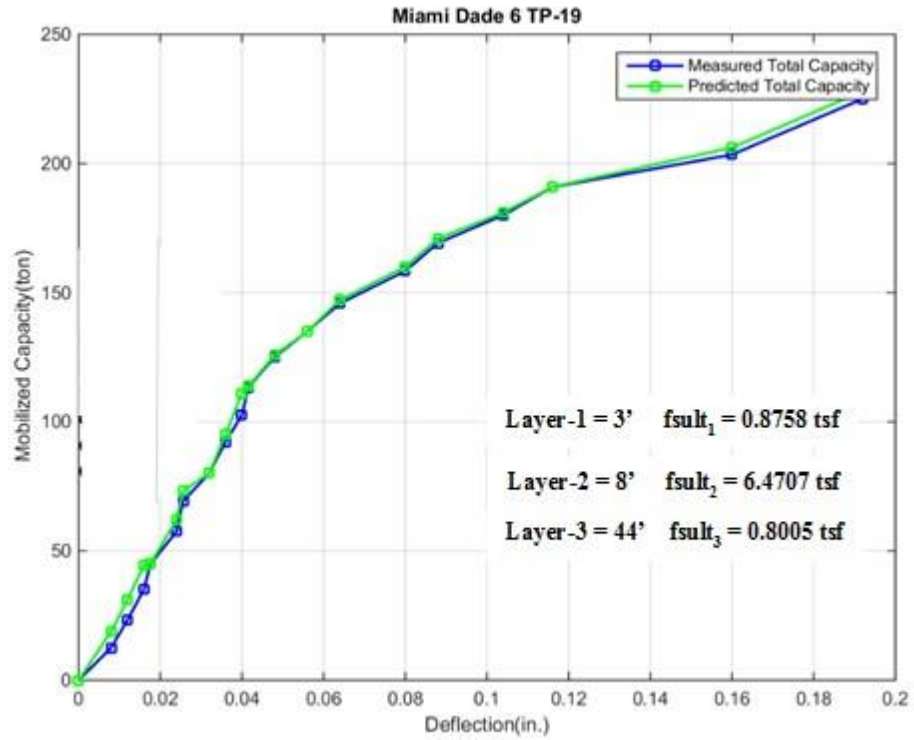


Figure 4.46 Measured and estimated load vs. displacement of Miami Dade 6 TP-19

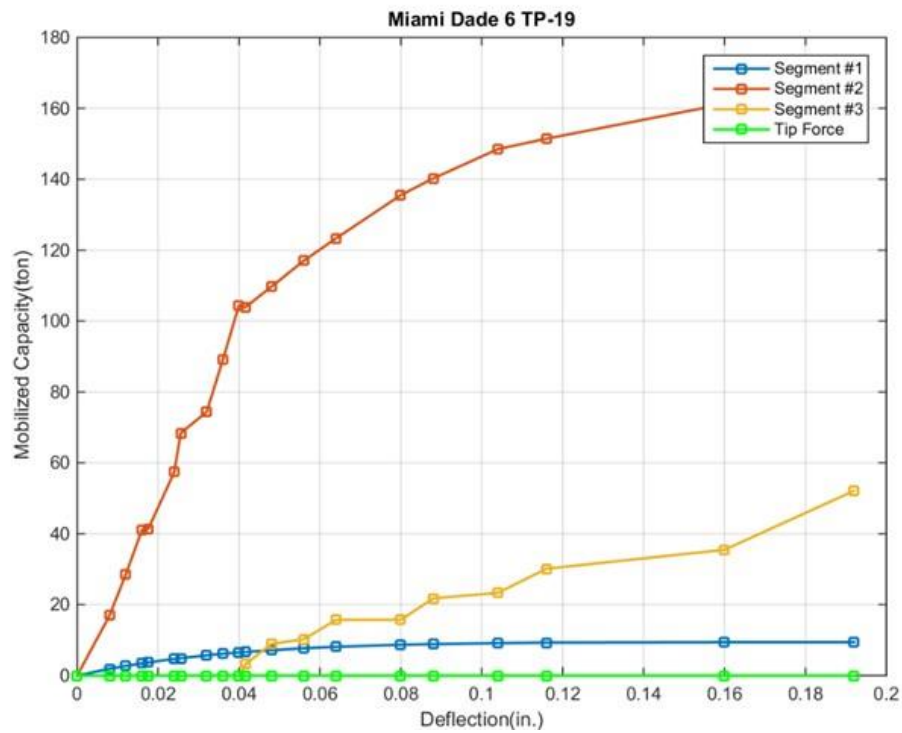


Figure 4.47 Mobilized unit side and tip resistance for 3 segments of Miami Dade 6 TP-19

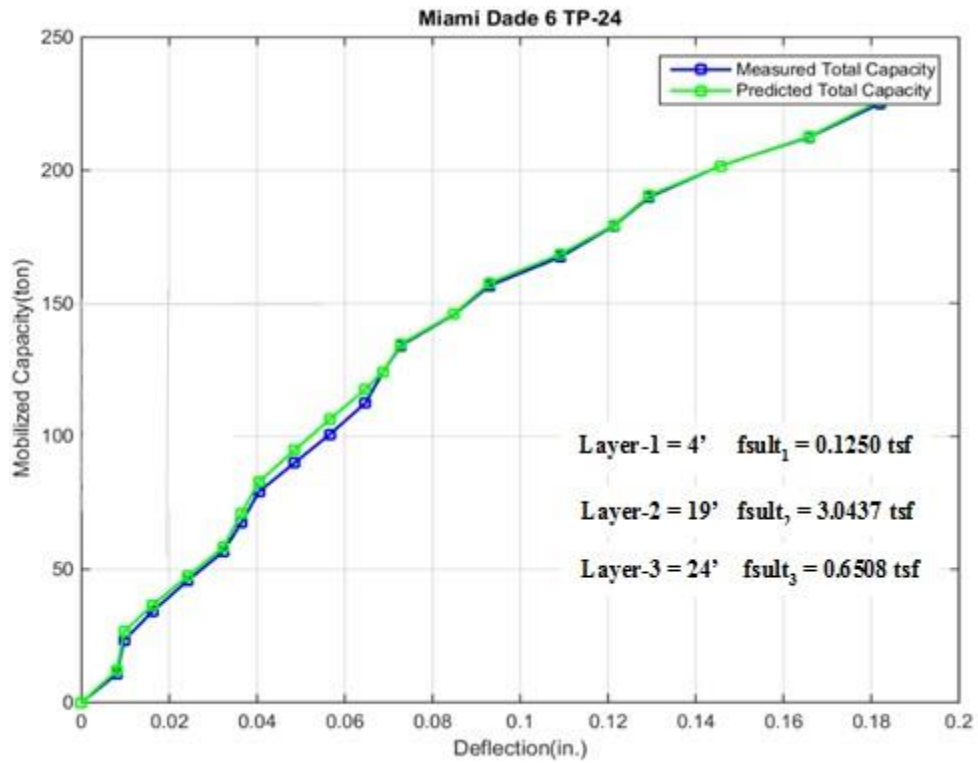


Figure 4.48 Measured and estimated load vs. displacement of Miami Dade 6 TP-24

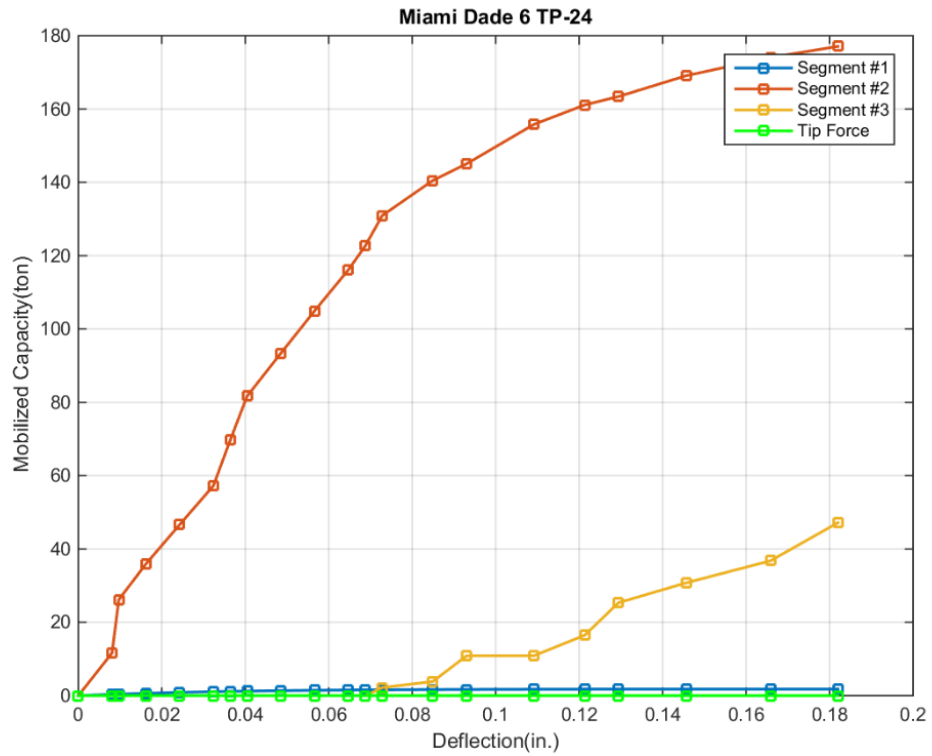


Figure 4.49 Mobilized unit side and tip resistance for 3 segments of Miami Dade 6 TP-19

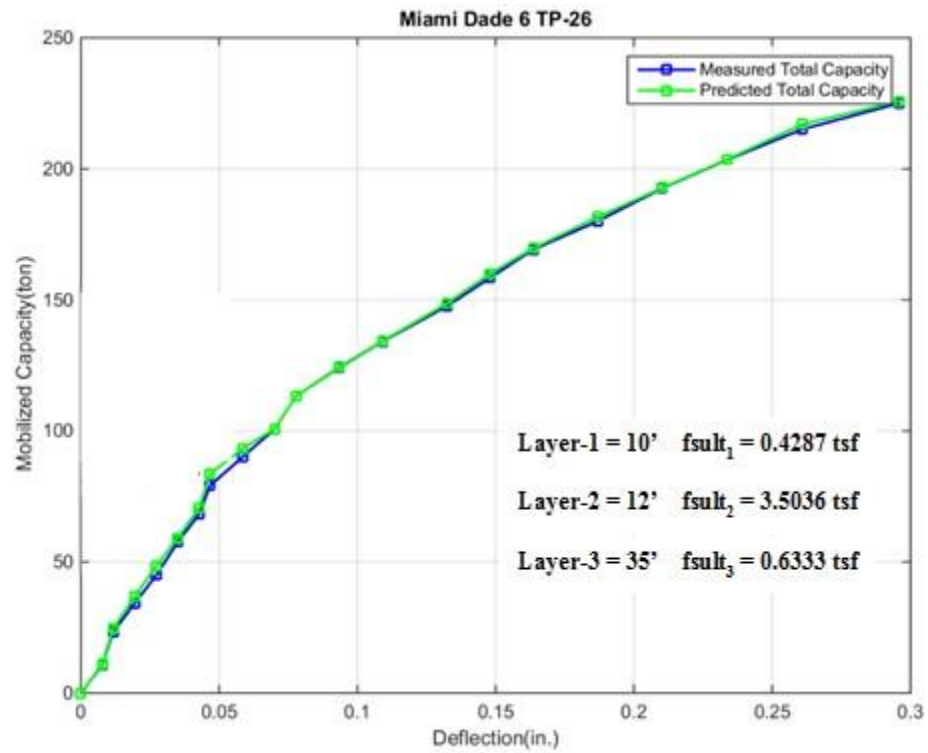


Figure 4.50 Measured and estimated load vs. displacement of Miami Dade 6 TP-26

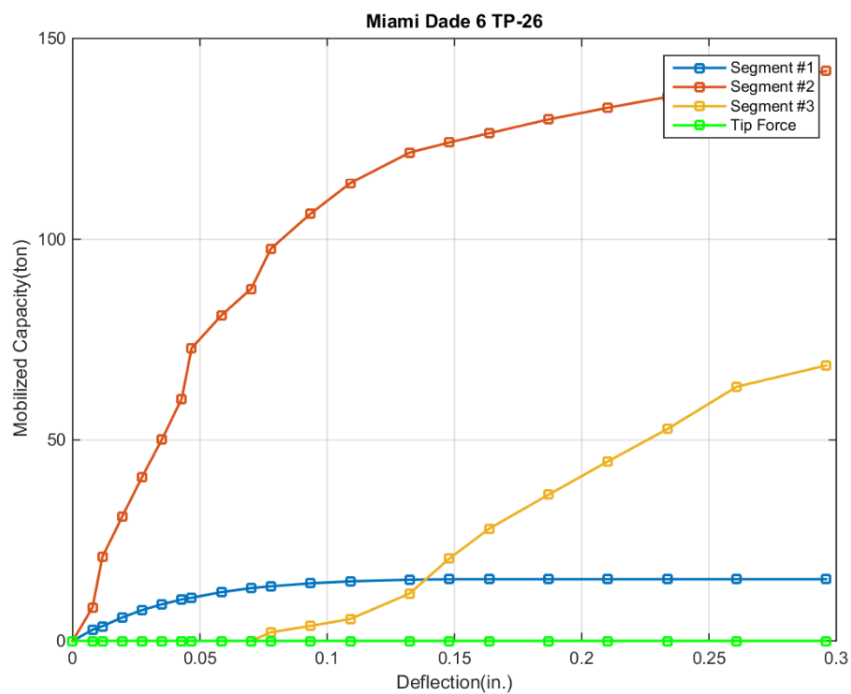


Figure 4.51 Mobilized unit side and tip resistance for 3 segments of Miami Dade 6 TP-26

#### 4.4 Estimated Nominal Resistance of All ACIPs in Florida

Inspection of the 78 load tests, revealed that the maximum pile head displacement was 1.18" (Hillsborough – 16" x 60', clay, and sand site), but a majority (> 90%) of pile top displacements were in the range of 0.1 to 0.3 inches (Table 2.2). Since typical failure (e.g. Davisson, FHWA, etc.) relate to displacements in the range of 0.4" to 0.8" for typical ACIP diameters (e.g. FHWA – 5% diameter:  $0.05 \times 14" = 0.75"$ ), most, if not all, of the load tests did not reach nominal resistance, or plunging failure, and were generally only loaded to twice the design load (ASTM D1143) since the database was collected mainly from the private sector. Moreover, given the nominal pile head displacements (0.1" to 0.3") as well as typical pile lengths (40 to 60 ft), observed mobilized tip resistance was small compared to applied top load. For instance, the maximum mobilized tip resistance in the database was 30% of top load and occurred with a large pile top displacement (i.e. Hillsborough >1.0") for a pile embedded in soil only. Generally, the average tip resistance for the database was less than 10% of applied top load; in the case of the Miami ACIP piles (embedded in 2 layers of limestone: Miami and Fort Thompson), small top movements (< 0.3") were observed and little if any tip resistance was found. Current practice is to design for side friction only to address load transfer characteristics (upper layers would be mobilized past ultimate into residual response to transfer load to deeper layers), punching shear when tipping near the bottom of the bearing layer, and quality control during installation/grouting. After discussions with FDOT engineers, the LRFD  $\Phi$  assessment for the project focused only on side friction of ACIPs.

Given in Table 4.1 are the estimated unit side frictions of the ACIP piles in Florida using the MatLAB code (segmental approach) identified in section 4.2. All reported numbers are estimated nominal unit skin friction values. Since the numbers are estimates, the bias,  $\lambda$ ,

(measured/estimated-segmental) and CV ( $\sigma_{\text{measured/segmental}} / \lambda_{\text{measured/segmental}}$ ) of the segmental approach will be found (chapter 6) by comparing the estimates side resistances against the 13 (see section 4.1) instrumented piles (i.e., embedded strain gauges) from which measured values were obtained,. Subsequently (section 6.1), the estimated resistance will be obtained by multiplying the estimated skin friction (Table 4.1) by the segmental approach method bias,  $\lambda$  (measured/estimated-segmental, section 6.1)

The results in Table 4.1 are separated by county/city with variable color coded segment length (depth range). The yellow segments represent sand, light green are clay, dark green are marl, light grey are Miami Limestone, light orange Ocala Limestone, light blue Anastasia Limestone and dark grey are Fort Thompson Limestone. All piles that had very small displacements ( $< 0.1''$ , e.g. Miami Dade 6, TP-7) were not considered, since the ultimate skin friction was not mobilized. Finally, the uplift or tension piles were not used (e.g. West Palm) due to possible differences with top down compression loading.

A total of 53 nominal estimated skin friction values were sand, 32 were clay (4 were Duval Marl – USC (CH)), 23 were Miami Limestone (Miami-Dade and Broward), 10 were Fort Thompson Limestone, 3 were Anastasia Limestone and 4 were Ocala Limestone. The average unit skin friction of sand ranged from 0.2 tsf to 1.5 tsf; the clay ranged from 0.3 tsf to 4.65 tsf; the Miami Limestone varied from 1.5 tsf to 6.5 tsf; the Fort Thompson varied from 4 tsf to 7.2tsf, the Anastasia Limestone varied from 2.06 to 4.6 and the Ocala IGM from 2.1 to 2.7 tsf. The depths of soil and rock varied significantly in the study (see Table 4.1). The sand and clay occurred from the ground surface to depths of 80ft. Miami Limestone occurred from 5ft to 30ft (Prieto, 1981). The north Florida IGM varied from 40ft to 64ft and the Fort Thompson varied from 25 ft to 80ft (Prieto, 1981) in South Florida.

The following is a number of general observations of the estimated ultimate unit skin friction:

- The estimated Fort Thompson range (4 – 7.5 tsf) agreed with Frizzi and Meyer (2000) range of 3 to 8 tsf as well as the estimated Miami (1.5 – 6.5 tsf) vs. 2 - 8 tsf (Frizzi and Meyer, 2000). The Anastasia Limestone varied from 2.1 to 4.6 tsf; since the highest value (4.6 tsf, Broward 2, TP-1) occurred at boundary with Miami Limestone Formation (see 2.3.3), and other values were within the Miami range, it was decided to combine the Anastasia (light blue) with the Miami (light grey) for total of 26 values.
- The Jacksonville Marl (Duval, Table 4.1), discussed in section 4.2.2, classified as CH (Wolf 2004), does not have the highest  $f_s$  (3 to 3.5 tsf); for instance, Hillsborough at depth of 55 to 60 ft has  $f_s = 4.65$  tsf (TP-5). The higher clay unit skin friction at deeper depths may be attributed to the undrained shear strength of the clay as function of vertical effective stress (e.g. Kulhway & Mayne), i.e.  $S_u/\sigma'_v = \text{constant}$ . Sowers (1979,) reports  $S_u$  greater than 6 tsf, for high blow count (SPT N) CH soils. Note, the marl could also be identified as Cohesive IGM ( $5\text{ksf} < S_u < 50\text{ksf}$ , Table 3.4); however there are insufficient number of values (3, Table 4.1) for separate evaluation. Consequently, the marl will be either considered part of the Clay data set or removed when evaluating the Clay methods LRFD resistances.
- The ultimate unit side friction of the sand had the lowest mean and smallest variability (0.2 tsf to 1.5 tsf) compared to clay and rock for the depth ranges considered.

Table 4.1 Estimated nominal unit skin friction of ACIP piles in Florida

Location	Project Name	Soil Type	Diameter (in)	Embedded Length (ft)	Test Type	Water Table Depth (ft)	Instrumentation	Peak Displacement Load Test (in)	Segment #1 (tsf)	Depth range (ft)	Segment #2 (tsf)	Depth range (ft)	Segment #3 (tsf)	Depth range (ft)
Alachua	Alachua-1 TP-2	Clay & IGM	16	64	Static	29	Load-Deflection	0.085	0.652	0~20	0.367	20~40	2.352	40~64
	Alachua-1 TP-3	Clay & IGM	16	64	Static	31	Load-Deflection	0.125	0.896	0~20	0.882	20~40	2.488	40~64
	Alachua-1 TP-4	Clay & IGM	16	64	Static	26	Load-Deflection	0.183	0.489	0~20	0.275	20~40	2.696	40~64
	Alachua-1 TP-5	Clay & IGM	16	64	Static	28	Load-Deflection	0.219	0.600	0~20	0.336	20~40	2.124	40~64
	Alachua-2 TP-1	Clay	14	42	Static	4.5	Load-Deflection	0.288	N/A		N/A		N/A	
	Alachua-2 TP-2	Clay	14	42	Static	5	Load-Deflection	0.325	0.461	0~15	1.609	15~30	1.496	30~42
	Alachua-2 TP-3	Clay	14	42	Static	6.5	Load-Deflection	0.295	0.555	0~15	1.498	15~30	1.493	30~42
	Alachua-2 TP-5	Clay	14	42	Static	5	T-Z & Load-Defl.	0.341	0.596	0~15	1.235	15~30	1.237	30~42
	Alachua-2 TP-XX-1	No Boring	14	42	Static	None	Load-Deflection	0.777	N/A		N/A		N/A	
	Alachua-2 TP-XX-2	No Boring	14	42	Static	None	Load-Deflection	0.460	N/A		N/A		N/A	
	Alachua-3 TP-1	Clay, Sand & IGM	14	15	Static	12	Load-Deflection	0.549	N/A		N/A		N/A	
	Alachua-5 TP-1	Sand & Clay	14	65	Static	6	T-Z & Load-Defl.	0.600	0.498	0~27	1.424	27~65		
Broward	Alachua-5 TP-2	Sand & Clay	14	65	Static	6	T-Z & Load-Defl.	1.000	0.497	0~15	1.453	15~40	3.040	40~50
	Alachua-5 TP-3	Sand & Clay	14	65	Tension	6	T-Z & Load-Defl.	0.088						
	Broward-1 TP-1	Sand & IGM	18	102	Static	5.7	T-Z & Load-Defl.	0.344	0.358	0~15	2.358	15~48	0.477	48~80
	Broward-1 TP-2	Sand & IGM	18	102	Tension	5.7	T-Z & Load-Defl.	0.009						
Duval	Broward-1 TP-5	Sand & IGM	30	140	Osterberg	1	O-Cell	0.400	0.212	0~30	2.069	30~70	2.706	70~95
	Broward-2 TP-1	Sand & IGM	14	40	Static	None	Load-Deflection	0.350	0.331	0~10	0.536	10~32	4.633	32~40
	Duval-1 TP 1-2	Sand, Marl & Clay	16	55	Static	4.5	Load-Deflection	0.289	0.341	0~30	3.197	30~45	0.967	45~55
	Duval-1 TP 2-2	Sand, Marl & Clay	16	54	Static	4.5	Load-Deflection	0.397	0.392	0~30	3.498	30~45	1.026	45~55
Hollywood	Duval-1 TP 3-2	Sand, Marl & Clay	18	54	Tension	4.5	Load-Deflection	0.192						
	Duval-1 TP 3-3	Sand, Marl & Clay	16	54	Static	4.5	Load-Deflection	0.267	0.279	0~30	3.528	30~45	1.000	45~55
	Hollywood-1 TP-1	No Boring	14	50	Static	No Boring	Load-Deflection	0.340	N/A		N/A		N/A	
	Hollywood-2 TP-1	No Boring	14	48	Static	No Boring	T-Z & Load-Defl.	0.200	N/A		N/A		N/A	
Hillsborough	Hollywood-2 TP-2	No Boring	14	48	Tension	No Boring	T-Z & Load-Defl.	0.032	N/A		N/A		N/A	
	Hillsborough-2 TP-1	No Boring	14	40	Static	None	Load-Deflection	0.079	N/A		N/A		N/A	
	Hillsborough-3 TP-1	Sand, and Clay	16	60	Static	5.2	Load-Deflection	0.548	0.543	0~43	0.570	43~55	4.650	55~60
	Hillsborough-3 TP-2	Sand, and Clay	16	60	Statnamic	5.2	T-Z & Load-Defl.	0.939	1.353	0~20	0.990	20~45	1.394	45~60
Nassau	Hillsborough-3 TP-3	Sand and Clay	16	60	Statnamic	5	T-Z & Load-Defl.	1.176	0.470	0~25	0.470	25~45	2.310	45~60
	Hillsborough-3 TP-4	Sand and Clay	16	60	Statnamic	5	T-Z & Load-Defl.	0.760	0.778	0~43	0.634	43~58	4.650	58~60
	Hillsborough-3 TP-5	Sand and Clay	16	69	Statnamic	4	T-Z & Load-Defl.	0.653	0.731	0~30	0.467	30~50	3.415	50~69
Palm Beach	Nassau-1 TP14	Sand	14	60	Static	3.8	T-Z & Load-Defl.	0.385	0.499	0~10	1.377	10~50	1.309	50~60
	Nassau-2 TP-1	Sand	16	39	Static	3	Load-Deflection	0.300	N/A		N/A		N/A	
	Nassua-3 TP-1	Sand	14	65	Static	5	T-Z & Load-Defl.	0.200	0.835	0~10	0.268	10~50	0.838	50~60
Polk	Palm Beach-1 TP-9	No Boring	16	61	Static	None	T-Z & Load-Defl.	0.113	N/A		N/A		N/A	
	Palm Beach-2 TP-8	No Boring	16	61	Static	None	T-Z & Load-Defl.	0.188	N/A		N/A		N/A	
Santa Rosa	Polk-1	Clay, Silt & Sand	18	65	Static	8.5	Load-Deflection	0.360	N/A		N/A		N/A	
	Santa Rosa-1 TP-1	Sand, Cayey Sand	24	47	Static	2.5	CPT Data	0.465	N/A		0.830	0~29	0.185	29~44
West Palm	West Palm-1 T2B	Sand	14	40	Tension	9	Load-Deflection	0.250						
	West Palm-1 T8	Sand	14	40	Tension	9	Load-Deflection	0.250						
	West Palm-1 T9B	Sand	14	40	Static	9	Load-Deflection	0.536	0.310	0~10	0.471	10~30	0.494	30~40

Green – clay; Yellow – sand; Dark Green – marl; Light Orange – Ocala Limestone; Light Blue – Anastasia Limestone; Light Grey – Miami Limestone



Table 4.1 Estimated nominal unit skin friction of ACIP piles in Florida (-continued)

Location	Project Name	Soil Type	Diameter (in)	Embedded Length (ft)	Test Type	Water Table Depth (ft)	Instrumentation	Peak Displacement Load Test (in)	Segment #1	Depth range (ft)	Segment #2	Depth range (ft)	Segment #3	Depth range (ft)
Miami Dade	Miami Dade-1 TP-1	IGM, Sand & FT Limestone	16	43	Static	5	Load-Deflection	0.343	2.100	0~18	0.441	18~35	3.910	35~43
	Miami Dade-1 TP-2	Sand & IGM	16	43	Tension	5	Load-Deflection	0.208						
	Miami Dade-5 TP-1	Sand & IGM	14	30	Static	(+) 2.5	Load-Deflection	0.148	N/A		N/A		N/A	
	Miami Dade-5 TP-2	Sand & IGM	14	30	Tension	(+) 2.5	Load-Deflection	0.270						
	Miami Dade-6 TP-1	IGM & Sand	14	25	Static	Not measured	Load-Deflection	0.183	6.425	5~14	1.500	14~25	N/A	
	Miami Dade-6 TP-2	IGM & Sand	14	40	Static	8	Load-Deflection	0.182	3.153	0~20	0.994	20~40	N/A	
	Miami Dade-6 TP-3	IGM & Sand	14	40	Static	8	Load-Deflection	0.303					N/A	
	Miami Dade-6 TP-5	IGM & Sand	14	40	Static	8	Load-Deflection	0.090	5.380	2~16	0.588	16~40	N/A	
	Miami Dade-6 TP-6	IGM, Sand & FT Limestone	14	40	Static	4	Load-Deflection	0.206	1.737	2~24	0.100	24~35	4.024	35~40
	Miami Dade-6 TP-7	IGM & Sand	14	40	Static	Not measured	Load-Deflection	0.060	N/A		N/A		N/A	
	Miami Dade-6 TP-8	IGM & Sand	14	40	Static	Not measured	Load-Deflection	0.093	N/A		N/A		N/A	
	Miami Dade-6 TP-9	IGM & Sand	14	40	Static	Not measured	Load-Deflection	0.142	3.005	1~24	0.478	24~40	N/A	
	Miami Dade-6 TP-10	IGM & Sand	14	40	Static	Not measured	Load-Deflection	0.572	3.431	5~22	0.404	22~40	N/A	
	Miami Dade-6 TP-11	IGM & Sand	14	23	Static	5.5	Load-Deflection	0.073	3.759	1~8	0.907	8~23	N/A	
	Miami Dade-6 TP-12	IGM & Sand	14	23	Static	5.5	Load-Deflection	0.346	N/A		N/A		N/A	
	Miami Dade-6 TP-13	IGM, Sand & FT Limestone	14	50	Static	Not measured	Load-Deflection	0.072	1.899	1~25	0.504	25~40	4.318	40~50
	Miami Dade-6 TP-14	IGM & Sand	14	58	Static	8	Load-Deflection	0.182	3.009	5~16	0.392	16~58	N/A	
	Miami Dade-6 TP-15	IGM & Sand	14	45	Static	7.5	Load-Deflection	0.119	3.199	3~11	0.616	11~45	N/A	
	Miami Dade-6 TP-16	IGM & Sand	14	25	Static	5.5	Load-Deflection	0.115	3.658	5~14	0.853	14~25	N/A	
	Miami Dade-6 TP-17	IGM & Sand	14	25	Static	5.5	Load-Deflection	0.135	3.315	4~21	0.159	21~25	N/A	
	Miami Dade-6 TP-18	Sand & IGM	14	20	Static	4	Load-Deflection	0.115	1.474	1~8	5.782	8~19	N/A	
	Miami Dade-6 TP-19	IGM, Sand & FT Limestone	14	55	Static	8	Load-Deflection	0.192	3.420	1~9	0.777	9~40	6.176	40~50
	Miami Dade-6 TP-20	IGM & Sand	14	30	Static	9	Load-Deflection	0.091	3.860	1~26	0.583	26~30	N/A	
	Miami Dade-6 TP-21	IGM & Sand	14	46	Static	12	Load-Deflection	0.110	3.008	4~17	0.612	17~46	N/A	
	Miami Dade-6 TP-22	IGM & Sand	14	41	Static	12	Load-Deflection	0.058	N/A		N/A		N/A	
	Miami Dade-6 TP-23	Sand	14	58.5	Static	10.5	Load-Deflection	0.560	0.275	0~58.5	N/A		N/A	
	Miami Dade-6 TP-24	IGM & Sand	14	47	Static	4	Load-Deflection	0.182	3.044	1~20	0.651	20~47	N/A	
	Miami Dade-6 TP-25	IGM & Sand	14	56	Static	10	Load-Deflection	0.095	N/A		N/A		N/A	
	Miami Dade-6 TP-26	IGM, Sand & FT Limestone	14	57	Static	10	Load-Deflection	0.296	2.755	20~32			4.634	32~57
	Miami Dade-6 TP-27	IGM, Sand & FT Limestone	14	47	Static	11	Load-Deflection	0.053	2.072	1~10	0.152	10~22	4.423	22~47
	Miami Dade-6 TP-28	IGM, Sand & FT Limestone	14	65	Static	8	Load-Deflection	0.408	1.564	1~9			7.230	60~65
	Miami Dade-6 TP-29	IGM, Sand & FT Limestone	14	56	Static	9	Load-Deflection	0.107	2.930	0~18	0.916	24~46	4.872	46~56
	Miami Dade-6 TP-30	IGM, Sand & FT Limestone	14	56	Static	9	Load-Deflection	0.107	3.490	1~15	0.659	15~45	4.248	45~56
	Miami Dade-6 TP-31	IGM, Sand & FT Limestone	14	44	Static	Not measured	Load-Deflection	0.432	2.026	1~12	0.137	12~30	4.332	30~40
	Miami Dade-7 TP-1	Sand & IGM	18	41	Static	4	Load-Deflection	0.064	N/A		N/A		N/A	
	Miami Dade-7 TP-2	Sand & IGM	18	41	Static	4	Load-Deflection	0.069	N/A		N/A		N/A	
	Miami Dade-8 TP-1	Sand & IGM	14	52	Static	1	Load-Deflection	0.300	N/A		N/A		N/A	
Total # of Test Piles				78	Total T-Z Curve		16							

Yellow – sand; light grey – Miami Limestone or North Florida IGM; dark grey – Fort Thompson Limestone

## CHAPTER 5 PREDICTED SIDE FRICTION OF ACIPs IN FLORIDA

### 5.1 Background

For all of the sites, with exception of Santa Rosa, site data consisted of SPT borings, laboratory soil classifications, and rock strength data for Limestone and IGM, if applicable. In addition a few of the sites (i.e. Alachua) had unconfined compression strength data for the clay. Santa Rosa had CPT data with no SPT data. In addition, Hillsborough – 3 had both CPT and SPT data. The Miami Dade Site also had dynamic cone data with SPT data. For those sites which had rock cores and laboratory strengths, core recoveries and RQD was available. None of the sites with the exception of Miami had borings within the footprint of any pile. The Miami site had 4 piles with borings within the footprint; however none had SPT data extended over the full length (e.g. half SPT and half dynamic cone). A few of the sites employed automatic SPT hammers (Alachua, Duval, and Broward). For these sites, the SPT blow count was corrected (i.e.  $1.24 \times N$ ) to obtain 60% hammer energies.

Due to limited data in the footprint, mean site representation of unit skin friction were predicted based on the total in situ and laboratory strength data. Specifically, all SPT N values, rock strengths, etc. for the site were used to obtain a mean site unit skin friction by layer. An individual layer was classified as one of the following, Sand, Clay, Marl, Miami Limestone, Fort Thompson Limestone, and North Florida IGM. In the case of soils, the Unified Soil Classification (USCS) which was given was used to separate the sands from the clays. All soils classified as SP, SW, and SM soils were considered Cohesionless and CH, CL, MH, SC and dual classifications (e.g. SM-SC) with PIs greater than 35 were represented as Cohesive.

In the case of cohesive soils, undrained shear strengths,  $S_u$ , are required for a number of the prediction methods. Only one site provided undrained shear strength (Alachua -2) from

laboratory testing. Estimated undrained shear strength from in situ SPT N values have been suggested by Sowers (1979), Figure 5.1, based on USCS soil classification. NAVFAC DM-7.1 (1982), provided a mean of Sowers  $S_u$  vs. N recommendations as well as Terzaghi and Peck (1967) recommendation for clays, Figure 5.2. Note, X and Y axis of Figure 5.2 are flipped from Figure 5.1, and the undrained shear strength,  $S_u$ , is presented as unconfined compressive strength,  $q_u$  ( $S_u = q_u/2$ ).

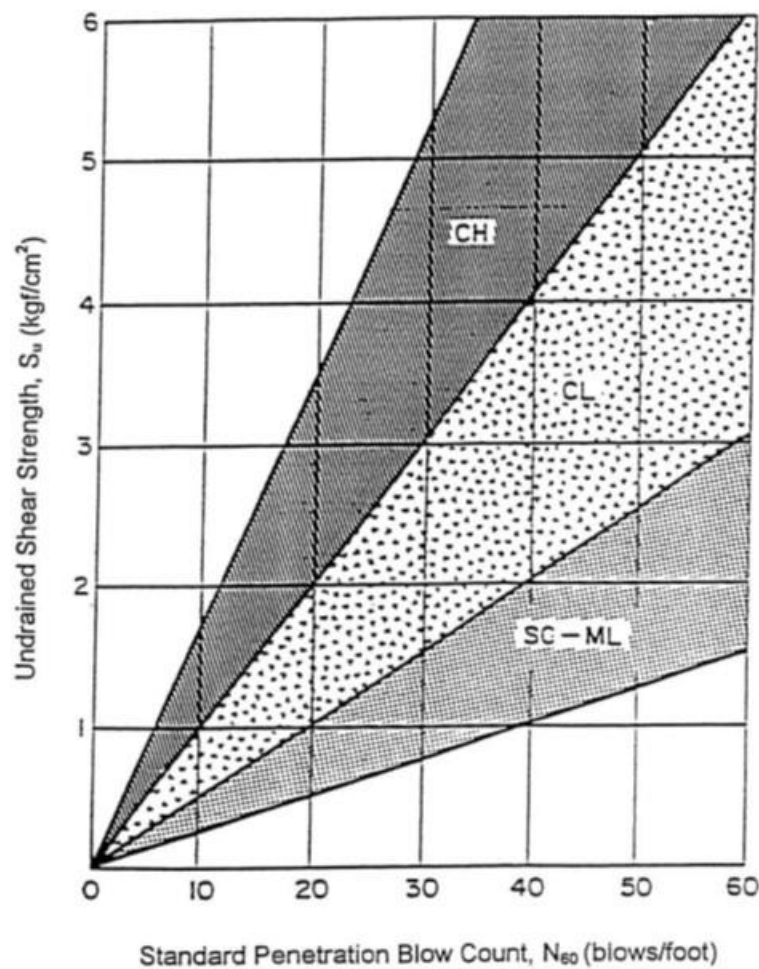


Figure 5.1 Undrained shear strength vs. SPT N, Sowers, 1979

Shown in Table 3, are equations of  $S_u$  (tsf) vs. SPT N for each of the lines presented in Figure 53 given by Aggour (2002) for MDOT. Presented in Figure 5.3 are three measured and predicted unconfined compressive strengths,  $q_u$  (NAVFAC, 1982) at Alachua-2 site which had both CH

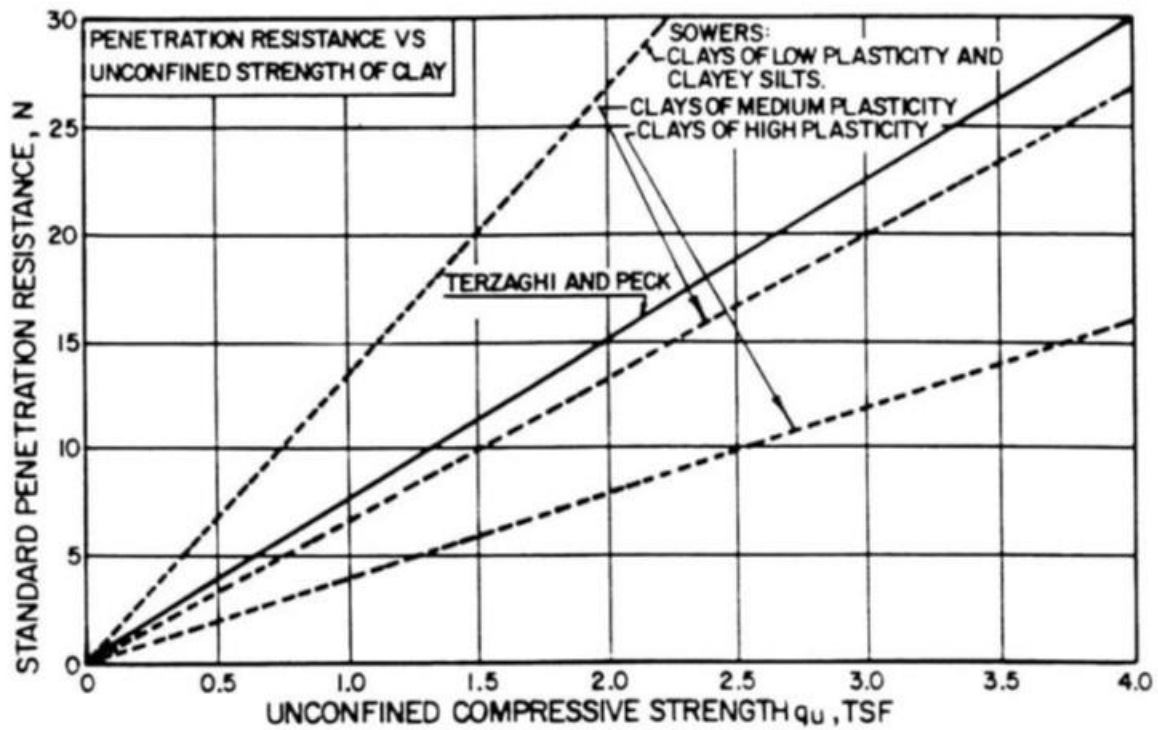


Figure 5.2 SPT N vs. unconfined compressive strength,  $q_u$  ( $S_u = q_u / 2$ ) (NAVFAC, 1982)

Table 5.1 Estimated undrained shear strength,  $S_u$ , from SPT N (Aggour, 2002)

Type of Clay (USCS)	Undrained Shear Strength, $S_u$ (tsf)	Source
Clay of High Plasticity (CH)	$S_u = 0.120N$	Sowers(1979)
Clay of Medium Plasticity (CL)	$S_u = 0.075N$	Sowers(1979)
Clay of Low Plasticity and Clayey Silt (SC-ML)	$S_u = 0.038N$	Sowers(1979)
Average relationship for all Clays	$S_u = 0.066N$	Terzaghi and Peck (1967)

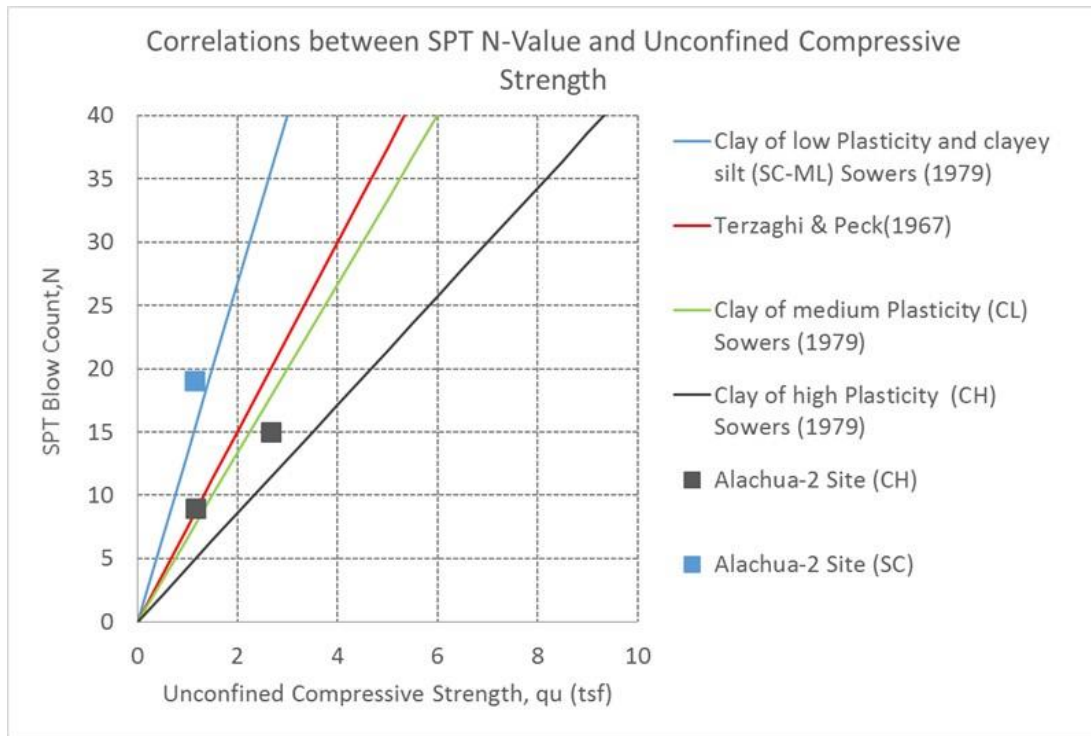


Figure 5.3 Measured and estimated unconfined compressive strength,  $q_u$  ( $S_u = q_u / 2$ ) vs. SPT N and SC soils. Evident from Figure 5.3, the measured and predicted are in reasonable agreement. Consequently, it was decided to use Sowers (Table 5.1) equations to represent CH and SC-ML soils and in the case of CL soils, Terzaghi ( $S_u = 0.066N$ ) would be used. In addition, all strengths were limited to blow counts, N, of 40 as shown in Figure 5.3. Note, this did not affect any of the Alachua sites, only the Duval site with marl.

For the Cohesionless soils, (SW, SP, etc.), the estimated unit skin frictions required the calculation of vertical effective stresses which require unit weights for layers on each site. Estimates of unit weights were provided in a few site Geotechnical reports (Miami – Prieto, 1981), other came from nearby Geotechnical Reports (Geosol), and personal communication (Universal – North Florida). All unit weights were given as ranges, and were subsequently correlated to the range of SPT N values.

For effective stress analyses (e.g. Beta), each boring's SPT value was converted to a unit weight, multiplied by a depth to obtain increment of total stress which was subsequently summed to obtain total stress at a specific depth. Then the effective vertical stress was obtained by subtracting the static pore pressure from the total stresses. The static pore pressures were obtained from the boring ground water elevation multiplied by depth. In the case of no reported boring groundwater, the site mean value was employed.

One of the Cohesionless prediction methods (Brown 2010, Table 3.1) requires the use of angle of internal friction,  $\phi'$ , and OCR. For  $\phi'$  estimation, a number of approaches were investigated, and the method by Hatanaka and Uchida (1996) was selected based on SPT N values

$$\phi' = [15.4(N_1)_{60}]^{0.5} + 20^0 \quad \text{Eq. 5.1}$$

$$(N_1)_{60} = \frac{N_{60}}{\left(\sigma'_{vo}/P_a\right)^{0.5}} \quad \text{Eq. 5.2}$$

A comparison with reported  $\phi'$  for Duval and Miami sites resulted in similar values. For OCR, Brown (2010) recommends that the maximum past stress be computed from

$$\frac{\sigma'_p}{P_a} \approx 0.47(N_{60})^m \quad \text{Eq. 5.3}$$

where  $m=0.6$  for clean sands and  $m=0.8$  for silty sands. Also, due to the uncertainty of estimating OCR from  $N_{60}$ , an additional modified Brown's method was also performed limiting the angle of internal friction,  $\phi'$ , to  $40^0$  and OCR to 10.

## 5.2 Predicted Ultimate Unit Skin Friction of Limestone

The prediction analysis began with Limestone formations of South Florida (Miami and Fort Thompson). As identified in Table 4.1 a significant number of the piles came from the

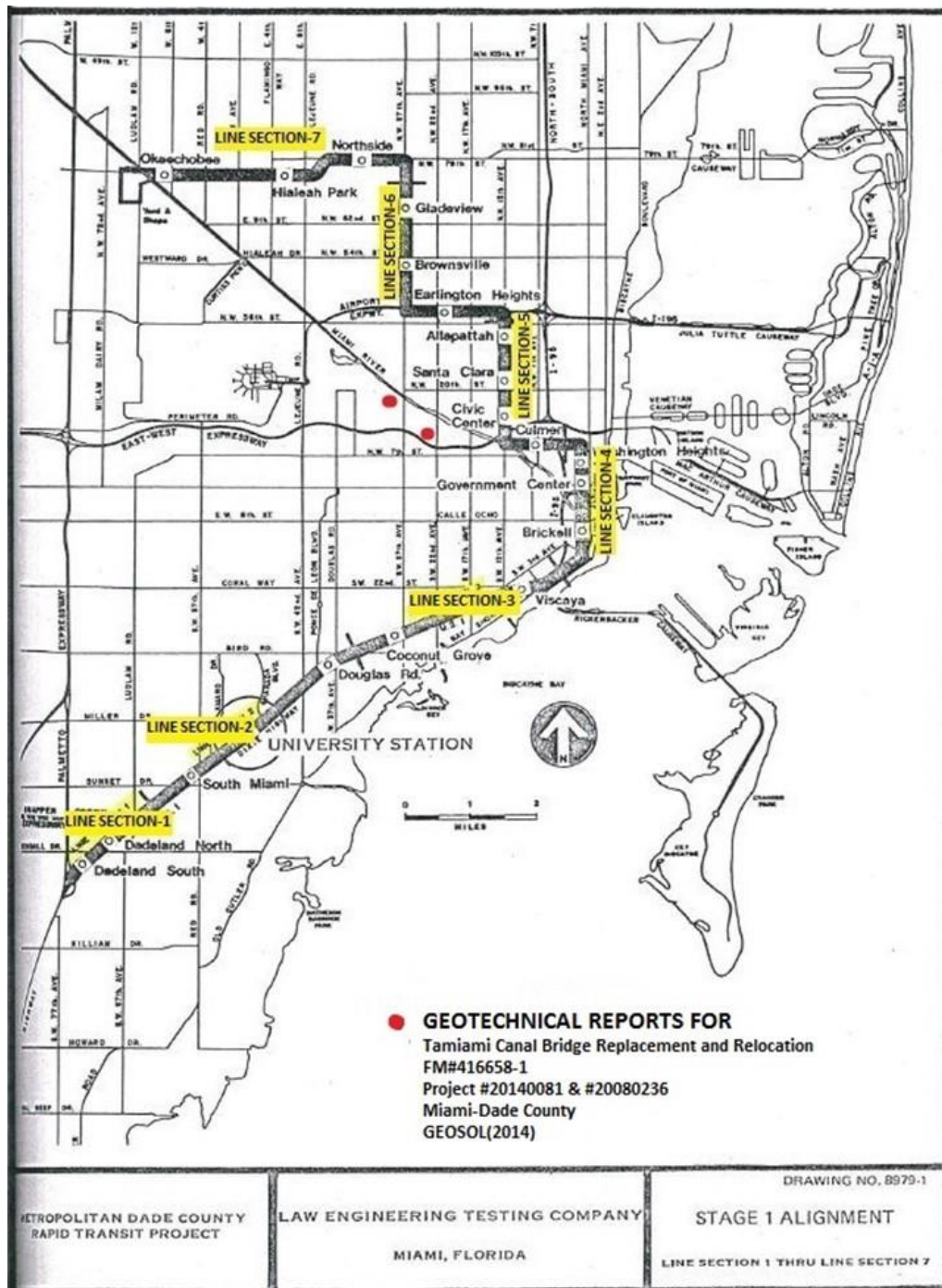


Figure 5.4 Line Sections 1 through 7 of Metro Dade Rapid Transit Project (Law Engineering, 1978)



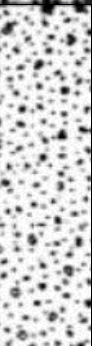

EPOCH	FORMATION	GEOLOGIC DESCRIPTION		DEPTH (FT.)	RANGE OF THICKNESS (FT.)	PHYSICAL PROPERTIES
PLEISTOCENE	PAMLICO	LOOSE TAN BROWN QUARTZ FINE SAND WITH LIMESTONE FRAGMENTS		3.00	0 - 6.0	----
	MIAMI LIMESTONE	SOFT TO MEDIUM TAN WHITE POROUS TO VERY POROUS OOLITIC <u>LIMESTONE</u>		9.50 ▼	3.0 - 24.0 Avg: 18.0	Modulus of Elasticity: Range: 3,300 - 39,200 ksf Avg: 13,500 ksf  Unconfined Compressive Strength: Range: 9.0 - 242.0 ksf Avg: 46.0 ksf  Split Tension: Range: 4.0 - 82.0 ksf Avg: 14.0 ksf
		LOOSE TO MEDIUM LIGHT GRAY QUARTZ FINE SAND WITH LIMESTONE FRAGMENTS		21.00	3.0 - 38.0 Avg: 20.0	Modulus of Elasticity: Range: 100 - 870 ksf Avg: 450 ksf  Static Cone Penetration Resistance Range: 5.0 - 100.0 kg/cm <sup>2</sup> Avg: 60.0 kg/cm <sup>2</sup>
	FORT THOMPSON	MEDIUM TO MODERATELY HARD TAN SLIGHTLY POROUS FOSSILIFEROUS QUARTZ SANDY <u>LIMESTONE</u>		41.00		Modulus of Elasticity: Range: 21,600 - 75,600 ksf Avg: 49,00 ksf  Unconfined Compressive Strength: Range: 84.0 - 261.0 ksf Avg: 155.0 ksf

Figure 5.5 Geological profile of Miami Stratigraphy (recreated from Prieto, 1981)



Metro Dade Rapid Transit Project, specifically Line sections 4 through 7, Figure 5.4 (Law Engineering, 1978). Preliminary rocks strengths for all line sections as well as available boring, depth and rock strength for Line Sections 4 through 7 were obtained from “System wide Preliminary Geotechnical Investigation of Metropolitan Dade County Transit Improvement Program,” by Law Engineering, 1978 (note other line sections were not available). Prieto (1981) reported a general profile for all of the line sections in Figure 5.5 along with mean strengths. Inspection of the figure shows that Miami Limestone had a mean unconfined compressive strengths,  $q_u$ , of 46ksf (23 tsf) and Fort Thompson had a strength of 155 ksf (77.5 tsf). Presented in Figure 5.6 is the frequency distribution of  $q_u$  for the Miami Limestone reported in the Geotechnical Report (Law 1978) for Line sections 4 and 7 (load test piles). Evident, from Figure 5.6, the distribution is highly log-normal with a mean of 51.8 ksf (similar to Prieto, 1981) and median of 37.4 ksf. No correlation or trends were observed with depth. Shown in Figure 5.7 is the frequency distribution of the split tension data reported in the Geotechnical Report (Law, 1978) for the Miami Limestone formation. Again the data is highly log-normal with mean of 13.8 ksf (14 ksf Prieto, 1981) and median of 11.5ksf.

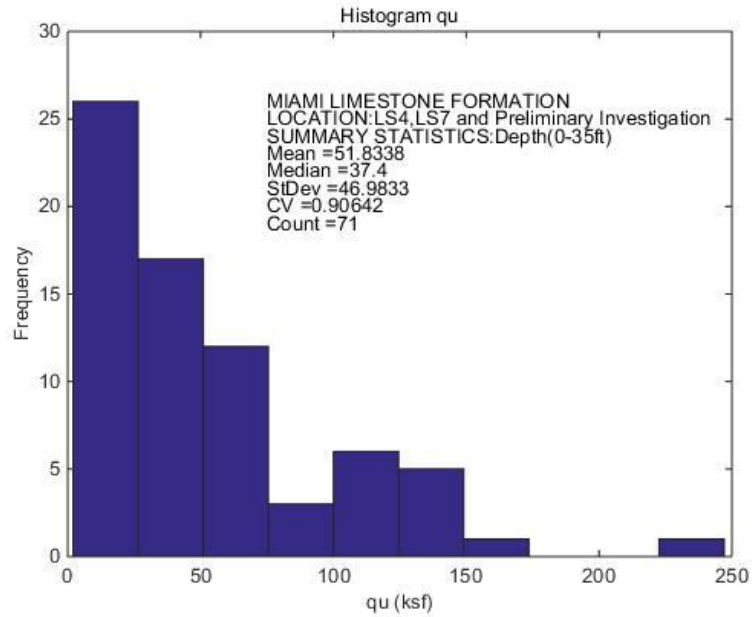


Figure 5.6 Frequency distribution of  $q_u$  for Miami Limestone

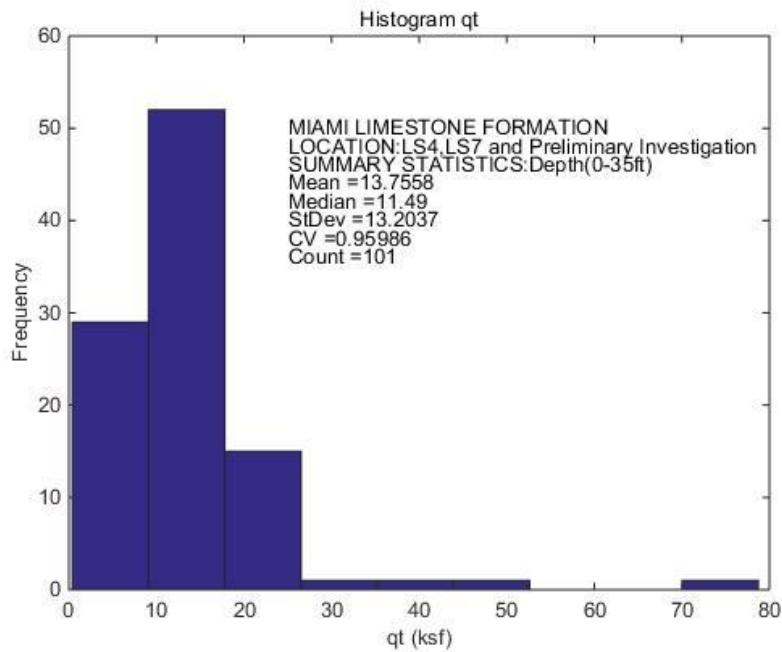


Figure 5.7 Frequency distribution of split tension,  $q_t$  for Miami Limestone

Shown in Figure 5.8 is the frequency distribution of the unconfined compressive strengths,  $q_u$  for the Fort Thompson formation. The data was obtained from “System wide

Preliminary Geotechnical Investigation of Metropolitan Dade County Transit Improvement Program,” by Law Engineering, 1978 for Line section 4 and all section preliminary data for Fort Thompson as well as nearby FDOT data (MIC data). Again, the data was log-normal with a mean of 130 ksf (vs. 155 ksf Prieto, 1981, Figure 5.5) and median of 114 ksf. Presented in Figure 5.9 is a frequency distribution of split tension,  $q_t$  of the Fort Thompson with mean of 32 ksf and median of 28 ksf. Note, the Fort Thompson Limestone exhibits lower coefficients of Variabilities (CV) than the Miami Limestone (Figures 5.6 and 5.7); also, the line sections with pile load tests that had segment within the Fort Thompson formation were located in sections 5 and 7.

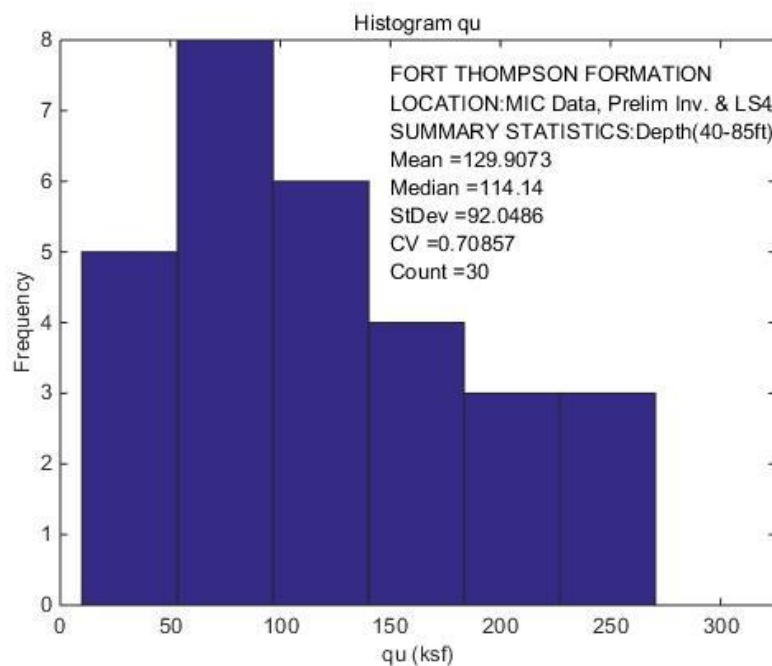


Figure 5.8 Frequency distribution of  $q_u$  for Fort Thompson Limestone

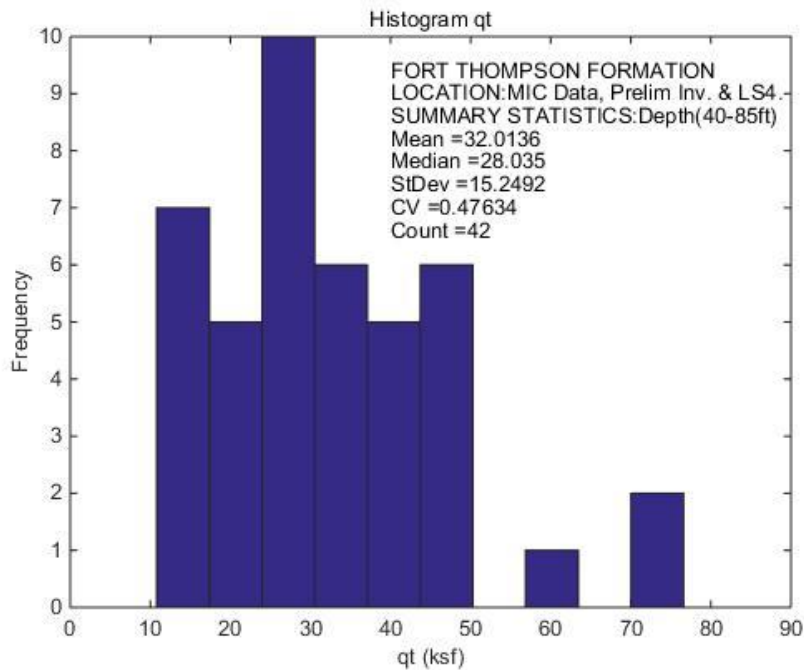


Figure 5.9 Frequency distribution of split tension, qt, for Fort Thompson Limestone

The frequency distribution of SPT N values for the Miami Limestone is presented in Figure 5.10. Unfortunately only two line sections (4 and 7, Figure 5.4) had SPT data; consequently data from nearby county bridge replacement and relocation (see Figure 5.4 for locations) was obtained. The Geotechnical reports (Tamiami Canal Bridge Replacement, Project 20140081 and Relocation, Project 20080236) by Geosol provided stratigraphy, as well as individual boring data. Presented in Figure 5.11 is the soil and rock stratigraphy and summary information at the two sites. The SPT data was obtained with an automatic hammer and was subsequently corrected ( $N_{60} = 1.24 \times N_{\text{auto}}$ ), whereas, the site data by Law Engineering (1978) was with safety hammer. A mean of 22 bpf and a median of 21 bpf was found for 86  $N_{60}$  values after combining the Law with Geosol data for the Miami Limestone.

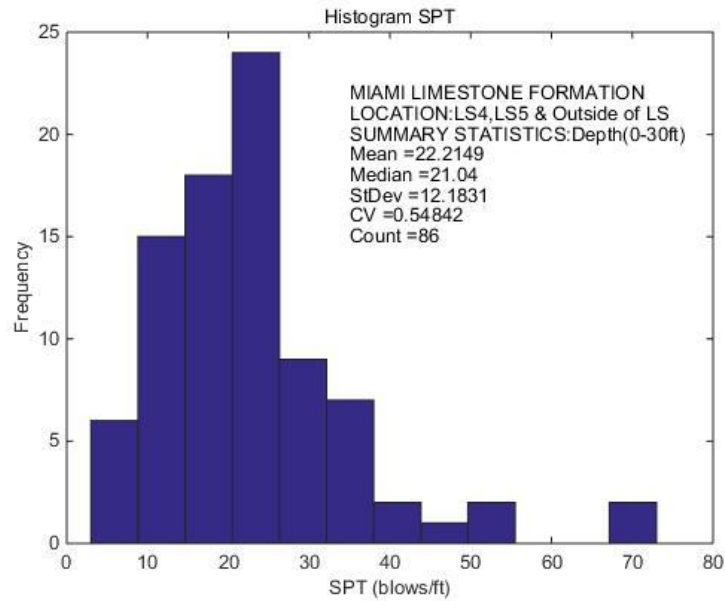


Figure 5.10 Frequency distribution SPT N values for Miami Limestone

FORMATION	GEOLOGIC DESCRIPTION		DEPTH (FT.)	RANGE OF THICKNESS (FT.)	PHYSICAL PROPERTIES
SAND	BROWN SLIGHTLY SILTY FINE TO MEDIUM SAND WITH TRACE OF LIMESTONE FRAGMENTS (FILL; SP-SM)		5	0-10	SPT: Range: 1-37 bpf Avg : 13 bpf  Unit Weight: 110 pcf
MIAMI LIMESTONE FORMATION	BROWN TO LIGHT GRAY SANDY LIMESTONE		22	20-22	SPT: Range: 5-53 bpf Avg : 19 bpf  Unit Weight: 115 pcf
FORT THOMPSON FORMATION	LIGHT GRAY SLIGHTLY SILTY FINE TO COARSE SAND WITH TRACE TO LITTLE LIMESTONE FRAGMENTS (FORT THOMPSON FORMATION SAND; SP-SM)		32	6-10	SPT: Range: 7-26 bpf Avg : 12 bpf  Unit Weight: 110 pcf
	LIGHT GRAY TO LIGHT BROWN SANDY LIMESTONE		65	30-38	SPT: Range: 6-50 blows per 2 in. Avg : 52 bpf  Unit Weight: 120 pcf

Geosol(2014)

Figure 5.11 Tamiami Canal Bridge Replacement and Relocation, Geosol Geotechnical Reports (2008, 2014)

Presented in Figure 5.12 are the Fort Thompson SPT data for Miami Dade site 6, Line sections 4 and 5 (see Figure 5.4). Unfortunately, very limited SPT data was available in “System wide Preliminary Geotechnical Investigation of Metropolitan Dade County Transit Improvement Program,” for line sections 1 and 6. Again, boring data from nearby sites (Geosol, Figure 5.11) was collected and added to the analysis, Figure 5.12. Review of data shows the distribution to be bimodal with refusal set as 100 bpf (e.g.  $50/4 = 150 \text{ bpf} \Rightarrow 100 \text{ bpf}$ ) which results in very different mean (52 bpf) and median (35 bpf) values for  $N_{60}$ .

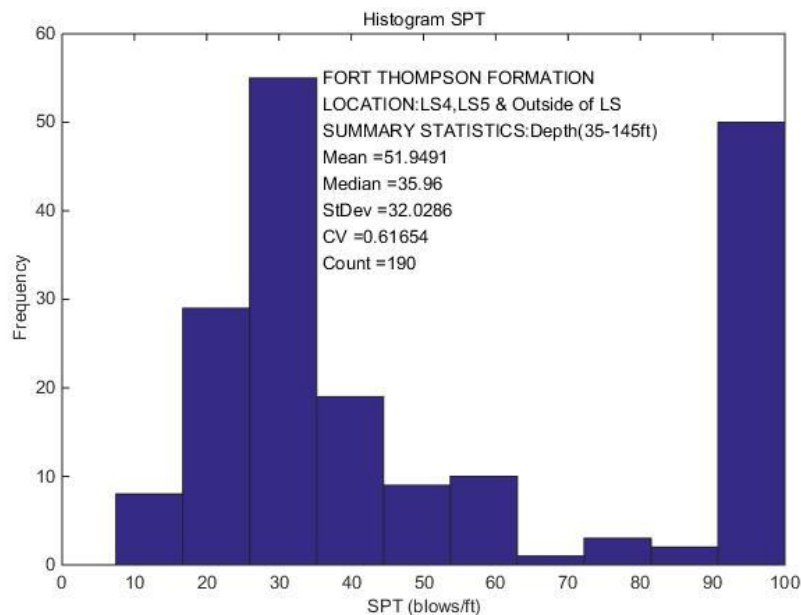


Figure 5.12 Frequency distribution SPT N values for Fort Thompson Limestone

Table 5.2. Predicted unit skin friction for Miami Limestone

<u>Predicted Unit Skin Friction (Miami Limestone Formation)</u>				
Design Method	Mean-qu (ksf)	51.85*	Mean-qu (ksf) (+/-) 1-StDev	35.13
	Mean-qt (ksf)	13.75	Mean-qt (ksf) (+/-) 1-StDev	11.70
	fs (tsf)		fs (tsf)	
FDOT	N/A		3.5485	
Herrera_qu (C=1.111)	N/A		3.2610	
Horvath and Kenney (1979)	3.4109		N/A	
Williams et al. (1980)	6.0824		N/A	
Reynolds and Kaderabek (1980)	7.7751		N/A	
Gupton and Logan (1984)	5.1834		N/A	
Reese and O'Neill (1987)	3.8875		N/A	
Rowe and Armitage (1987)	7.3818		N/A	
Carter and Kulhawy (1988)	3.2072		N/A	
Ramos et al. (1994)	3.11		N/A	
Kulhawy et al. (2005)	5.2367		N/A	
Design Method	Mean-SPT (blows/ft)	22.21	Mean-SPT (blows/ft) (+/-) 1-StDev	21.27
	fs (tsf)		fs (tsf)	
Herrera_SPT (C=0.15)	N/A		3.1905	
Frizzi & Meyer (2000)	6.2752		N/A	
Ramos et al. (1994)-SPT (Blows/ft)	6.443		N/A	
Crapps (IGM)	1.7795		N/A	
*ACIP piles considered IGM with q <sub>u</sub> between 10 ksf and 100 ksf.				

Using the identified ACIP methods (Table 3.5), the unit skin friction (tsf) was predicted for the Miami Limestone, Table 5.2. All predicted values are based on each site's frequency distribution, identified in Figures 5.6 through 5.12. The first predicted column is for the methods that use all of the data, whereas the second column is for the methods (FDOT and Herrera) which use a revised mean value. The revised mean value is obtained by first calculating the mean of all the data, subsequently removing data outside +/- on standard deviation from the original mean, and then re-computing the average of the revised data set. See Table 3.5 and Figures 5.6 through 5.12. For the Miami Limestone Formation, the mean and median SPT N values are quite close and have little impact on predicted fs values based on N.

Besides the methods given in Table 3.5, Herrera (FDOT, Assistant State Geotechnical Engineer) has proposed:

$$f_s(tsf) = C \sqrt{q_u(tsf)} \times Rec \quad \text{Eq. 5.4}$$

$$f_s = C (N_{60}) \quad \text{Eq. 5.5}$$

where  $q_u$  in units of tons per square foot (tsf) is the **revised** value of  $q_u$  (i.e., the mean  $q_u$  value after data outside +/- one standard from the original mean has been removed). The coefficient C was calibrated (back-calculated) using the measured mean unit skin friction for the layer and resulted in a value of  $C = 1.11$  for material with strength characteristics similar to the Miami Limestone. The Recovery used in the calculations presented in Table 5.2 for FDOT & Herrera Methods was 70% for the Miami Formation based on all boring data.

It should be noted that both FDOT and Herrera methods partially address variability in strength *prior* to computing skin friction through the use of revised strength parameters. In addition, they reflect the site specific characteristics of the bearing strata by applying local Recovery values (e.g., results from the nearest core). These features bring uniformity to the evaluation of overall site variability in design, as well consideration of localized subsurface conditions.

The proposed correlation with the corrected SPT “ $N_{60}$ ” blow count was calibrated in the same manner, using SPT data. Values of the C constants for the Miami Limestone are shown for each method in Table 5.2.

In the case of Ocala Limestone (North Florida IGM rock), no rock strength or recovery data was available; in addition, the North Florida site’s SPT N showed a higher mean compared to Miami Limestone. The mean estimated skin friction (Table 4.1) for North Florida was lower (2.4 tsf) vs. Miami (3.3 tsf) and therefore, all of the IGM SPT methods over predicted capacity (bias ~ 0.3). This suggests that the material needs to be separated to calculate a separate bias and



LRFD for North Florida IGM; unfortunately with only 4 values (Table 4.1), a reliable assessment could not be performed with the collected data but recommended for further testing in Chapter 7.

The Fort Thompson Limestone predicted unit skin friction (tsf) is given in Table 5.3 for Table 3.5 design methods. Note, Reynolds and Kaderabek (1980) were developed specifically for Miami Limestone. Gupton and Logan (1984) was developed for Key Largo, Anastasia, Miami, and Fort Thompson Limestone formations. Frizzi & Meyer (2000) have different and independent assessment ( $N_{60}$ ) for Miami (Table 5.2) and Fort Thompson (Table 5.3) formations. Again both the mean and mean  $\pm$  one standard deviation were computed (FDOT and Herrera). Because of the bimodal (refusal) distribution of N values (Figure 5.12), mean and mean  $\pm$  one standard deviation values are quite different. Note the Fort Thompson formation rock strengths exceeds the IGM 100 ksf upper limit (FHWA, 2010). The Recovery used in the calculations for FDOT & Herrera Methods was 40% for the Fort Thompson Formation based on all boring data. Note that for Herrera, the *revised* value of  $q_u$  is in units of tsf, along with  $C = 1.643$  which corresponds to material of similar strength to the Ft. Thompson formation.

Table 5.3 Predicted unit skin friction for Fort Thompson Limestone

Predicted Unit Skin Friction (Fort Thomspson Limestone Formation)				
Design Method	Mean-qu (ksf)	129.91*	Mean-qu (ksf) (+/-) 1-StDev	114.77*
	Mean-qt (ksf)	32.01	Mean-qt (ksf) (+/-) 1-StDev	31.65
	fs (tsf)		fs (tsf)	
FDOT	N/A		6.0275	
Herrera_qu (C=1.643)	N/A		4.9795	
Horvath and Kenney (1979)	5.3998		N/A	
Williams et al. (1980)	8.5215		N/A	
Reynolds and Kaderabek (1980)	19.4861		N/A	
Gupton and Logan (1984)	12.9907		N/A	
Reese and O’Neill (1987)	9.7430		N/A	
Rowe and Armitage (1987)	11.6861		N/A	
Carter and Kulhawy (1988)	5.0774		N/A	
Ramos et al. (1994)	7.7944		N/A	
Kulhawy et al. (2005)	8.2903		N/A	
Design Method	Mean-SPT (blows/ft)	51.95	Mean-SPT (blows/ft) (+/-) 1-StDev	35.54
	fs (tsf)		fs (tsf)	
Herrera_SPT (C=0.15)	N/A		5.3310	
Frizzi & Meyer (2000)	8.2729		N/A	
Ramos et al. (1994)-SPT (Blows/ft)	12.3898		N/A	
Crapps (IGM)	19.8296		N/A	
*Note outside IGM design values (q_u between 10 ksf and 100 ksf).				

### 5.3 Predicted Ultimate Unit Skin Friction for Cohesionless Soils

As identified in FHWA GEC #8 (Design and Construction of Continuous Flight Augers) all soils are separated into either Cohesive or a Cohesionless category (undrained or drained behavior) for design. Silty soils require judgment on the part of engineer to determine if the material will act undrained (Cohesive) or drained (Cohesionless) under loading.

All Cohesionless unit skin friction predictions were computed on an individual site basis. The SPT N from an individual boring and depth was substituted into a prediction methods with vertical effective stress to compute an individual beta, and  $f_s$  as shown in Figure 5.13 for the FHWA (O'Neil & Reese 1999)  $\beta$  method, and Figure 5.14 for the Brown method. Then a trend

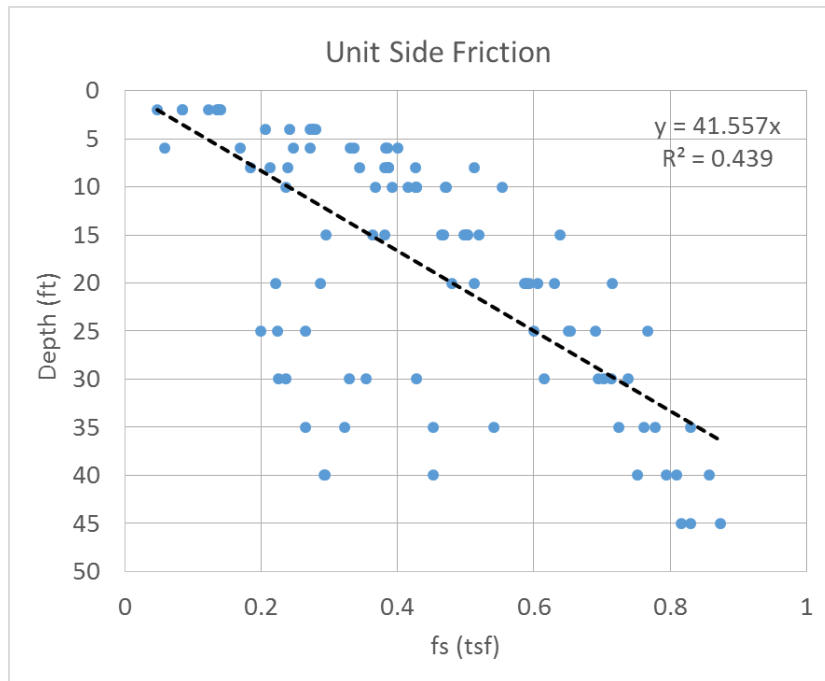


Figure 5.13 Predicted FHWA unit skin friction Hillsborough-3 using all borings

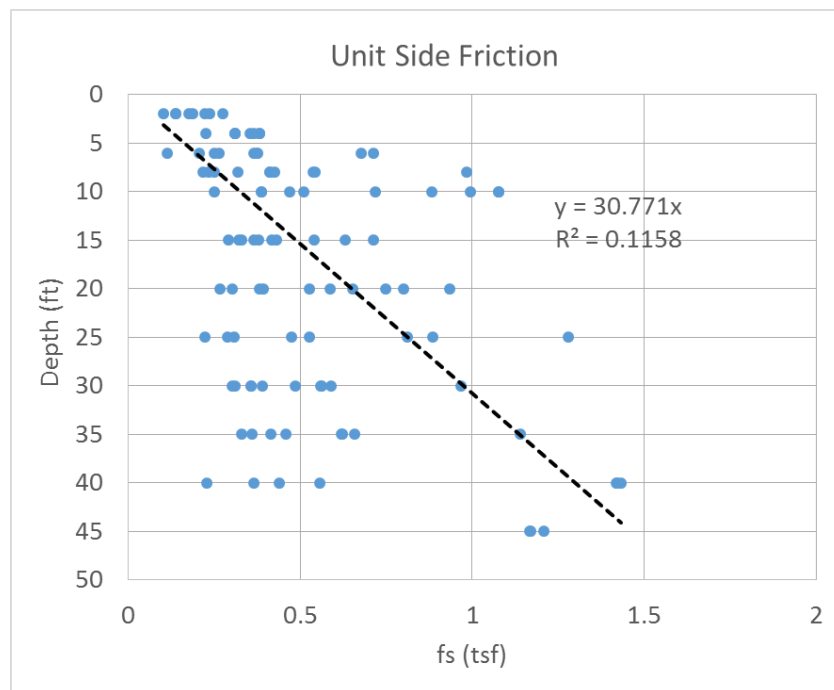


Figure 5.14 Predicted Brown unit skin friction Hillsborough-3 using all borings

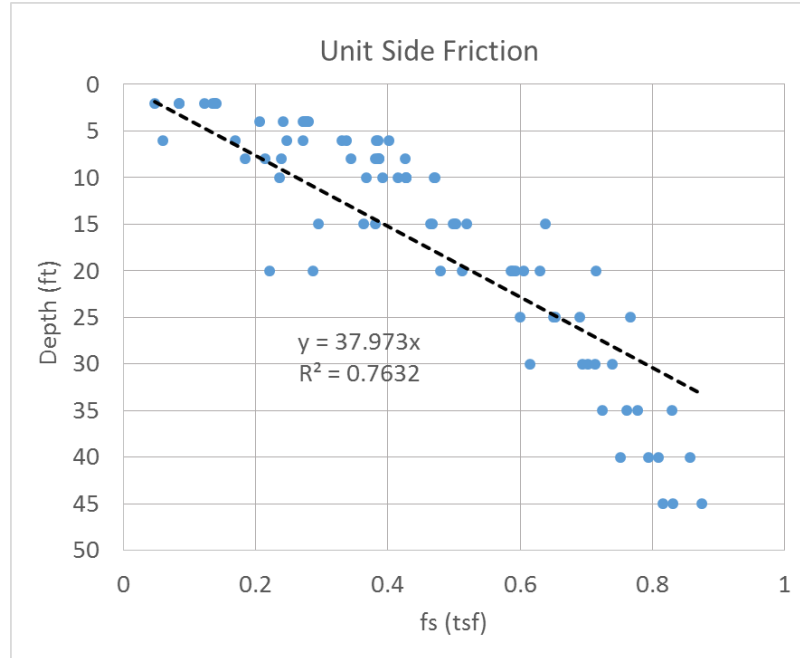


Figure 5.15 Predicted FHWA unit skin friction Hillsborough-3,  $\pm 2$  standard deviation

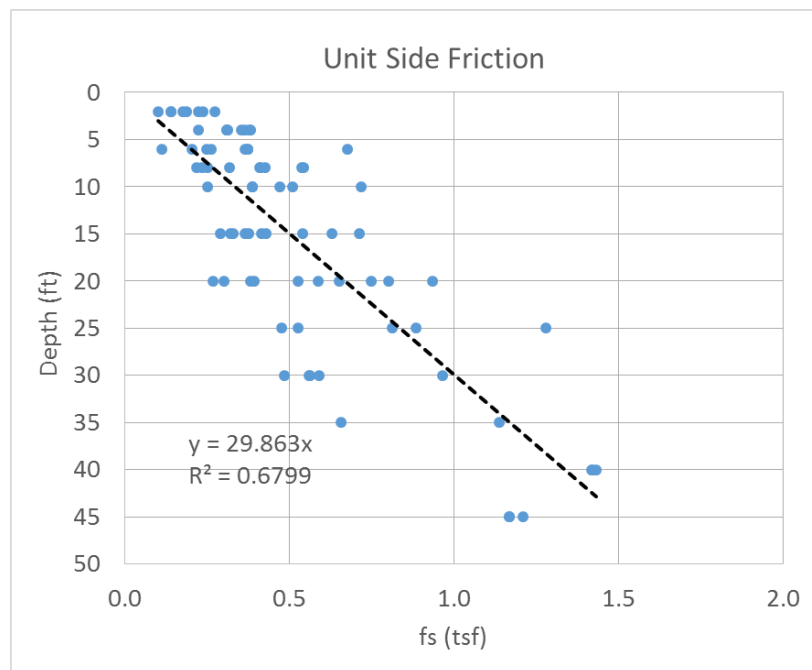


Figure 5.16 Predicted Brown unit skin friction Hillsborough-3,  $\pm 2$  standard deviation

line was fit to  $f_s$  vs. depth, and data 2 standard deviations away from the line were removed and a new trend line was found. Shown in Figure 5.15 is FHWA  $\beta$  method and Figure 5.16 is the Brown method. Using the trend line, the  $f_{s_{avg}}$  for middle of layer was found (e.g. Hillsborough - 3, TP-1, length of layer=55', mid depth =  $55'/2 = 27.5 \Rightarrow$  for FHWA, Figure 5.15,  $f_{s_{avg}} = 0.72$  tsf). The results for all sites by counties for both estimated and predicted unit skin friction is shown in Table 5.4 for Cohesionless soils using the design methods identified (FHWA, Zelada and Brown), Table 3.5. Note, a number of the estimated values (Table 4.1), had similar values over two segment lengths (e.g. Hillsborough -3, TP-1); for such segments, their values were averaged for one reported value in Table 5.4. For instance, Hillsborough-3, TP4 for depth of 0 to 58ft Table 5.4 shows 0.74 tsf [using Table 4.1,  $f_{s_{avg}} = (0.778 \times 43' + 0.634 \times 15)/58' = 0.74$  tsf]. For other sites, e.g. Nassau-1 TP-14 adjacent layers were not averaged due to the large difference of layer unit skin friction values.

Evident from Table 5.4, the Zelada & Stevenson (2000) predictions are more conservative (i.e. lower) than the FHWA (O'Neil & Reese, 1999) and Brown (2010) methods. Also presented in Table 5.4 are minimum and maximum unit values, as well as the computed bias (estimated/predicted) for each case with summary statistics (bottom of table). Again note, in the bias computation, the numerator is the estimated resistance based on the segmental approach (Table 4.1) and the denominator is the predicted value (e.g. FHWA, Brown, etc.). After bias correction (chapter 6), the numerator will be the measured resistance.

Table 5.4 Predicted unit skin frictions for ACIP piles in cohesionless soils in Florida

Cohesionless Unit Skin Friction Bias-All Sites											
Site	Pile	Depth (ft)	fs <sub>EST</sub> (tsf)	fs <sub>PRED-FHWA</sub> (tsf)	Bias <sub>FHWA</sub>	fs <sub>PRED-ZELDA</sub> (tsf)	Bias <sub>ZELDA</sub>	*fs <sub>Brown</sub> (tsf)	*Bias <sub>BROWN</sub>	**fs <sub>Brown</sub> (tsf)	**Bias <sub>BROWN</sub>
Miami Dade	Miami Dade-1 TP-1	18~35	0.4413	0.4879	0.9046	0.3903	1.1307	0.4808	0.9179	0.4756	0.9279
	Miami Dade-6 TP-2	20~40	0.9938	0.6028	1.6486	0.4823	2.0605	0.6491	1.5310	0.6089	1.6321
	Miami Dade-6 TP-5	16~40	0.5885	0.6028	0.9762	0.4823	1.2202	0.6491	0.9066	0.6089	0.9665
	Miami Dade-6 TP-9	24~40	0.4783	0.6028	0.7934	0.4823	0.9917	0.6491	0.7368	0.6089	0.7855
	Miami Dade-6 TP-10	22~40	0.4040	0.6028	0.6702	0.4823	0.8377	0.6491	0.6224	0.6089	0.6635
	Miami Dade-6 TP-11	8~23	0.9067	0.6028	1.5041	0.4823	1.8798	0.6491	1.3968	0.6089	1.4890
	Miami Dade-6 TP-13	25~40	0.5040	0.6028	0.8361	0.4823	1.0450	0.6491	0.7765	0.6089	0.8277
	Miami Dade-6 TP-14	16~58	0.3923	0.6028	0.6508	0.4823	0.8134	0.6491	0.6044	0.6089	0.6443
	Miami Dade-6 TP-15	11~45	0.6156	0.6028	1.0212	0.4823	1.2763	0.6491	0.9484	0.6089	1.0110
	Miami Dade-6 TP-16	14~25	0.8525	0.6028	1.4143	0.4823	1.7677	0.6491	1.3134	0.6089	1.4001
	Miami Dade-6 TP-19	9~30	0.7771	0.6028	1.2891	0.4823	1.6112	0.6491	1.1971	0.6089	1.2762
	Miami Dade-6 TP-20	26~30	0.5832	0.6028	0.9675	0.4823	1.2092	0.6491	0.8985	0.6089	0.9578
	Miami Dade-6 TP-21	17~46	0.6123	0.6028	1.0158	0.4823	1.2696	0.6491	0.9433	0.6089	1.0056
	Miami Dade-6 TP-23	0~58.5	0.2750	0.6028	0.4562	0.4823	0.5702	0.6491	0.4237	0.6089	0.4516
	Miami Dade-6 TP-24	20~47	0.6508	0.6028	1.0796	0.4823	1.3494	0.6491	1.0026	0.6089	1.0688
	Miami Dade-6 TP-29	24~46	0.9164	0.6028	1.5203	0.4823	1.9001	0.6491	1.4118	0.6089	1.5050
	Miami Dade-6 TP-30	15~45	0.6590	0.6028	1.0932	0.4823	1.3664	0.6491	1.0153	0.6089	1.0823
Alachua	Alachua-5 TP-1	0~27	0.4980	0.5356	0.9298	0.4285	1.1622	0.8814	0.5650	0.6864	0.7255
	Alachua-5 TP-2	0~27	0.4510	0.5356	0.8420	0.4285	1.0525	0.8814	0.5117	0.6864	0.6571
Broward	Broward-1 TP-1	0~15	0.3580	0.1601	2.2362	0.1281	2.7953	0.1018	3.5167	0.0972	3.6831
	Broward-1 TP-1	48~80	0.4770	0.6513	0.7324	0.5210	0.9155	0.8714	0.5474	0.8295	0.5750
	Broward-2 TP-1	0~10	0.3311	0.4000	0.8278	0.3200	1.0347	1.0461	0.4560	0.9395	0.3524
	Broward-2 TP-1	10~32	0.5364	1.0750	0.4990	0.8604	0.6234	1.0234	0.3235	0.9355	0.5734
Duval	Duval-1 TP 1-2	0~30	0.3410	0.3924	0.8690	0.3140	1.0860	0.3756	0.9079	0.3639	0.9371
	Duval-1 TP 2-1	0~30	0.3920	0.3924	0.9990	0.3140	1.2484	0.3756	1.0437	0.3639	1.0772
	Duval-1 TP 3-3	0~30	0.2790	0.3924	0.7110	0.3140	0.8885	0.3756	0.7428	0.3639	0.7667
Hillsborough	Hillsborough-3 TP-1	0~55	0.5489	0.7242	0.7579	0.5793	0.9475	0.9209	0.5960	0.8006	0.6856
	Hillsborough-3 TP-3	0~45	0.4700	0.5925	0.7932	0.4740	0.9916	0.7534	0.6238	0.6551	0.7174
	Hillsborough-3 TP-4	0~58	0.7407	0.7637	0.9699	0.6109	1.2125	0.9711	0.7627	0.8443	0.8773
	Hillsborough-3 TP-5	0~50	0.6254	0.6584	0.9499	0.5267	1.1874	0.8372	0.7470	0.7278	0.8593
Nassua	Nassau-1 TP14	0~10	0.4990	0.2540	1.9646	0.2030	2.4581	0.371	1.3450	0.2539	1.9653
	Nassau-1 TP14	10~50	1.3773	0.8280	1.6634	0.6620	2.0805	0.9103	1.5130	0.8274	1.6646
	Nassua-3 TP-1	10~60	0.3818	0.4736	0.8062	0.3789	1.0077	0.9103	0.4194	0.8274	0.4614
West Palm	West Palm-1 T9B	0~10	0.3100	0.3034	1.0218	0.2427	1.2773	0.4735	0.6547	0.4688	0.6613
	West Palm-1 T9B	10~30	0.4710	0.5282	0.8917	0.4226	1.1145	1.017	0.4631	0.9302	0.5063
	West Palm-1 T9B	30~40	0.4936	0.7679	0.6428	0.6143	0.8035	1.022	0.4830	0.9348	0.5280
Summary Statistics		Mean			1.0264		1.2829		0.9130		0.9991
		Median			0.9398		1.1748		0.7696		0.8683
		StDev			0.3950		0.4940		0.5573		0.5967
		CV			0.3849		0.3851		0.6104		0.5972
		count	36	36	36	36	36	36	36	36	36
		min	0.2750	0.1601	0.4562	0.1281	0.5702	0.1018	0.3235	0.0972	0.3524
		max	1.3773	1.0750	2.2362	0.8604	2.7953	1.0461	3.5167	0.9395	3.6831
* Predicted Unit Skin Friction using the Brown Method as Presented in GEC10											
** Predicted Unit Skin Friction using the Brown Method as presented in GEC10 with OCR Limited -10 & Angle of internal friction limited -40 degree											

#### 5.4 Predicted Ultimate Unit Skin Friction for Cohesive Soils

In the case of cohesive soils, the individual borings on a site were used to estimate the undrained shear strength as a function of depth based on Figure 5.3 (Table 5.1). For instance, shown in Figure 5.17 is the undrained shear strength,  $S_u$ , for Alachua-2 as a function of depth with  $\pm 2$

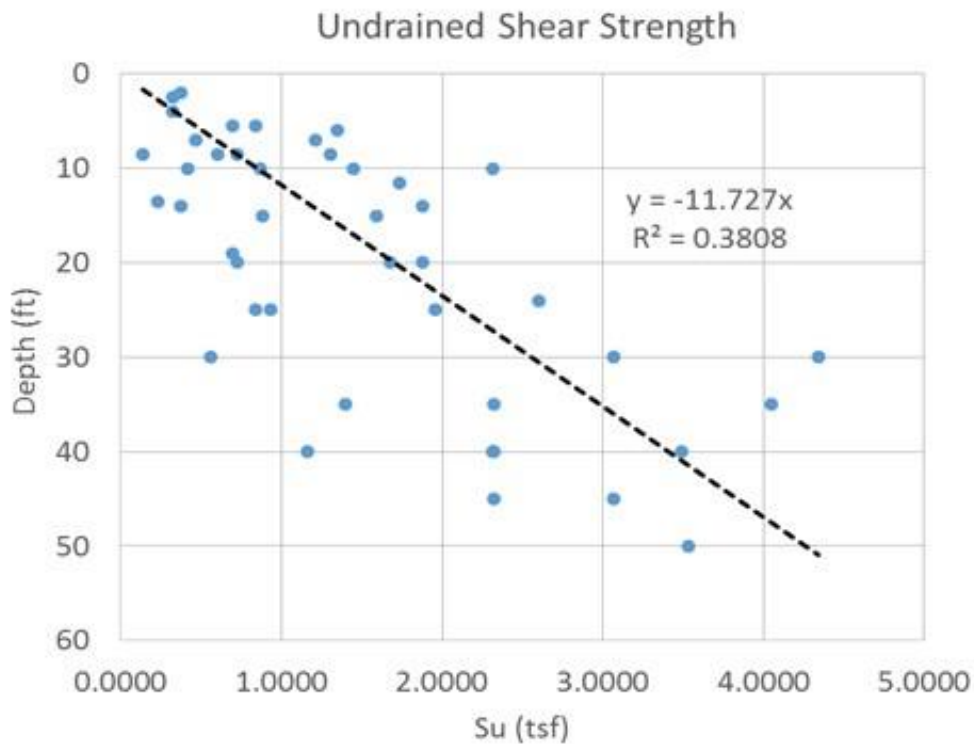


Figure 5.17 Estimated undrained shear strength,  $S_u$ , Alachua-2,  $\pm 2$  standard deviations

standard deviation data removed. Subsequently, the alpha for each point (method dependent), and fs as function of depth was obtained, Figure 5.18. Fitting a linear equation to the data (Figure 5.18), the mean fs for a layer was found (e.g. Alachua-2, TP-2, depth =  $15'/2 = 7.5 \Rightarrow$  Figure 5.18,  $f_{s_{avg}} = 0.30$  tsf, see Table 5.4). A number of sites did not exhibit any  $S_u$  correlation with depth (e.g. over consolidation, sandy clay, etc.), then a mean value per layer (Hillsborough,

Duval, and Alachua 1) was found directly. Table 5.4 reports all of the predicted and estimated  $f_s$  values for each segment on the pile. Note, the Duval site also included the Marl unit skin friction (CH material, see section 2.3.2) values which occurred at depths from 45 to 55 ft. Maximum and minimum predicted values are given in the bottom of the table. Evident from Table 5.4, the FHWA method is very conservative; consequently the Duval marl and maximum bias (Hillsborough-3, TP-5) data was removed to identify their influences. The new bias and CV (far right column) only changed 6%. Data in Tables 5.1 through 5.4 were used subsequently in LRFD assessment, Chapter 6.

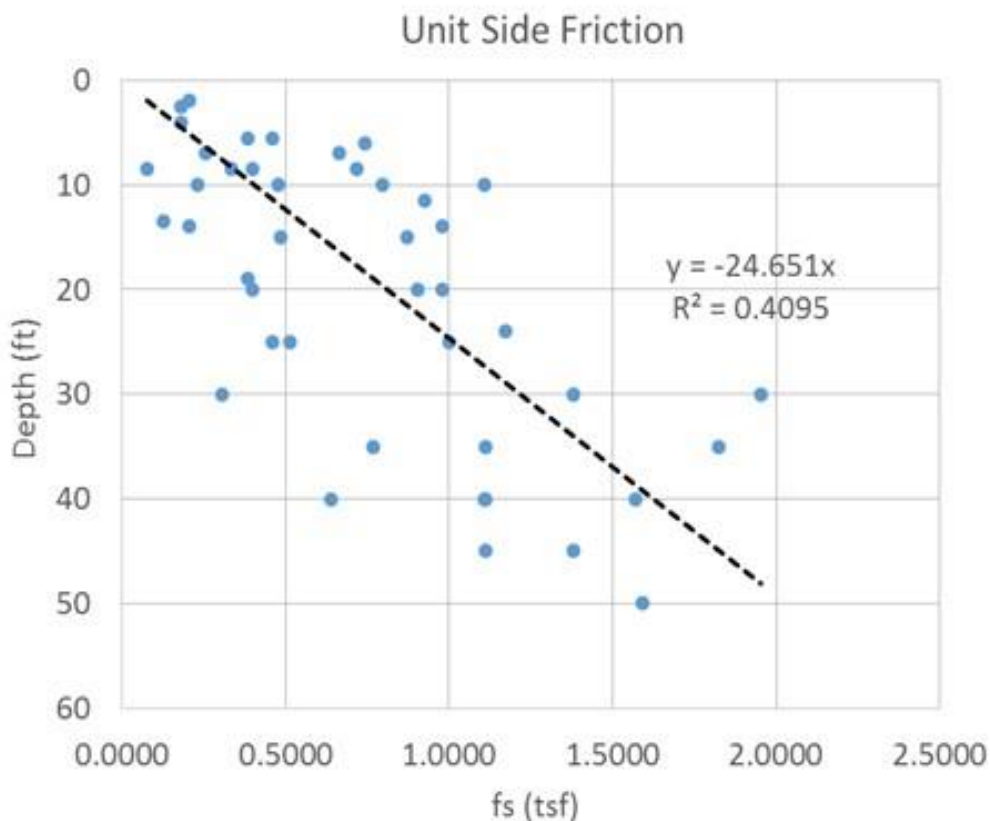


Figure 5.18 FHWA estimated unit skin friction, Alachua-2,  $\pm 2$  standard deviations



Table 5.5 Predicted unit skin frictions for ACIP piles in cohesive soils in Florida

Cohesive Unit Skin Friction Bias-All Sites						
Site	Pile	Depth(ft)	fs <sub>EST</sub> (tsf)	fs <sub>PRED</sub> (tsf)*	Bias <sub>FHWA</sub>	Bias <sub>FHWA</sub>
Alachua	Alachua-1 TP-2	0~20	0.6520	0.4840	1.3471	1.3471
	Alachua-1 TP-3	0~20	0.8960	0.4840	1.8512	1.8512
	Alachua-1 TP-4	0~20	0.4890	0.4840	1.0103	1.0103
	Alachua-1 TP-5	0~20	0.6000	0.4840	1.2397	1.2397
	Alachua-1 TP-2	20~40	0.3670	0.3370	1.0890	1.0890
	Alachua-1 TP-3	20~40	0.8820	0.3370	2.6172	2.6172
	Alachua-1 TP-4	20~40	0.2750	0.3370	0.8160	0.8160
	Alachua-1 TP-5	20~40	0.3360	0.3370	0.9970	0.9970
	Alachua-2 TP-2	0~15	0.4610	0.3040	1.5164	1.5164
	Alachua-2 TP-3	0~15	0.5550	0.3040	1.8257	1.8257
	Alachua-2 TP-5	0~15	0.5960	0.3040	1.9605	1.9605
	Alachua-2 TP-2	15~30	1.6090	0.9127	1.7629	1.7629
	Alachua-2 TP-3	15~30	1.4980	0.9127	1.6413	1.6413
	Alachua-2 TP-5	15~30	1.2350	0.9127	1.3531	1.3531
	Alachua-2 TP-2	30~42	1.4960	1.4604	1.0244	1.0244
	Alachua-2 TP-3	30~42	1.4930	1.4604	1.0223	1.0223
	Alachua-2 TP-5	30~42	1.2370	1.4604	0.8470	0.8470
	Alachua-5 TP-1	27~50	1.4240	0.6230	2.2857	2.2857
	Alachua-5 TP-2	27~50	0.7050	0.6230	1.1316	1.1316
Duval	Duval-1 TP 1-2	30~45	0.9670	0.9700	0.9969	0.9969
	Duval-1 TP 2-2	30~45	1.0260	0.9700	1.0577	1.0577
	Duval-1 TP 3-3	30~45	1.2110	0.9700	1.2485	1.2485
	Duval-1 TP 1-2	45~55	3.1970	1.9024	1.6805	
	Duval-1 TP 2-2	45~55	3.4980	1.9024	1.8387	
	Duval-1 TP 3-3	45~55	3.5280	1.9024	1.8545	
Hillsborough	Hillsborough-3 TP-2	45~60	1.394	1.1345	1.2287	1.2287
	Hillsborough-3 TP-3	45~60	2.31	1.1345	2.0361	2.0361
	Hillsborough-3 TP-5	50~69	3.415	1.1345	3.0101	
Summary Statistics		Mean			1.5104	1.4128
		Median			1.3501	1.2441
		StDev			0.5470	0.4821
		CV			0.3622	0.3412
		count	28	28	28	24
		min	0.2750	0.3040	0.8160	0.8160
		max	3.5280	1.9024	3.0101	2.6172
* FHWA-Predicted Unit Skin Friction, fs (tsf)						

## CHAPTER 6

### LRFD RESISTANCE FACTOR ASSESSMENT FOR ACIPs IN FLORIDA

#### 6.1 Introduction

Prior to the LRFD resistance factor assessment of the various design methods, an evaluation of the resistance bias (section 6.1) for the summary statistics, goodness of fit against the normal and lognormal cumulative density models, updating for the uncertainty of the segmental method, and exclusion of outliers was performed.

#### 6.2 Assessing Segmental Method Uncertainty

Since the segmental method was used in this project to estimate the measured unit skin friction along the length of the piles, an assessment and inclusion of its error or uncertainty was required. In order to determine the error, the measured load distribution at depths along the instrumented piles presented in section 4.2 (e.g. Alachua-2 TP-5, Alachua-5 TP-1, Alachua 5 TP-2, Broward 1 TP-1, Hillsborough 3 TP2, Hillsborough 3 TP3, Hillsborough 3 TP4, Hillsborough 3 TP5, Nassau 1 TP14, Nassau 3 TP-1, and Santa Rosa 1 TP-1) was compared with the estimated load (segmental method) at the same depths. That is, the bias,  $\lambda_{\text{segmental}}$  was found (i.e. measured unit skin friction/segmental unit skin friction for instrumented piles). Table 6.1 shows the measured/predicted (segmental approach), and the mean bias,  $\lambda$ , for those pile segments in sand. Table 6.2 shows the measured/predicted (segmental approach), and the mean bias,  $\lambda$ , for those pile segments in clay. Table 6.3 shows the measured, predicted (segmental approach), and the bias,  $\lambda$ , for those pile segments in all soil.

Table 6.1 Measured and predicted loads on test pile segments in sand

Sand				
Measured		Predicted		Lamda- $\lambda$
Load (tons)	Depth (ft)	Load (tons)	Depth (ft)	
190.246	20.172	201.230	20.172	0.945
230.229	0.000	237.698	0.000	0.969
249.522	0.000	256.405	0.000	0.973
0.000	80.000	0.000	80.000	1.000
405.587	0.000	413.967	0.000	0.980
94.624	44.967	79.570	44.967	1.189
154.839	24.923	154.839	24.923	1.000
295.161	0.000	287.097	0.000	1.028
225.175	25.265	235.269	25.265	0.957
290.449	0.000	286.524	0.000	1.014
139.497	45.066	148.654	45.066	0.938
206.284	24.891	211.670	24.891	0.975
300.000	0.000	290.305	0.000	1.033
274.909	31.916	277.091	31.916	0.992
346.909	5.088	348.364	5.088	0.996
346.182	0.000	361.455	0.000	0.958
0.000	60.000	0.000	60.000	1.000
65.633	40.000	66.763	40.000	0.983
150.474	20.000	141.434	20.000	1.064
180.277	10.000	182.537	10.000	0.988
200.287	0.000	198.404	0.000	1.009
10.208	60.000	9.527	60.000	1.071
35.161	50.000	36.068	50.000	0.975
70.095	10.000	72.817	10.000	0.963
99.811	0.000	102.306	0.000	0.976
40.041	46.066	33.881	46.066	1.182
54.928	28.934	52.875	28.934	1.039
199.692	0.000	199.692	0.000	1.000
Summary Statistics			mean	1.007
			median	0.994
			StDev	0.060
			CV	0.059
			Count	28
			MSE <sub>mean</sub>	0.00012786
			MSE <sub>var</sub>	9.4938E-07

After assessing the segmental bias estimates (Tables 6.1 -6.3), the measured ultimate skin friction was found from

$$f_{s,measured} = \lambda_{measured/segmental} f_{s,segmental} \quad \text{Eq. 6.1}$$

based on soil type (Tables 6.1 and 6.2). For the Miami limestone and Fort Thompson limestone data sets, the bias correction was made using the bias determined from all soil (sand, clay, and two values in limestone).

Table 6.2 Measured and predicted loads on test pile segments in clay

<b>Clay</b>				
<i>Measured</i>		<i>Predicted</i>		<i>Lamda-<math>\lambda</math></i>
Load (tons)	Depth (ft)	Load (tons)	Depth (ft)	
44.848	42.051	45.981	42.051	0.975
160.192	15.095	157.178	15.095	1.019
180.174	9.155	170.004	9.155	1.060
189.997	0.000	189.243	0.000	1.004
29.877	5.032	19.772	64.129	1.511
140.158	40.043	128.735	40.043	1.089
24.665	50.000	18.929	49.070	1.303
114.723	40.000	109.560	40.000	1.047
150.287	30.000	160.038	30.000	0.939
0.000	60.000	5.376	59.077	1.000
39.247	54.989	26.882	54.989	1.460
70.112	57.996	74.599	57.996	0.940
180.678	47.111	174.510	47.111	1.035
114.722	58.035	114.183	58.035	1.005
2.500	67.996	11.636	67.996	0.215
229.818	51.806	221.091	51.806	1.039
Summary Statistics			mean	1.040
			median	1.027
			StDev	0.281
			CV	0.270
			Count	16
			MSE <sub>mean</sub>	0.00491762
			MSE <sub>var</sub>	0.00082545

Table 6.3 Measured and predicted loads on test pile segments in all soils

All Soils				
Measured		Predicted		Lamda- $\lambda$
Load (tons)	Depth (ft)	Load (tons)	Depth (ft)	
44.848	42.051	45.981	42.051	0.975
160.192	15.095	157.178	15.095	1.019
180.174	9.155	170.004	9.155	1.060
189.997	0.000	189.243	0.000	1.004
29.877	65.032	19.772	64.129	1.511
140.158	40.043	128.735	40.043	1.089
190.246	20.172	201.230	20.172	0.945
230.229	0.000	237.698	0.000	0.969
24.665	50.000	18.929	49.070	1.303
114.723	40.000	109.560	40.000	1.047
150.287	30.000	160.038	30.000	0.939
249.522	0.000	256.405	0.000	0.973
0.000	80.000	0.000	80.000	1.000
39.386	47.081	39.386	47.081	1.000
390.503	15.081	387.989	15.081	1.006
405.587	0.000	413.967	0.000	0.980
0.000	60.000	5.376	59.077	1.000
39.247	54.989	26.882	54.989	1.460
94.624	44.967	79.570	44.967	1.189
154.839	24.923	154.839	24.923	1.000
295.161	0.000	287.097	0.000	1.028
70.112	57.996	74.599	57.996	0.940
180.678	47.111	174.510	47.111	1.035
225.175	25.265	235.269	25.265	0.957
290.449	0.000	286.524	0.000	1.014
114.722	58.035	114.183	58.035	1.005
139.497	45.066	148.654	45.066	0.938
206.284	24.891	211.670	24.891	0.975
300.000	0.000	290.305	0.000	1.033
2.500	67.996	11.636	67.996	0.215
229.818	51.806	221.091	51.806	1.039
274.909	31.916	277.091	31.916	0.992
346.909	5.088	348.364	5.088	0.996
346.182	0.000	361.455	0.000	0.958
0.000	60.000	0.000	60.000	1.000
65.633	40.000	66.763	40.000	0.983
150.474	20.000	141.434	20.000	1.064
180.277	10.000	182.537	10.000	0.988
200.287	0.000	198.404	0.000	1.009
10.208	60.000	9.527	60.000	1.071
35.161	50.000	36.068	50.000	0.975
70.095	10.000	72.817	10.000	0.963
99.811	0.000	102.306	0.000	0.976
40.041	46.066	33.881	46.066	1.182
54.928	28.934	52.875	28.934	1.039
199.692	0.000	199.692	0.000	1.000
Summary Statistics			mean	1.018
			median	1.000
			StDev	0.169
			CV	0.166
			Count	46

## 6.3 LRFD Measured/Predicted Bias Assessment

### 6.3.1 Granular Soils

Table 6.4 lists the bias (measured/predicted) values for the sites with ACIPs located in sand layers. For each site and depth where the pile was embedded in the sand, both the measured and predicted unit skin friction using the FHWA, Zelada and Brown methods are given. In the case of Brown,  $f_s^*$  were the un-factored and  $f_s^{**}$  were for OCR limited to 10 and  $\phi'$  to  $40^\circ$ . With these, the bias (measured/predicted) were calculated for each sand layer. As a result, there are 36 bias values for the FHWA, Zelada and Brown methods based on all the sites. Miami Dade provided the most measured with 17 values from load tests. The other sites had fewer load tests per site (2 to 4), however, 19 values in all were found for all sites.

Figure 5.19 shows the distribution of the FHWA and Zelada bias values plotted against the normal and lognormal models based on each data set's summary statistics. For both methods, it is apparent that the data is described by the lognormal model.

### 6.3.2 Cohesive Soils

Table 6.5 lists the bias values for the sites with ACIPs embedded in layers of clay. For the specific depth the pile was embedded in the clay, the measured unit skin friction and the predicted unit skin friction using the FHWA method are given. With these, the bias (measured/predicted) were calculated for each layer. As a result there are 28 bias values for the FHWA method based on all the sites. Most of the values are from sites in Alachua County, with 19 values from 3 sites and 9 load tests. Duval County had provided 6 values from 1 site and 3 load test. Hillsborough County had 3 values from 1 site and 3 test piles. Figure 5.20 shows the distribution of the FHWA bias values plotted against the normal and lognormal models based on

Table 6.4 Bias values of FHWA, Zelada, and Brown methods for ACIPs in granular soils

Pile	Depth (ft)	$f_s$ MEAS (tsf)	$f_s$ FHWA (tsf)	Bias <sub>FHWA</sub>	$f_s$ ZELADA (tsf)	Bias <sub>ZELADA</sub>	* $f_s$ Brown (tsf)	*Bias <sub>BROWN</sub>	** $f_s$ Brown (tsf)	**Bias <sub>BROWN</sub>
Miami Dade-1 TP-1	18~35	0.4413	0.4879	0.9046	0.3903	1.1307	0.4808	0.9179	0.4756	0.9279
Miami Dade-6 TP-2	20~40	0.9938	0.6028	1.6486	0.4823	2.0605	0.6491	1.5310	0.6089	1.6321
Miami Dade-6 TP-5	16~40	0.5885	0.6028	0.9762	0.4823	1.2202	0.6491	0.9066	0.6089	0.9665
Miami Dade-6 TP-9	24~40	0.4783	0.6028	0.7934	0.4823	0.9917	0.6491	0.7368	0.6089	0.7855
Miami Dade-6 TP-10	22~40	0.4040	0.6028	0.6702	0.4823	0.8377	0.6491	0.6224	0.6089	0.6635
Miami Dade-6 TP-11	8~23	0.9067	0.6028	1.5041	0.4823	1.8798	0.6491	1.3968	0.6089	1.4890
Miami Dade-6 TP-13	25~40	0.5040	0.6028	0.8361	0.4823	1.0450	0.6491	0.7765	0.6089	0.8277
Miami Dade-6 TP-14	16~58	0.3923	0.6028	0.6508	0.4823	0.8134	0.6491	0.6044	0.6089	0.6443
Miami Dade-6 TP-15	11~45	0.6156	0.6028	1.0212	0.4823	1.2763	0.6491	0.9484	0.6089	1.0110
Miami Dade-6 TP-16	14~25	0.8525	0.6028	1.4143	0.4823	1.7677	0.6491	1.3134	0.6089	1.4001
Miami Dade-6 TP-19	9~30	0.7771	0.6028	1.2891	0.4823	1.6112	0.6491	1.1971	0.6089	1.2762
Miami Dade-6 TP-20	26~30	0.5832	0.6028	0.9675	0.4823	1.2092	0.6491	0.8985	0.6089	0.9578
Miami Dade-6 TP-21	17~46	0.6123	0.6028	1.0158	0.4823	1.2696	0.6491	0.9433	0.6089	1.0056
Miami Dade-6 TP-23	0~58.5	0.2750	0.6028	0.4562	0.4823	0.5702	0.6491	0.4237	0.6089	0.4516
Miami Dade-6 TP-24	20~47	0.6508	0.6028	1.0796	0.4823	1.3494	0.6491	1.0026	0.6089	1.0688

Miami Dade-6 TP-29	24~46	0.9164	0.6028	1.5203	0.4823	1.9001	0.6491	1.4118	0.6089	1.5050
Miami Dade-6 TP-30	15~45	0.6590	0.6028	1.0932	0.4823	1.3664	0.6491	1.0153	0.6089	1.0823
Alachua-5 TP-1	0~27	0.4980	0.5356	0.9298	0.4285	1.1622	0.8814	0.5650	0.6864	0.7255
Alachua-5 TP-2	0~27	0.4510	0.5356	0.8420	0.4285	1.0525	0.8814	0.5117	0.6864	0.6571
Broward-1 TP-1	0~15	0.3580	0.1601	2.2362	0.1281	2.7953	0.1018	3.5167	0.0972	3.6831
Broward-1 TP-1	48~80	0.4770	0.6513	0.7324	0.5210	0.9155	0.8714	0.5474	0.8295	0.5750
Broward-2 TP-1	0~10	0.3311	0.4000	0.8278	0.3200	1.0347	1.0461	0.4560	0.9395	0.3524
Broward-2 TP-1	10~32	0.5364	1.0750	0.4990	0.8604	0.6234	1.0234	0.3235	0.9355	0.5734
Duval-1 TP 1-2	0~30	0.3410	0.3924	0.8690	0.3140	1.0860	0.3756	0.9079	0.3639	0.9371
Duval-1 TP 2-1	0~30	0.3920	0.3924	0.9990	0.3140	1.2484	0.3756	1.0437	0.3639	1.0772
Duval-1 TP 3-3	0~30	0.2790	0.3924	0.7110	0.3140	0.8885	0.3756	0.7428	0.3639	0.7667
Hillsborough-3 TP-1	0~55	0.5489	0.7242	0.7579	0.5793	0.9475	0.9209	0.5960	0.8006	0.6856
Hillsborough-3 TP-3	0~45	0.4700	0.5925	0.7932	0.4740	0.9916	0.7534	0.6238	0.6551	0.7174
Hillsborough-3 TP-4	0~58	0.7407	0.7637	0.9699	0.6109	1.2125	0.9711	0.7627	0.8443	0.8773
Hillsborough-3 TP-5	0~50	0.6254	0.6584	0.9499	0.5267	1.1874	0.8372	0.7470	0.7278	0.8593
Nassau-1 TP14	0~10	0.4990	0.2540	1.9646	0.2030	2.4581	0.371	1.3450	0.2539	1.9653
Nassau-1 TP14	10~50	1.3773	0.8280	1.6634	0.6620	2.0805	0.9103	1.5130	0.8274	1.6646
Nassua-3 TP-1	10~60	0.3818	0.4736	0.8062	0.3789	1.0077	0.9103	0.4194	0.8274	0.4614
West Palm-1 T9B	0~10	0.3100	0.3034	1.0218	0.2427	1.2773	0.4735	0.6547	0.4688	0.6613



West Palm-1 T9B	10~30	0.4710	0.5282	0.8917	0.4226	1.1145	1.017	0.4631	0.9302	0.5063
West Palm-1 T9B	30~40	0.4936	0.7679	0.6428	0.6143	0.8035	1.022	0.4830	0.9348	0.5280
Summary Statistics	Mean			1.0264		1.2829		0.9130		0.9991
	Median			0.9398		1.1748		0.7696		0.8683
	StDev			0.3950		0.4940		0.5573		0.5967
	CV			0.3849		0.3851		0.6104		0.5972
	count	36	36	36	36	36	36	36	36	36
	min	0.2750	0.1601	0.4562	0.1281	0.5702	0.1018	0.3235	0.0972	0.3524
	max	1.3773	1.0750	2.2362	0.8604	2.7953	1.0461	3.5167	0.9395	3.6831

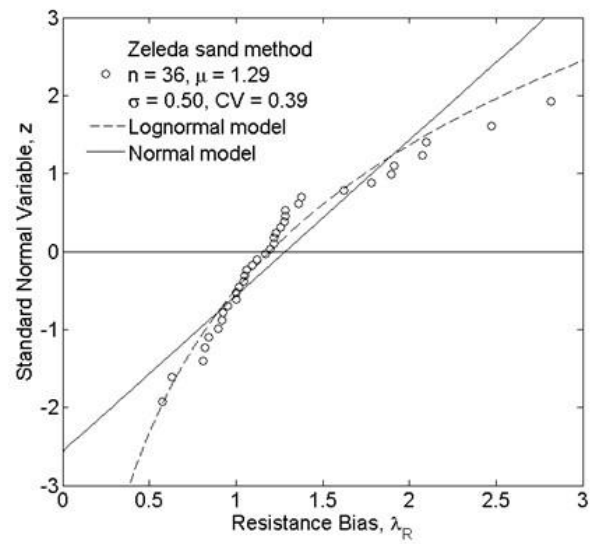
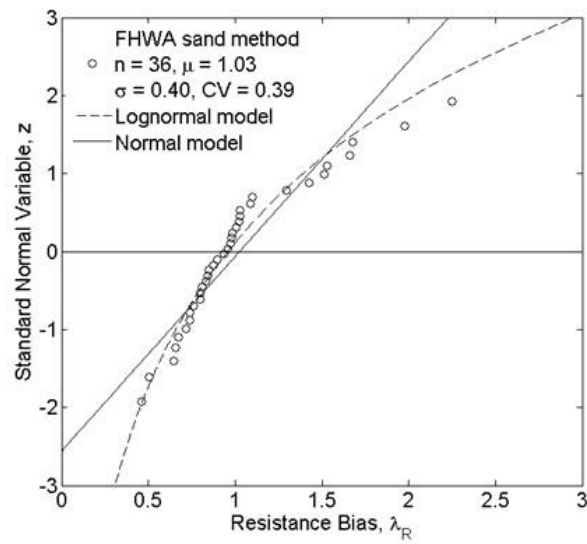


Figure 5.19 FHWA and Zelada sand method bias distributions

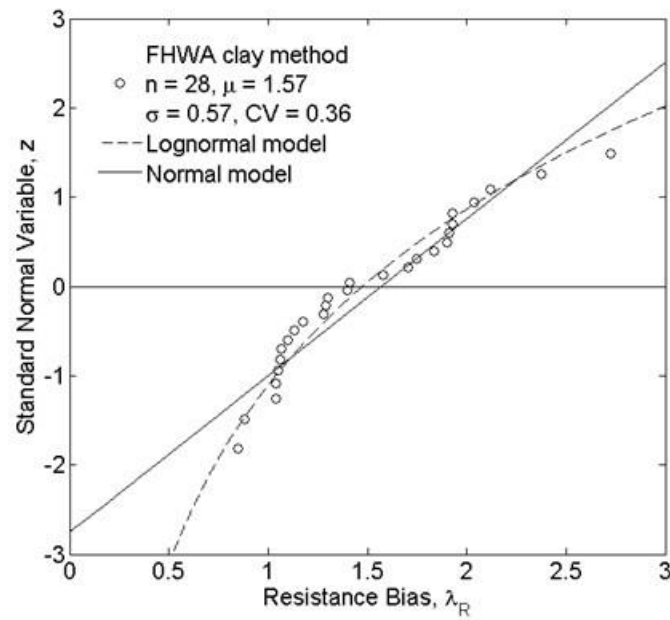


Figure 5.20 FHWA clay model bias distribution

Table 6.5 Bias values of FHWA method for ACIP piles in clay

Site	Pile	Elev. Range (ft)	fs MEAS(tsf)	fs PRED (tsf)	Bias <sub>FHWA</sub>
Alachua	Alachua-1 TP-2	0~20	0.6781	0.4840	1.4011
	Alachua-1 TP-3	0~20	0.9319	0.4840	1.9255
	Alachua-1 TP-4	0~20	0.5086	0.4840	1.0508
	Alachua-1 TP-5	0~20	0.6241	0.4840	1.2894
	Alachua-1 TP-2	20~40	0.3817	0.3370	1.1327
	Alachua-1 TP-3	20~40	0.9174	0.3370	2.7222
	Alachua-1 TP-4	20~40	0.2860	0.3370	0.8487
	Alachua-1 TP-5	20~40	0.3495	0.3370	1.0370
	Alachua-2 TP-2	0~15	0.4795	0.3040	1.5773
	Alachua-2 TP-3	0~15	0.5773	0.3040	1.8989
	Alachua-2 TP-5	0~15	0.6199	0.3040	2.0391
	Alachua-2 TP-2	15~30	1.6735	0.9127	1.8336
	Alachua-2 TP-3	15~30	1.5581	0.9127	1.7071
	Alachua-2 TP-5	15~30	1.2845	0.9127	1.4074
	Alachua-2 TP-2	30~42	1.5560	1.4604	1.0655
	Alachua-2 TP-3	30~42	1.5529	1.4604	1.0633
	Alachua-2 TP-5	30~42	1.2866	1.4604	0.8810
	Alachua-5 TP-1	27~50	1.4811	0.6230	2.3774
	Alachua-5 TP-2	27~50	0.7333	0.6230	1.1770
Duval	Duval-1 TP 1-2	30~45	1.0058	0.9700	1.0369

	Duval-1 TP 2-2	30~45	1.0671	0.9700	1.1001
	Duval-1 TP 3-3	30~45	1.2596	0.9700	1.2985
	Duval-1 TP 1-2	45~55	3.3252	1.9024	1.7479
	Duval-1 TP 2-2	45~55	3.6383	1.9024	1.9125
	Duval-1 TP 3-3	45~55	3.6695	1.9024	1.9289
Hillsborough	Hillsborough-3 TP-2	45~60	1.4499	1.1345	1.2780
	Hillsborough-3 TP-3	45~60	2.4026	1.1345	2.1178
	Hillsborough-3 TP-5	50~69	3.5519	1.1345	3.1308
Summary Statistics		Mean	1.3875	0.8779	1.5709
		Median	1.1634	0.9127	1.4043
		StDev	1.0237	0.5201	0.5689
		CV	0.7378	0.5924	0.3622
		count	28	28	28
		min	0.2860	0.3040	0.8487
		max	3.6695	1.9024	3.1308

the data set's summary statistics. The comparison suggest that the data best described by the lognormal model.

### 6.3.3 Miami Limestone (Intermediate GeoMaterial, IGM)

As identified in section 5.2 (predictions of ACIP piles in Limestone), the site means were used to predict the mean side friction for both the Miami and Fort Thompson formation. Since there were only two sites (Miami Metro Rail and Broward, see Table 2.2), only 2 predicted means were available, i.e. insufficient data to assess CV of bias, even though 26 load tests (e.g.

estimated/measured Miami data) were available. To overcome deficiency of data near the load test (i.e. predicted), the variability of the predicted ultimate side friction could be estimated from the recorded site data ( $q_u$ ,  $q_t$ ,  $N$ ). For example, all the rock data (Figure 5.6 – Miami, or Figure 5.8 – Fort Thompson) may be inputted to a given method (e.g. Horvath, Gupton, etc.) and its associated predicted mean ( $\mu_Y$ ) and standard deviation ( $\sigma_Y$ ) could be obtained. Similarly, for any formation (Miami or Fort Thompson) the estimated mean ( $\mu_X$ ) ultimate skin (Table 2.2), bias corrected ( $f_{s, \text{estimated-segmental}} \lambda_{\text{measured/segmental}}$ ) and standard deviation ( $\sigma_X$ ) may be determined. Then based on the distribution of both X and Y, the variance (VAR, i.e. standard deviation squared) of the ratio may be found. In the case of two normally distributed random variables (i.e. Gaussian distribution) that are correlated (i.e., COV), the VAR is given by Eq. 6.2. Again, the variables X and Y represent the “measured” and “predicted”, respectively, analyzed for each of the data sets. This expression was used to determine the variance of the bias for the data sets that could be described as normally distributed, which were the FDOT and Herrera following the removal of  $q_u$  and  $N$  values according to  $\pm\sigma$  (i.e., FDOT method).

$$VAR\left(\frac{X}{Y}\right) = \frac{\sigma_X^2}{\mu_Y^2} + \frac{\mu_X^2}{\mu_Y^4} \sigma_Y^2 - 2 \frac{\mu_X}{\mu_Y^3} COV(X, Y) \quad \text{Eq. 6.2}$$

Equation 6.3 is the variance of a ratio of two lognormally distributed random variables that are correlated (i.e., COV). This expression was used to determine the variance of the bias for the data sets that could be described as lognormally distributed, which were all data sets besides the FDOT and Herrera.

$$VAR\left(\frac{X}{Y}\right) = VAR(e^z) = e^{(2\mu_z + 2\sigma_z^2)} - e^{(2\mu_z + \sigma_z^2)} \quad \text{Eq. 6.3}$$

where

$$\sigma_z^2 = \sigma_X^2 + \sigma_Y^2 - 2COV(X, Y) \quad \text{Eq. 6.4}$$

Tables 6.6 and 6.7 are the calculated summary statistics (including standard deviation and CV = Square root of VAR / mean bias-measured/predicted) for all of methods based on  $q_u$  and SPT N, respectively, for Miami Limestone which is an Intermediate GeoMaterial (IGM). Note, for the FDOT and Herrera methods, the  $q_u$  data was trimmed using the  $\pm\sigma$  approach. This generally results in normally distributed data sets, and thus the CV of each was initially calculated based on the normal variance expression, i.e. Equation 6.3. The Reynolds, Gupton, and Reese methods showed a high variances that led to CVs of about 1.2. Each of the three method are quite similar, they only vary due to different constants. Subsequently, for the three methods, the values were limited to  $5 \text{ tsf} < q_u < 50 \text{ tsf}$  (FHWA guidelines for grouping IGM). After trimming, the calculated CVs for these methods were reduced to approximately 0.47 (Table 6.6). Similarly, the data set for the Frizzi SPT N method only includes unit side friction  $2 \text{ tsf} < f_{s,ult} < 6.5 \text{ tsf}$  (range reported by Frizzi and Meyer, 2000).

#### **6.3.4 Fort Thompson Limestone**

Similar to the approach used on the Miami Limestone dataset, i.e. no boring near load test results and the use of only one mean site prediction, the estimated mean and variance of the measured and predicted ultimate skin friction individually was performed. Specifically, Equations 6.2 and 6.3 were used to calculate the variance of the bias knowing the individual measured and predicted mean and standard deviation. Subsequently, the bias and CV of each method was calculated.

Tables 6.8 and 6.9 are the calculated summary statistics (including Standard Deviation, and CV) of the bias for methods based on  $q_u$  and SPT N, respectively, for the Fort Thompson formation. The data sets of predicted unit side friction are much more limited than the Miami

Limestone data set, with only 11 values of measured unit side friction. Similarly, for the FDOT and Herrera methods, the  $q_u$  data was trimmed using the  $\pm\sigma$  approach, which resulted in normally distributed data sets. The CV of each was initially determined based on the calculated variance expression in Equation 6.2. The Reynolds, Gupton, and Reese methods again showed high variances that led to CVs of about 1.2. Each method is similar and only varies due to different constants, which are similar. Subsequently, values  $5 \text{ tsf} < q_u < 50 \text{ tsf}$  (FHWA guidelines for grouping IGM) were only considered. As a result the calculated CVs for these methods were less, about 0.50 (Table 6.8). The data set for the Frizzi SPT N method only includes unit side friction  $2 \text{ tsf} < f_{s,ult} < 6.5 \text{ tsf}$  (reported range of Frizzi and Meyer, 2000).

Table 6.6 Summary statistics of bias for prediction methods using rock strengths for Miami Limestone

Statistic	FDOT	Herrera	Horvath	Williams	Reynolds	Gupton	Reese	Rowe	Carter	Ramos	Kulhawy
Mean	1.05	0.851	0.988	0.554	0.564	0.846	1.13	0.456	1.05	1.08	0.648
StDev	0.453	0.282	0.449	0.207	0.267	0.401	0.534	0.208	0.478	0.410	0.295
CV	0.434	0.331	0.454	0.373	0.474	0.474	0.474	0.455	0.455	0.379	0.455

Table 6.7 Summary statistics of bias for prediction methods using SPT N for Miami Limestone

Statistic	Herrera	Frizzi	Ramos
Mean	0.977	0.713	0.511
StDev	0.756	0.582	0.256
CV	0.774	0.817	0.50



Table 6.8 Summary statistics of bias for prediction methods using rock strengths for Fort Thompson Limestone

Statistic	FDOT	Herrera	Horvath	Williams	Reynolds	Gupton	Reese	Rowe	Carter	Ramos	Kulhawy
Mean	0.841	1.01	0.937	0.594	0.557	0.836	1.11	0.433	0.997	0.649	0.615
StDev	0.27	0.35	0.378	0.16	0.278	0.417	0.556	0.15	0.346	0.37	0.213
CV	0.321	0.351	0.403	0.271	0.50	0.50	0.50	0.346	0.347	0.571	0.347

Table 6.9 Summary statistics of bias for prediction methods using SPT N for Fort Thompson Limestone

Statistic	Herrera	Frizzi	Ramos
Mean	0.652	0.67	0.41
StDev	0.254	0.339	0.246
CV	0.376	0.505	0.598

## 6.4 LRFD Resistance Factors

Resistance factors,  $\Phi$ , for each of the selected methods used to predicted the ACIP pile unit skin friction in the sand, clay, Miami IGM, and Fort Thompson Limestone are calculated using the First Order Second Moment (FOSM) approach. While the FOSM is a closed form method, it works on the assumption that the load and resistance are lognormally distributed. An alternative approach to determining the  $\Phi$ 's is the First Order Reliability Method (FORM). Paikowsky et al. (2004) showed in an NCHRP 507 study of LRFD for deep foundations,  $\Phi$ 's developed using the FORM were 10% - 15% greater than those developed using FOSM. Styler (2006) showed a revised expression for the coefficient of variation,  $CV (\sigma / \mu)$ , of the load that, when used in the FOSM method, resulted in  $\Phi$ 's about 5% less than those developed using the FORM. The revised expression for  $CV$  of the load will be used here.

For the calibration, the following load parameters according to the AASHTO (2014) recommendation for load cases, I, II, and IV, and used by Paikowsky et al. (2004) in the NCHRP 507 study, were used: dead to live load ratio  $q_D/q_L = 2$ , dead load factor  $\gamma_D = 1.25$ , live load factor  $\gamma_L = 1.75$ , dead load bias factor  $\lambda_D = 1.05$ , live load bias factor  $\lambda_L = 1.15$ , dead load coefficient of variation  $CV_D = 0.10$ , and live load coefficient of variation  $CV_L = 0.20$ .

Note, in Equation 6.5, LRFD  $\Phi$  equation by FHWA, the uncertainty in the load is represented by  $CV_Q$  as presented by Styler (2006). In Equation 6.6, the  $CV_Q$  can be represented in terms of its dead and live load  $CV$  components. In FHWA's Eq. 10,  $\lambda_R = \lambda$ , i.e. mean bias that was presented earlier.

$$\Phi = \frac{\lambda_R \cdot \left( \gamma_D \cdot \frac{q_D}{q_L} + \gamma_L \right) \cdot \sqrt{\frac{(1 + CV_Q^2)}{(1 + CV_R^2)}}}{\left( \lambda_D \cdot \frac{q_D}{q_L} + \lambda_L \right) \cdot e^{\beta \sqrt{\ln[(1 + CV_R^2)(1 + CV_Q^2)]}}} \quad \text{Eq. 6.5}$$

$$CV_Q^2 = \frac{\left( \frac{q_D}{q_L} \lambda_D CV_D \right)^2 + (\lambda_L CV_L)^2}{\left( \frac{q_D}{q_L} \lambda_D \right)^2 + 2 \frac{q_D}{q_L} \lambda_D \lambda_L + \lambda_L^2} \quad \text{Eq. 6.6}$$

where the parameters  $\lambda_R$ ,  $CV_R$  are from the data sets being analyzed and  $\beta$  is selected according to the AASHTO (2014). The target reliability used was  $\beta = 2.33$  which corresponds to a probability of failure of 1 in 100.

Tables 6.10 through 6.11 are the calculated  $\Phi$ 's for the methods based on the bias and CV data presented in the previous tables. Table 6.10 are the calculated  $\Phi$ 's for sand and clay using FHWA, Zeleda, and Brown design methods based on mean SPT N site values. An evaluation of the methods based on their efficiency ( $\Phi/\lambda$  (%)-McVay et al., 2000) shows that the FHWA and Zeleda methods to be most efficient and with  $\Phi$ 's of 0.51 and 0.64, respectively. For the FHWA clay method, the  $\Phi$  is 0.83.

In Table 6.11 are the calculated  $\Phi$ 's for methods based on rock strength for Miami Limestone or IGM. The  $\Phi$ 's range from 0.19 to 0.55, with the most efficient method being the Herrera ( $\Phi/\lambda = 55\%$ ). In Table 6.12 are the calculated  $\Phi$ 's for methods based on SPT N values for Miami Limestone or IGM. The  $\Phi$ 's range from 0.14 to 0.20, with the most efficient method being the Ramos ( $\Phi/\lambda = 38\%$ ).

In Table 6.13 are the calculated  $\Phi$ 's for methods based on rock strength for Fort Thompson Limestone. The  $\Phi$ 's range from 0.21 to 0.55, with the most efficient method being

the Herrera ( $\Phi/\lambda = 55\%$ ). Shown in Table 6.14 are the calculated  $\Phi$ 's for methods based on SPT N values for Fort Thompson Limestone. The  $\Phi$ 's range from 0.13 to 0.33, with the most efficient method being the Herrera ( $\Phi/\lambda = 55\%$ ). Note, the current FDOT design guideline suggests the use of the FHWA methods for sand and clay and a  $\Phi$  of 0.6 when performing LRFD design for ACIP's (FDOT, 2013).

Table 6.10 Resistance factors for ACIP pile methods in sand and clay

Method	$\Phi$	$\Phi/\lambda$ (%)
Sand		
FHWA	0.51	0.50
Zelada	0.64	0.50
Brown	0.27	0.30
Brown <sup>†</sup>	0.31	0.31
Clay		
FHWA	0.83	53

<sup>†</sup> Brown method using limited data determined by using  $OCR < 10$  and  $\phi < 40^\circ$ .

Table 6.11 Resistance factors for ACIP pile methods based on  $q_u$  for Miami Limestone

Method	$\Phi$	$\Phi/\lambda$ (%)
Miami Formation		
$q_u$		
Horvath	0.42	43
Williams	0.29	52
Reynolds	0.23	41
Gupton	0.34	41
Reese	0.46	41
Rowe	0.19	42
Carter	0.45	42
Ramos	0.55	51
Kulhawy	0.28	42
Herrera $\pm\sigma q_u$	0.48	56
FDOT ( $\pm\sigma q_u$ and $q_t$ )	0.47	45

Table 6.12 Resistance factors for ACIP pile methods based on SPT N for Miami Limestone

Method	$\Phi$	$\Phi/\lambda$ (%)
Miami Formation		
SPT		
Herrera	0.20	21
Frizzi	0.14	19
Ramos	0.20	38

Table 6.13 Resistance factors for ACIP pile methods based on  $q_u$  for Fort Thompson Limestone

Method	$\Phi$	$\Phi/\lambda$ (%)
Fort Thompson		
$q_u$		
Horvath	0.45	48
Williams	0.39	66
Reynolds	0.21	38
Gupton	0.32	38
Reese	0.42	38
Rowe	0.24	55
Carter	0.55	55
Ramos	0.21	32
Kulhawy	0.34	55
Herrera $\pm\sigma q_u$	0.55	55
FDOT ( $\pm\sigma q_u$ and $q_t$ )	0.49	58

Table 6.14 Resistance factors for ACIP pile methods based on SPT N for Fort Thompson  
Limestone

Method	$\Phi$	$\Phi/\lambda$ (%)
Fort Thompson		
SPT N		
Herrera	0.33	51
Frizzi	0.25	37
Ramos	0.13	30

## CHAPTER 7 RECOMMENDATIONS FOR DESIGN AND SELECTION OF MINIMUM NUMBER OF LOAD TESTS PER SITE

### **7.1 Collected Load Test Data and Soil/Rock Data**

The focus of this research project was the development of LRFD Resistance Factors,  $\Phi$ , for Auger Cast in Place Piles (ACIP) constructed in Florida. A total 78 pile load tests (see Table 2.2) from 21 sites identified by county were collected for the research. The distribution of piles based on diameter were 53-14 inch, 17-16 inch, 6-18 inch, 1-24 inch, and 1-30 inch. Most of the test piles were between 20 and 68 feet in length, but three were greater than 100 ft and one was only 15 feet in length. Forty-four of the test piles were in a layer of limestone with a layer of sand and/or clay above or below. Seven of the test piles were in sand, 4 in clay, 15 piles were in multiple layers of sand, clay or silt and 8 had no borings. Sixteen of the top down compression loaded piles were instrumented along their length from which skin friction distribution measurements as well as T-Z curves were available. The in situ data reported was generally SPT blow counts with lab testing for soil classification. One site (Santa Rosa) had conventional CPT sounding, and another, a Miami site, had dynamic cone data. The Miami sites had limestone with measured rock strength (unconfined compressive strength,  $q_u$ , and split tensile strength,  $q_t$ ) for both the Miami and Fort Thompson formations.

Inspection of the 78 load tests revealed that the maximum pile head displacement was 1.18" (Hillsborough – 16" x 60', clay, and sand site), but a majority (> 90%) of pile top displacements were in the range of 0.1 to 0.3 inches (Table 2.2). Since typical failure (e.g. Davisson, FHWA, etc.) has movements of 0.4" to 0.8" (e.g. FHWA – 5% diameter:  $0.05 \times 14" = 0.75"$ ), most, if not all, the load tests did not reach failure and were generally only loaded to twice the design load (ASTM D1143). Moreover, given the nominal pile head displacements (0.1" to 0.3") as well as



typical pile lengths (40 to 60 ft), observed mobilized tip resistance was small compared to applied top load. For instance, the maximum mobilized tip resistance in the database was 30% of top load and occurred with a large pile top displacement (i.e. Hillsborough >1.0") for a pile embedded in only soil. Generally, the average tip resistance for the database was less than 10% of applied top load; in the case of the Miami ACIP piles (embedded in 2 layers of limestone: Miami and Fort Thompson), small top movements (< 0.3") were observed and little if any tip resistance was found. Therefore, current practice suggests that most if not all ACIP piles are designed for side friction only (i.e. minimal tip resistance). Consequently, the LRFD  $\Phi$  assessment for the project focused only on side friction of ACIP piles.

Many of the soil and rock design methods for ACIPs been reported in FHWA GEC 18 (Brown et al., 2007). Generally, the methods have been developed independently for piles in Cohesionless & Cohesive soils, and rock (e.g., limestone). The methods generally estimate resistance based soil properties ( $S_u$ ,  $\phi$ ), rock properties ( $q_u$ ,  $q_t$ , RQD), in situ stresses (vertical effective stress) or in situ measurements (SPT-N, CPT- $q_c$ ). A number of the methods distinguish between weak and strong rock, as well as specific formations (e.g., Miami Limestone, Frizzi and Meyer, 2000). In addition, intermediate geomaterial (IGM – strength between soil and rock) designs are available for ACIPs for both Cohesive ( $S_u$  between 5 ksf and 50 ksf) and Cohesionless soils ( $N_{60}$  between 50 and 100). All of the methods estimate the nominal (failure) unit skin and/or tip resistance of ACIPs.

Based on the geotechnical information (in situ and laboratory) reported for all of the sites, most designs were based on boring logs, laboratory soil classification, strength testing (unconfined compression, and split tension) and SPT  $N_{60}$  values. Very few sites (only Santa Rosa) performed any CPT testing, even though 23 of the 78 load test piles were in sand, clay or a

mixture of soils. However, it should be noted that a number of these sites had strong/stiff clay (Hillsborough), marl (Duval) and sand (Nassau) layers that would be difficult for CPT penetration. Consequently, design methods based on CPT (Task 2 report): Bustamante & Gianeselli (LPC), Rizkalla (1988), and Viggiani (1993) were not evaluated for the collected ACIP database.

Besides in situ and laboratory data collected, a number of the design methods required other strength parameters, e.g.  $S_u$  (undrained shear strengths), and angle of internal friction,  $\phi$ . Some sites (Alachua-2) provided this data, for other sites, it had to be estimated. A review of the literature, resulted in the selection of Sowers (1979) for SC and CH soils (USCS), and Terzaghi for CL clays based on  $N_{60}$  values within a boring. Limited data from one site (Alachua) agreed with the selected relationships. In the case of angle of internal friction, the method by Hatanaka and Uchida (1996) was selected based on SPT  $N$  values. A comparison of limited data (Miami and Duval) showed similar results (predicted and reported).

## **7.2 Discussion of Design Methods Evaluated and Their Associated Bias & CVs**

The evaluation of LRFD resistance factors for unit skin friction design methods began by identifying the methods that were applicable to Florida soil and rock conditions. A method was evaluated if 1) soil, rock or pile placement were similar to the Florida conditions; and 2) all parameters for any method could be assessed for all sites. A discussion of methods considered and eliminated are presented along with a discussion of results (Bias and CV).

In the case of sand, the methods developed by FHWA, Zelada (2000), and Brown (2010) were evaluated since they depend on site data that was readily available: SPT  $N_{60}$ , and unit weights, or could be estimated (angle of internal friction). However, the method by Neely (1991) was not considered, since it was developed only for piles embedded in a single sand layer

(e.g. vertical stress at midpoint of pile, and beta function of total pile length). Methods by Wright and Reese (1979) and Douglas (1983) were also not considered due to lack of information (e.g.  $K_s$  – lateral earth pressure coefficient – no guidance on selection). Finally, Stuedlein et al (2013) was not considered since it was developed in Northwest soil conditions and had only 6 case studies.

For clays, all of the unit skin friction design methods identified (Table 3.2) are based on undrained shear strength,  $S_u$  multiplied by a constant coefficient. However, a number of the methods, were developed for a specific locale (e.g. Clemente, 2000) or condition (e.g. saturated clays - Coleman and Arcement, 2002), i.e. non-Florida conditions and thus were not evaluated. The method identified by FHWA or Reese and O'Neill (1999) was evaluated, since it has been used in Florida soils.

In the case of rock and IGM materials, a total of 14 methods Table 6.6 were evaluated, since all the methods have been used in Florida (e.g. ACIP and drilled shafts) with required laboratory strengths ( $q_u$ , and  $q_t$ ) as well as in situ SPT  $N_{60}$  for each site. Unfortunately, many of the borings were far from the load test data. For instance in the case of Miami Dade, 6 borings located between 100 ft to more than a mile from the load test results were available. Consequently, as suggested in FDOT report BD-545, RPWO#76 (Modification of LRFD Resistance Factors Based on Site Variability), the mean site predictions of unit skin friction based on all the boring or laboratory data on the site was compared to the mean measured side friction on the site.

Based on the analysis, a number of similarities and differences between the computed bias (measured/predicted) and CV (coefficient of variation of bias) and reported values in the literature were found:

- For clays, the computed (Table 6.5) bias (measured/predicted) of 1.57, and CV of 0.36 are very similar to O'Neill's (Axial Performance of CFA piles to TDOT, 1999) bias, 1.52 and CV, 0.39 for the FHWA method for clays.
- In the case of sands, O'Neill (1999) reports a bias of 0.98 and a CV of 0.27 versus a bias of 1.02 and CV of 0.38 in Table 6.4 for the FHWA method. It should be noted that bias is generally more accurate with fewer points than CV. In the case of the TDOT report, O'Neill had 12 points whereas, Table 6.4 had 36 points.
- Zelada and Stephenson (2000) reported a bias of 1.1 and a CV of 0.37 versus Table 6.4 bias of 1.28 and CV of 0.38 for sands. The difference in bias may be attributed to Zelada and Stephenson (2000) inclusion of end bearing in the pile's nominal resistance (defined failure as settlement = 10% diameter of shaft).
- For Brown's (2010) sand method, Table 6.4, the bias (measured/predicted) were quite reasonable (0.91 non modified and 0.999 modified by limiting  $OCR < 10$ , and  $\phi' < 40$ ); however the CVs (0.61 non modified and 0.60 modified) were appreciably larger than the FHWA and Zelada CVs values, 0.38. This difference may be attributed to estimation of OCR and  $\phi'$  from SPT N values from multiple borings at large distances from the load tests. In addition, multiple borings were used to compute mean values, since all borings were generally greater than 50 ft. from load test piles.
- In the case of rock, a number of methods (Tables 6.6-6.9) had reasonable bias values ( $0.6 < \lambda < 1.2$ ): FDOT, Herrera, Gupton, Reese, Carter, Ramos, and Kulhawy, and Frizzi for both Miami and Fort Thompson Limestone (Tables 6.13-6.15). However, very few had CVs less than 0.4 (Herrera, FDOT-Fort Thompson,

Ramos – Miami, Rowe – Fort Thompson). The high CV were attributed to using all borings on the site to obtain site mean and associated variability vs. limited boring data in the vicinity of the pile load test (< 50 ft).

### **7.3 Discussion of LRFD Resistance Values for ACIPs in Florida**

In the case of ACIP installed in soils, the computed LRFD resistance values,  $\Phi$ , varied by method and soil type:

- For the FHWA (1999) method in sands, Table 6.10, reports  $\Phi = 0.51$  and  $\Phi/\lambda = 0.5$  while Zelada (2000) has  $\Phi = 0.64$  and  $\Phi/\lambda = 0.5$ . The higher  $\Phi$  for Zelada vs. FHWA may be attributed to the more conservative predictions of Zelada ( $\lambda = 1.28$ , Table 6.4) vs. FHWA ( $\lambda = 1.03$ , Table 6.4); however both had the same CV (0.38, Table 6.4) and  $\Phi/\lambda$ .
- Brown's method (2010) original and modified ( $\text{OCR} < 10$ ,  $\phi < 40^\circ$ ) for sand had the lowest  $\Phi$ s for sand: 0.27 and 0.31 (modified) as well as  $\Phi/\lambda$ : 0.30 and 0.31 (modified) (Table 6.10). The reduced values are due to the high CVs (0.61 and 0.60 - modified, Table 6.4) which were attributed to the estimation of OCR and  $\phi$  from multiple borings (mean estimate) at large distances.
- In the case of clays, the FHWA (1999) method had a  $\Phi = 0.83$  and  $\Phi/\lambda = 0.53$  (Table 6.10). The high  $\Phi$  may be attributed to the high bias (1.57, Table 6.5), suggesting the method is conservative; however the  $\Phi/\lambda$  is similar to the sand methods. Also, the clay dataset considered the Duval Marls (USCS – CH); Table 5.5, section 5.4 identified only a 6% change if the data set was removed.

In the case of ACIPs installed in Florida Limestone, the LRFD resistance values,  $\Phi$ , varied by method and rock formation:

- For Miami Limestone ( $q_u$  values ranging from 2 ksf to 144 ksf), only one method had an LRFD  $\Phi$  above 0.5 (Ramos,  $\Phi = 0.55$  and  $\Phi/\lambda = 0.51$ ). In addition, the more efficient methods were based on laboratory rock strength approaches ( $0.4 < \Phi < 0.55$ , and  $0.40 < \Phi/\lambda < 0.56$ ) versus SPT methods ( $0.14 < \Phi < 0.22$ , and  $0.19 < \Phi/\lambda < 0.38$ ) – Tables 6.11 & 6.12. Besides Ramos method the following other rock strength methods gave reasonable values: Herrera ( $\Phi = 0.48$  and  $\Phi/\lambda = 0.56$ ), FDOT ( $\Phi = 0.47$  and  $\Phi/\lambda = 0.45$ ), Carter ( $\Phi = 0.45$  and  $\Phi/\lambda = 0.42$ ), Reese ( $\Phi = 0.46$  and  $\Phi/\lambda = 0.41$ )
- In the case of Fort Thompson Limestone ( $q_u$  values ranging from 10 ksf to 260 ksf), one method had an LRFD  $\Phi$  above 0.5 (Carter,  $\Phi = 0.55$  and  $\Phi/\lambda = 0.55$ ). Like the Miami Limestone, the more efficient methods for Fort Thompson were based on laboratory rock strength approaches ( $0.40 < \Phi < 0.55$ , and  $0.48 < \Phi/\lambda < 0.66$ ) versus SPT methods ( $0.13 < \Phi < 0.33$ , and  $0.30 < \Phi/\lambda < 0.51$ ) – Tables 6.13 & 6.14. Besides Carter's method, the following other rock strength methods gave reasonable values: FDOT ( $\Phi = 0.49$  and  $\Phi/\lambda = 0.58$ ), Herrera ( $\Phi = 0.55$  and  $\Phi/\lambda = 0.55$ ), Horvath ( $\Phi = 0.45$  and  $\Phi/\lambda = 0.48$ ), Reese ( $\Phi = 0.42$  and  $\Phi/\lambda = 0.38$ )
- For all design methods in Miami and Fort Thompson Limestone, every boring and laboratory strength data was used to estimate site predicted means due to limited individual boring data and distance to each load test. In order to estimate the CV of the bias (measured/predicted), the individual variance of measured and predicted based on all data was used to calculate the variance of ratio (i.e. bias – measured over predicted) through Eqs. 6.2 and 6.3. Generally, this approach results in large variance, CV and lower  $\Phi$  (i.e. use of full site data). Specifically, it is expected that

smaller variability of strength data would occur if only borings near the load test (e.g. 50 ft) were used.

- There was limited Limestone data for other Florida formations. In the case of North Florida (Alachua), 4 piles were embedded in an IGM rock material. Unfortunately, no rock strength or recovery data was available; in addition, the North Florida site SPT N showed a higher mean compared to Miami Limestone. In addition, the mean estimated skin friction for North Florida was lower (2.4 tsf) vs. Miami (3.3 tsf) and therefore, all of the IGM SPT methods over predicted capacity (bias ~ 0.3) and not considered with IGM material. It is suggested that additional data be collected in this and other rock formations that have ACIP piles for further analysis.

#### **7.4 Discussion and Recommendations for the Selection of Minimum Number of Load Tests per Site**

As identified in sections 7.1 and 7.3, the ACIP and site boring data collected was limited by: 1) number of fully instrumented pile load tests, 2) vertical movements of the piles tested, 3) number of rock formations piles were located and 4) distance of boring, and laboratory data from pile load test. For instance, only 16 of the top down compression piles were monitored along their length, requiring the use of segmental modeling approach to estimate ultimate skin friction which was subsequently bias corrected for measured resistance. In addition, since most borings were greater than 50 ft from an individual load test, a site mean for both measured and predicted could only be determined. Finally, the primary rock formations evaluated were only Miami and Fort Thompson, and no other Florida formations (i.e. Tampa, Alachua, Suwanee, etc.).

Consequently, it is recommended that a minimum of one static load test be performed on any planned FDOT site employing ACIP piles to improve current and future designs. The selection of number of load tests, should be based on the preliminary or phase I boring and

laboratory data. In the case of rock, sufficient laboratory strength data should be obtained for a number of the borings within the site to identify the mean strength and estimated pile capacity in multiple separate areas/zones on the site. If the mean estimate pile resistance in each area/zone is similar then the use of one or possibly two load tests should be considered on the site.

However, if the estimate of pile capacity varies significantly ( $> 50\%$ ) over the site from multiple areas or zones, then two or more load tests, depending on site variability, may be warranted based on the size of the site.

For an individual load test it is recommended that multiple levels of instrumentation on each ACIP test pile be performed. In this study, many of the tested piles had only 3 or 4 levels of instrumentation. Increased level of instrumentation provides multiple benefits: 1) differentiates skin from tip resistance which are mobilized quite differently, 2) separates soil from rock which may have significantly different ultimate skin friction, and 3) separates different rock formations (Anastasia, Fort Thompson, Miami, etc.) which may overlay one another. In addition, having a boring within the footprint of the tested pile, coupled with coring of the bearing layer (if the layer is cohesive/calcareous) and the associated laboratory testing will significantly reduce the variability (i.e. spatial) and CV of the bias (measured/predicted), resulting in better assessment of method error and improvements in proposed LRFD resistance factors,  $\Phi$ , for existing methods and soil/rock formations as well as others (e.g. North Florida, Anastasia, Suwanee, etc.).

Finally monitoring the ACIP installation is now possible on many rigs. These systems monitor torque, crowd force, penetration rate, concrete pressure and concrete volume during drilling (BAUER, 2013-B-tronic, Jean Lutz, etc.). With real time feedback during the drilling and grouting, it may be possible to estimate rock strength during drilling, and assess change in



conditions from one foundation to another. For instance, in case of drilled shaft installation, FDOT BDV 31 977-20, has shown comparison of rock strength ( $q_u$ ) estimated from crowd, torque, and penetration rate vs. laboratory strength data. Such systems are of value for cast in situ foundations that do not remove the drilling equipment for visual inspection.

## REFERENCES

AASHTO (2014). *AASHTO LRFD Bridge Design Specifications (US Customary Units), Fourth Edition*, AASHTO, Washington, D.C.

Ang, A. and Tang, W.H. (1975). *Probability concepts in engineering, planning, and design*, Vol. I: Basic Principles, John Wiley & Sons, New York.

Bauer (2013). *Product Monitoring System Brochure*, <http://www.bauerfoundations.com>

Brown, D.A., Dapp, S.D., Thompson, W.R., and Lazarte, C.A. (2007). "Design and Construction of Continuous Flight Auger (CFA) Piles", FHWA-HIF-07-03, Geotechnical Engineering Circular No. 8.

Brown, D.A., Turner, J.P., and Castelli, R.J. (2010). "Drilled shafts: construction procedures and LRFD design methods," FHWA-NHI-10-016, Geotechnical Engineering Circular No. 10.  
Carter, J. P., and Kulhawy, F. H. (1988). "Analysis and design of drilled shaft foundations socketed into rock," EPRIReport EI-5918, Electric Power Res. Inst., Palo Alto, Calif.

Clemente, J.L.M., Davie, J.R., and Senapathy, H. (2000). "Design and Load Testing of Augercast Piles in Stiff Clay," Geotechnical Special Publication No. 100, Ed. By N. D. Dennis, R. Castelli, and M. W. O'Neill (Eds.), ASCE, August, pp. 398–403.

Coleman, D.M. and Arcement, B.J. (2002). "Evaluation of Design Methods for Auger Cast Piles in Mixed Soil Conditions," Proceedings of the International Deep Foundations Congress 2002, February 14-16, 2002 Orlando, Florida; M.W. O'Neill and F.C. Townsend (Eds.), ASCE, pp. 1404–1420.

Crapps, D. K. (1986). "Design, construction and inspection of drilled shafts in limerock and limestone," Proc. Annual Meeting of Florida Section, ASCE.

Crapps, D. K. (1992). "Acosta Bridge Piling and Drilled Shafts," Schmertmann and Crapps, Inc. Report to the Florida Department of Transportation.

Decourt, L. (2003). "Behaviour of a CFA Pile in a Lateric Clay," Proceedings of the 4th International Geotechnical Seminar on Deep Foundations on Bored and Auger Piles, BAP IV, Ghent, Belgium, pp. 301–308.

Douglas, D. J. (1983). "Discussion on Paper 17-22: Case Histories," Proceeding, Conference on Piling and Ground Treatment, Institution of Civil Engineering, London, pp. 283.

Frizzi, R.P. and Meyer, M.E. (2000). "Augercast Piles: South Florida Experience," Geotechnical Special Publication No. 100, N. D. Dennis, R. Castelli, and M. W. O'Neill (Eds.), ASCE, August, pp. 382–396.

Gupton, C, and Logan, T. (1984). "Design guidelines for drilled shafts in weak rocks of south Florida," Proc. South Florida Annual ASCE Meeting, ASCE.

Hasofer, A. M. and Lind, N.C. (1974). "An exact and invariant first order reliability format", *Journal of Engineering Mechanics*, Vol. 100, No. 1, pp. 111-121.

Hassan, K., O'Neill, M., Sheikh, S, and Ealy, C. (1997) "Design method for drilled shafts in soft argillaceous rock," *Journal of Geotechnical and Geoenvironmental Engineering*, ASCE, Vol, 123, No. 3, pp 272-280.

Horvath, R. G., and Kenney, T. C. (1979). "Shaft resistance of rock-socketed drilled piers," Proc. Symp. on Deep Foundation, ASCE.

Kwak, K., Kim, K.J., Huh, J., Lee, J.H., and Park, J.H. (2010). "Reliability-based calibration of resistance factors for static bearing capacity of driven steel pipe piles", *Canadian Geotechnical Journal*, 47, pp. 528-538.

Lai, P. (1998). "Determination of design skin friction for drilled shafts socketed in Florida limestone," Notes of FDOT Design Conference, Tallahassee, pp. 140-146.

Neely, W. J. (1991) "Bearing Capacity of Auger-Cast Piles in Sand," *Journal of Geotechnical Engineering*, ASCE, Vol. 117, No. 2, pp. 331–345.

O'Neill, M., Townsend, F., Hassan, K., Buller, A., and Chan, P (1996) "Load Transfer for Drilled Shafts in Intermediate Geomaterials," FHWA-RD-95-171, FHWA, U.S. Department of Transportation

O'Neill, M.W. and Reese, L.C. (1999). "Drilled Shafts: Construction Procedures and Design Methods," FHWA Report No. IF-99-025, Federal Highway Administration, Washington, D.C.

O'Neill, M. W., Ata, A., Vipulanandan, C., and Yin, S. (2002). "Axial Performance of ACIP Piles in Texas Coastal Soils," Geotechnical Special Publication No. 116, Ed. by M. W. O'Neill and F. C. Townsend (Eds.), ASCE, February, Vol. 1, pp. 1290–1304.

Paikowsky, S. G., (2004). Load and resistance factor design (LRFD) for deep foundations." *NCHRP Report 507*, Transportation Research Board, Washington D.C.

Styler, M. A. (2006). *Development and implementation of the Diggs format to perform LRFD resistance factor calibration of driven concrete piles in Florida*, Master Thesis, Department of Civil and Coastal Engineering, University of Florida.

Ramos, H.R., Antorena, J.A., and McDaniel, T.G. (1994) Correlations between the Standard Penetration Test (SPT) and the Measured Shear Strength of Florida Natural Rock. Proc. Int. Conf. on Design and Construction of Deep Foundations, FHWA, pp. 699-711.

Reese, L. C., and O'Neill M. W. (1988). "Drilled Shaft: Construction Procedures and Design Methods," FHWA-HI-88-042, Federal Highway Administration, Washington, D.C.

Reese, L. C, and O'Neill, M. W. (1987). "Drilled shafts: construction procedures and design methods." Design manual, U.S. Department of Transportation, Federal Highway Administration, McLean, Va.

Reynolds, R. T., and Kaderabek, T. J. (1980). "Miami limestone foundation design and construction," ASCE, New York, N.Y.

Rizkallah, V. and Bruns, T. (1988). "Estimation of Pile Bearing Capacity of Cast-in-Place Screwed Piles," Proceedings of the 3rd International Geotechnical Seminar on Deep Foundations on Bored and Auger Piles, BAP III, Ghent, Belgium, pp. 417–424.

Rowe, R. K., and Armitage, H. H. (1987). "A design method for drilled piers in soft rock," Can. Geotech. J. 24(1), 126-142.

Stuedlein, A. W., and Gurtowski, T. M. (2012). "Reliability of shaft resistance for augered cast-in-place piles in granular soils," Full scale testing and foundation design: Honoring Bengt Fellenius, GSP No. 227, ASCE, Reston, VA.

Viggiani, C. (1993) "Further Experiences with Auger Piles in Naples Area," Proceedings of the 2nd International Geotechnical Seminar on Deep Foundations on Bored and Auger Piles, BAP II, Ghent, Belgium, pp. 445–458.

Williams, A. F., Johnston, I. W., and Donald, I. B. (1980). "The design of socketed piles in weak rock," Proc. Int. Conf. on Struct. Foundations in Rock, A.A. Balkema Publishers, Netherlands, 327-347.

Wright, S.J. & Reese, L.C. (1979). "Design of Large Diameter Bored Piles," Ground Engineering, Vol. 12, No. 8, pp. 17–51.

Yu, Y. (2006). “Bayesian updating for improving the accuracy and precision of pile capacity predictions”, *IAEG2006*, Geotechnical Society of London.

Zelada, G. A., and Stephenson, R. W. (2000). “Design Methods for Auger CIP piles in Compression,” *New Technological and Design Developments in Deep Foundations*, ASCE Geotechnical Special Publication No. 100, N. D. Dennis, R. Castelli and M. W. O’Neill (Eds.), ASCE, August, pp. 418–432.

Zhang, L. and Tang, W.H. (2002). “Use of load tests for reducing pile length”, *An International Perspective on Theory, Design, Construction, and Performance, Geotechnical Special Publication*, 116, pp. 993-1005.